ENERGY

CONSERVATION

ORNL/Sub/81-7762/5 & 01

Performance and Simulation of Once-Through and Separating Cycles Using Nonazeotropic Refrigerant Mixtures

D. Boggs
W. F. Stoecker

Prepared by

UNIVERSITY OF ILLINOIS AT URBANA-CHAMPAIGN
Department of Mechanical and Industrial Engineering
1206 West Green Street
Urbana, Illinois 61801

under
Subcontract 7762-X01

for

OAK RIDGE NATIONAL LABORATORY
operated by
MARTIN MARIETTA ENERGY SYSTEMS, INC.
for the

U.S. DEPARTMENT OF ENERGY

OFFICE OF BUILDINGS
AND COMMUNITY SYSTEMS

Printed in the United States of America. Available from
National Technical Information Service
U.S. Department of Commerce
5285 Port Royal Road, Springfield, Virginia 22161
NTIS price codes—Printed Copy: Microfiche A05

This report was prepared as an account of work sponsored by an agency of the United States Government. Neither the United States Government nor any agency thereof, nor any of their employees, makes any warranty, express or implied, or assumes any legal liability or responsibility for the accuracy, completeness, or usefulness of any information, apparatus, product, or process disclosed, or represents that its use would not infringe privately owned rights. Reference herein to any specific commercial product, process, or service by trade name, trademark, manufacturer, or otherwise, does not necessarily constitute or imply its endorsement, recommendation, or favoring by the United States Government or any agency thereof. The views and opinions of authors expressed herein do not necessarily state or reflect those of the United States Government or any agency thereof.

ORNL/Sub/81-7762/5 & 01
UILU ENG-86-4005

PERFORMANCE AND SIMULATION OF ONCE-THROUGH AND SEPARATING CYCLES USING NONAZEOTROPIC REFRIGERANT MIXTURES

D. Boggs
W. F. Stoecker

Date of Issue—June 1986

Prepared by

UNIVERSITY OF ILLINOIS AT URBANA-CHAMPAIGN
Department of Mechanical and Industrial Engineering
1206 West Green Street
Urbana, Illinois 61801

under
Subcontract 7762-X01

for

OAK RIDGE NATIONAL LABORATORY
Oak Ridge, Tennessee 37831
operated by
MARTIN MARIETTA ENERGY SYSTEMS, INC.
for the
U.S. DEPARTMENT OF ENERGY
under Contract DE-AC05-84OR21400

TABLE OF CONTENTS

Page

LIST OF FIGURES....iv

ABSTRACT....vi

1. RESEARCH IN REFRIGERANT MIXTURES....1
   1.1 Mixture Properties....1
      1.1.1 Thermodynamics....1
      1.1.2 Heat-Transfer Coefficients....4
   1.2 Some Recent Work on Refrigerant Mixtures....4
   1.3 Previous Work on this Project....5
      1.3.1 Two-Evaporator-System Studies....5
      1.3.2 Condensing Heat-Transfer Coefficients....7
   1.4 Objective of this Phase of the Project....7

2. TEST FACILITY....9
   2.1 Description of System....9
      2.1.1 Compressor and Oil Separator....9
      2.1.2 Condensers....12
      2.1.3 Heat Exchangers....12
      2.1.4 Evaporators....15
   2.2 Upgrading the System....15
      2.2.1 Model 214 Positive Displacement Flow Meter....15
      2.2.2 Expansion Valve....15
   2.3 Changes to Allow Separating Cycle....15
      2.3.1 Liquid Receiver....16
      2.3.2 Model 213 Positive Displacement Flow Meter....16
      2.3.3 Expansion Valve for Separating Cycle....16
   2.4 Operating Procedures....16

3. SIMULATION OF THE ONCE-THROUGH CYCLE....17
   3.1 Comparison of Simulation and Experiments....17
   3.2 Matching Test Parameters....17
   3.3 Downing Equations....20
      3.3.1 Vapor Pressure....21
      3.3.2 Vapor Enthalpy....21
      3.3.3 Specific Volume....21
   3.4 Heat-Transfer Evaporators and Condensers....22
   3.5 Enthalpy Expressions....23
   3.6 Comparison of Simulated and Experimental Results....25
      3.6.1 Heat-Transfer Coefficients....25
      3.6.2 Condensing Temperatures....32
      3.6.3 Position at Which Condensation Begins....35
      3.6.4 Evaporating Temperatures....35
      3.6.5 Superheat Boundary in the High-Temperature Evaporator....35
      3.6.6 Refrigerant Flow Rate....38
   3.7 Energy Savings Using Refrigerant Mixtures....38
   3.8 Summary of Equations Used in the Simulation Program....41

4. PERFORMANCE OF THE ONCE-THROUGH CYCLE USING R-22/R-114 AND R-13B1/R-152a MIXTURES....43
4.1 Comparison of R-22/R-114 with R-12/R-114 Mixtures....43
4.2 R-22/R-114 Properties....44
4.3 R-22/R-114 Test Conditions and Results....44
4.4 Comparison of Temperature Profiles of R-22/R-114 and R-12/R-114 Mixtures....45
4.5 Comparison of Compressor Power....46
4.6 Tests with R-13B1/R-152a Mixture....47

5. SEPARATING CYCLE....51
5.1 Description of Separating Cycle....51
5.2 Operating The Test Facility on Separating Cycle....51
5.2.1 Specifying Saturated Vapor Point....54
5.2.2 Condenser Water Flow....54
5.3 Test Data....56
5.4 Temperature Profiles....57
5.5 Compressor Power Comparisons....62

6. CONCLUSIONS....63
6.1 Scope of this Study....63
6.2 Comparison of Experimental and Simulated Results with a Once-Through, Two-Evaporator System....63
6.3 Other Combinations of Refrigerants....64
6.4 Separating Cycle....65
6.5 Capacity Modulating Using the Separating Cycle....65

APPENDIX I. OPERATING PROCEDURE....69
APPENDIX II. LISING OF PROGRAM SIMULATION....72
APPENDIX III. EXPERIMENTAL DATA ON TESTS OF THE SEPARATING CYCLE....95
REFERENCES....97

LIST OF FIGURES

Page

Figure 1.1 Temperature-concentration diagram of a nonazeotropic mixture....2

Figure 1.2 Temperature profiles in a counterflow evaporator for single and binary refrigerants....3

Figure 1.3 System for capacity control from Jakobs [3]....6

Figure 2.1 Schematic flow diagram of system....10

Figure 2.2 Temperature and pressure measurements....11

Figure 2.3 Condenser water control....14

Figure 3.1 Simulation diagram with designations of components and variables. Imposed parameters in parentheses....19

Figure 3.3 Condenser section boundaries....24

Figure 3.4 U-value of desuperheating section of condenser, UDSH....26

Figure 3.5 U-value of first condensing section of condenser, UCO1....27

Figure 3.6 U-value of second condensing section of condenser, UCO2....28

Figure 3.7 U-value of first pass of low temperature condenser, ULTC1....29

Figure 3.8 U-value of second pass of low temperature condenser, ULTC2....30

Figure 3.9 U-value of third pass of low temperature condenser, ULTC3....31

Figure 3.10 Comparison of simulated and actual refrigerant temperatures in condensers at several mass percentages of R-114....33

Figure 3.11 Comparison of simulated and actual refrigerant temperatures in evaporators at several mass percentages of R-114....37

Figure 3.12 Comparison of simulated and actual refrigerant flow rate....39

Figure 3.13 Isentropic compression power from simulation for actual U-values and constant U-values....42

Figure 5.1 Diagram of separating cycle.....52

Figure 5.2 Temperature-concentration diagram for separating cycle.....53

Figure 5.3 Temperature-concentration diagram showing condensation processes.....55

Figure 5.4 Separating cycle showing temperatures (°C) from Test 97.....58

Figure 5.5 Temperature concentration diagram showing separation in condenser.....59

Figure 5.6 Evaporator temperature profile for separating cycle.....60

Figure 5.7 Condensing temperatures in the separating cycle.....61

Figure 6.1 Separating cycle used for capacity modulation--two evaporators.....66

Figure 6.2 Separating cycle used for capacity modulation--single evaporator.....68

ABSTRACT

A simulation program developed at the University of Illinois at Urbana-Champaign was refined to match the performance of an experimental refrigeration facility located in the laboratory of the Department of Mechanical and Industrial Engineering in which the working fluid was a nonazeotropic mixture of two refrigerants, R-12/R-114. When simulating this two-evaporator system the program provided insight on how to control the physical system while independently regulating the refrigerating capacity and temperature level of each evaporator. A further role of the simulation program was to identify the extent to which the reduction in heat-transfer coefficients affected the cycle efficiency. The reduction in compressor power for given refrigeration loads and temperatures when using R-12/R-114 mixtures was of the order of 2 percent in comparison to using R-12 alone. Were it possible to maintain the same heat-transfer coefficients as with R-12 alone, the simulation program predicted an energy saving of 3.5 percent.

Experiments with R-22/R-114 mixtures verified the capability of achieving a 20°C temperature change during condensing or evaporation, but showed no improvements in cycle efficiency over R-12. This change of temperature, particularly when combined with desuperheating in the condenser and superheating in the evaporator, may exceed the optimum change in refrigerant temperature.

The experimental facility was revised for one series of tests so that the refrigerant flow was changed from a once-through mode to parallel branches through the two evaporators. This separating cycle performed a partial condensation, with the R-114-rich condensate thus formed passing through an expansion valve and then to the high-temperature evaporator. The vapor remaining after the partial condensation was condensed at lower temperature and directed to the low-temperature evaporator. Some of the practical consideration arising when operating such a cycle were discovered, such as the need for a low-temperature cooling sink in the after condenser. Extensions to the separating cycle will offer some potential concepts for rapidly changing the active concentration in capacity-modulating systems.

1. RESEARCH IN REFRIGERANT MIXTURES

Refrigerant mixtures have the potential to conserve energy in refrigeration systems and heat pumps both by virtue of their thermodynamic behavior and also through capacity modulation. The research work at the University of Illinois at Urbana-Champaign (UIUC) sponsored by the Oak Ridge National Laboratory (ORNL) through the Department of Energy (DOE) Office of Buildings and Community Systems, has concentrated thus far on thermodynamic cycles for energy conservation. Present emphasis is broadening to also include capacity modulation cycles. A heat pump using refrigerant mixtures could be more energy-effective than one using a single refrigerant if its heat pumping capacity were increased at low outdoor temperatures. The separating cycle discussed in Chapter 6 gives the flexibility to explore some capacity modulation ideas.

1.1 Mixture Properties

1.1.1 Thermodynamics

The property that gives a nonazeotropic mixture a theoretical advantage over a single substance in a refrigeration system is that it changes temperature as it passes at constant pressure through the two-phase region (i.e. evaporating or condensing). Figure 1.1 shows a temperature-concentration (T-x) diagram for a binary mixture at a given pressure.

The advantage occurs when the fluid being cooled drops in temperature in a counterflow heat exchanger. Figure 1.2 shows temperature profiles of a counterflow heat exchanger employing a single refrigerant (1.2a) and a binary mixture (1.2b).

In order to make a fair comparison of a heat pump operating with a binary mixture with that using a single refrigerant, the heat-transfer areas should be the the same. Also, in order to maintain the same refrigeration duty, the mean temperature difference must be constant, assuming that the heat-transfer coefficients are the same. Therefore temperature 1' in Fig. 1.2b must necessarily be lower than temperature 1.

The advantage of binary mixtures comes by virtue of reducing the entropy production that occurs in the heat exchange processes. In Fig. 1.2 the area between the curves, 1-2-3-4 or 1'-2'-3-4, is indicative of the entropy

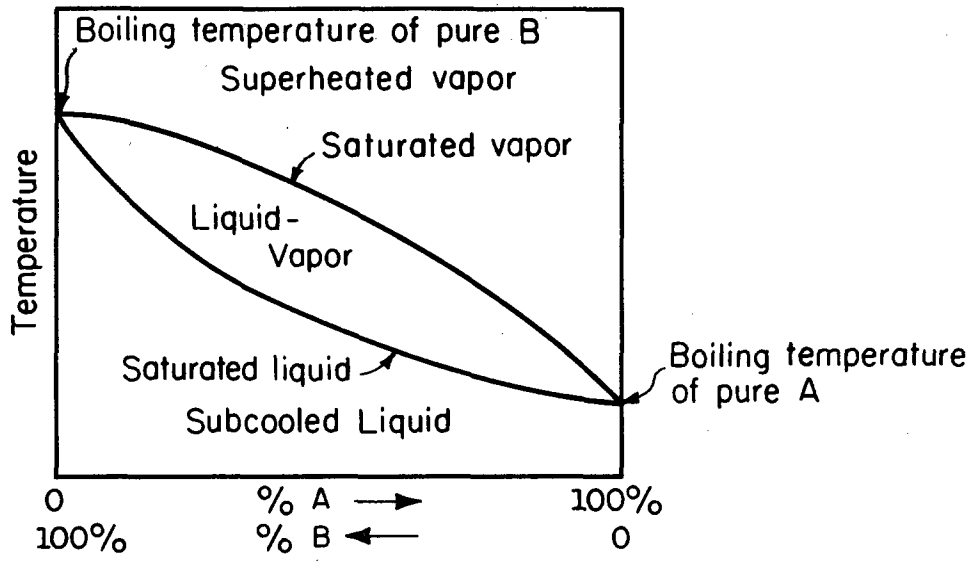

Figure 1.1 Temperature-concentration diagram of a nonazeotropic mixture

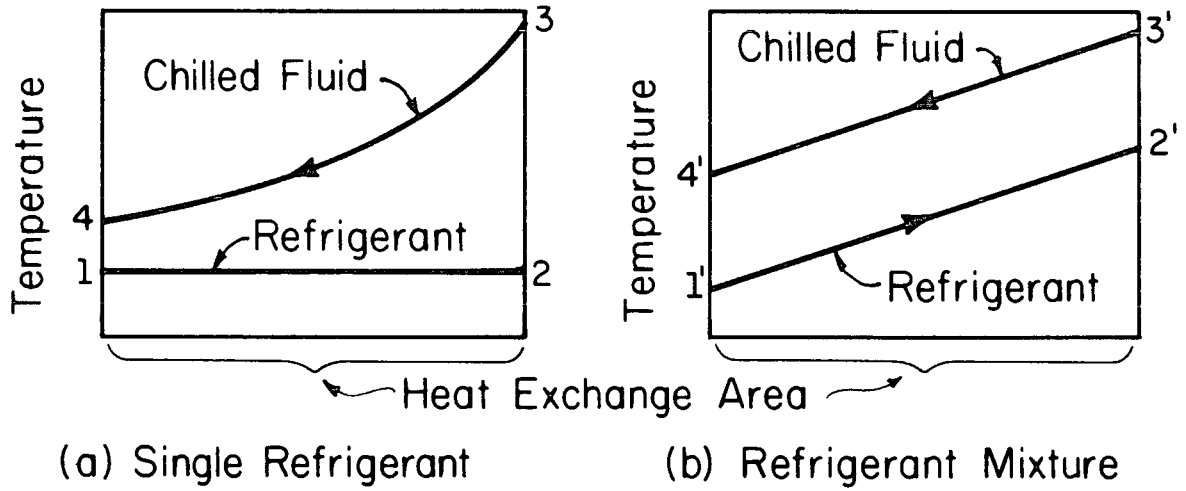

Figure 1.2 Temperature profiles in a counterflow evaporator for single and binary refrigerants

produced in the process. If area 1'-2'-3-4, representing entropy production with a binary mixture, is less than area 1-2-3-4, representing entropy production with a single refrigerant, the binary mixture has a thermodynamic advantage over the single refrigerant. However, the assumption of constant heat-transfer coefficients is an important one. If they are lower for a mixture, then temperature curve 1'-2' will be lower, and some advantage will be lost.

1.1.2 Heat-Transfer Coefficients

Aurora (1) has measured the convective heat-transfer coefficients for mixtures of R-12/R-114 and found that the coefficients were lower than the value predicted by weight averaging the two single refrigerant coefficients. Indeed, the data from our experiments confirms his findings. About half way through the condenser, the coefficients decrease 40 percent with mixtures compared to R-12 alone. Section 3.4.3 gives more information on the actual heat transfer coefficients.

1.2 Some Recent Work on Refrigerant Mixtures

Most of the current research on refrigerant mixtures concentrates on four main topics: 1) experimental heat-transfer coefficients of mixtures, 2) developing expressions for predicting the thermodynamic properties of mixtures for use in computer simulation, 3) applying refrigerant mixtures to familiar and new cycles (especially heat pump applications), and 4) using refrigerant mixtures as a means of capacity modulation.

Aittomaki (2) investigated an exhaust-air heat pump using mixtures of R-12/R-13B1 and R-22/R-114. The air streams undergo large temperature changes (25°C) so this heat pump seemed well-suited for refrigerant mixtures with gliding evaporation and condensation temperatures. Test results showed that mixtures did not improve the coefficient of performance (COP). Aittomaki states that part of the reason was the loss of temperature rise through the evaporator because of flashing. This occurred because there was subcooling with pure R-12 but none or very little with mixtures.

Jakobs and Kruse (3) tested a heat pump with mixtures of R-12/R-114. Their results show a 16 percent improvement in heating COP using 60 percent R-12 in an R-12/R-114 mixture in comparison to R-12 alone. The heat output of

the heat pump varied as the mixture concentration changed. Also, the maximum condensing temperature and the minimum evaporating temperature were held constant. Therefore, the mean temperature of condensation was probably lower with mixtures than with either pure refrigerant, and likewise the mean evaporating temperature was higher with mixtures than with either pure refrigerant.

Jakobs also tested a system for capacity control (Fig. 1.3) using a rectifier to accomplish changes in the working concentration. The working concentration of R-12 in R-114 changed from 50 percent to 90 percent. With this change, a heating increase of 30 percent can be obtained.

Cooper and Borchardt (4) proposed an ingenious method for capacity modulation in heat pumps by using refrigerant mixtures. In a heat pump with a capillary tube or an orifice as the restrictor between the condenser and the evaporator, there is a transfer of liquid from the high side to the low side as the evaporating temperature drops. An accumulator placed between the evaporator and condenser collects liquid during winter operation. If refrigerant mixtures are used in such a system, the liquid that collects in the accumulator contains a high concentration of the higher-boiling-point refrigerant. Therefore, the circulating fraction of refrigerant will become enriched in the low-boiling-point component which increases the compressor mass flow rate. This shift to a more-dense refrigerant occurs when additional heating capacity is needed. Tests were run with mixtures of R-13B1/R-152a and showed a 60 percent increase in compressor capacity compared to using a single refrigerant.

1.3 Previous Work on this Project

1.3.1 Two-Evaporator-System Studies

The two main thrusts of Stoecker and McCarthy's work (5) were: 1) to experimentally verify the expected power saving potential of refrigerant mixtures, and 2) to update the simulation program and demonstrate that it was useful for predicting cycle performance with refrigerant mixtures. McCarthy took data over the range of 0 percent to 70 mass percent R-114 in R-12 and found at best a 2 percent power reduction using 15 percent R-114. He also reported data on the heat-transfer coefficients as functions of refrigerant concentration, showing the decreases mentioned previously.

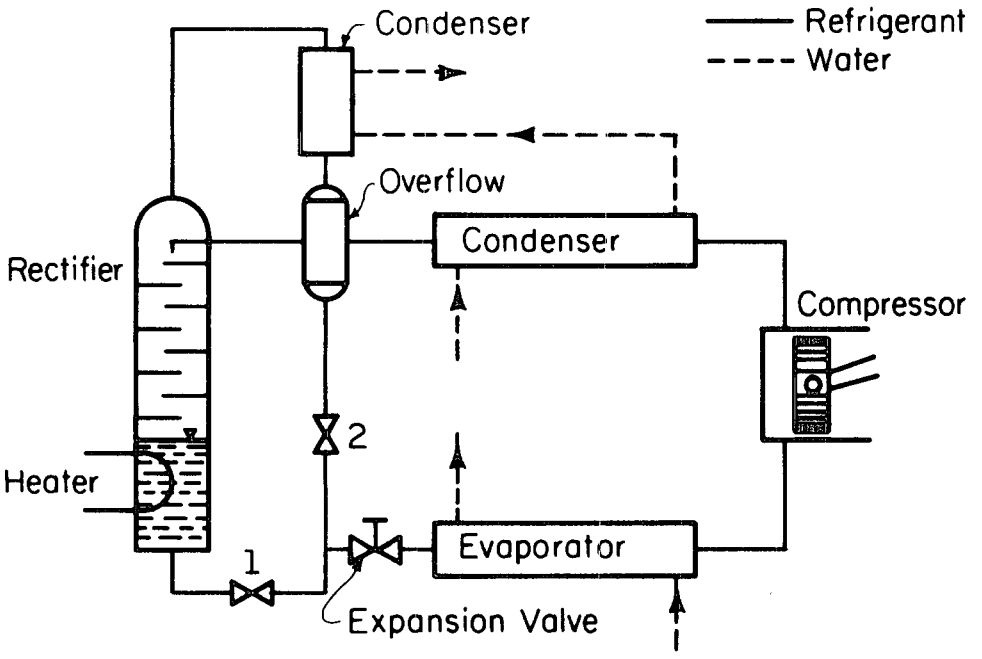

Figure 1.3 System for capacity control from Jakobs [3]

1.3.2 Condensing Heat-Transfer Coefficients

Kornota (6) investigated both qualitatively refrigerant mixture condensation in a glass-tube condenser and quantitatively at the University of Illinois at Urbana-Champaign. He measured temperature profiles along the condenser length and temperature fluctuations which represent the temperature gradient from liquid to vapor. Gas chromatography measurements showed that the R-114 concentration in the liquid increased along the length as condensation proceeds. He identified the flow regimes in condensing R-12/R-114 mixtures and discussed reasons why the heat-transfer coefficients are lower with mixtures. One of the factors is that with binary mixtures a diffusion/counter-diffusion action must be set up near the wall which creates a concentration boundary layer. This diffusion resistance contributes to the heat-transfer degradation. Another factor is that slip occurs between the vapor and liquid streams causing nonequilibrium liquid-vapor effects.

1.4 Objective of this Phase of the Project

The purpose of this phase of the project is to expand the knowledge base of working with refrigerant mixtures, mainly from a system performance point of view. Specifically the simulation of the two-evaporator, two-condenser, two-heat exchanger cycle has been refined and the results compared with test data from that cycle. Also, some mixtures in addition to R-12/R-114 have been explored, namely R-22/R-114 and R-13B1/R-152a. Furthermore, a new separating cycle has been tested in which there are two evaporators having different mixture compositions.

2. TEST FACILITY

The system used in the initial phase of the work sponsored by ORNL at the University of Illinois was built by Launay (7) and McCarthy (5). Several modifications were made to upgrade the accuracy and repeatability of refrigerant flow rate measurements. Changes were also made which allow the possibility of running either a once-through cycle or a separating cycle. In the once-through cycle the refrigerant flows in a single continuous circuit, whereas in the separating cycle two refrigerant streams diverge in the condensation process and meet again at the compressor inlet. The once-through cycle was used by Launay and McCarthy and during the portion of this current report covered in Chapters 3, and 4. The separating cycle study began during this phase of the project and is discussed in Chapter 5.

2.1 Description of System

A schematic flow diagram of the combined once-through and separating cycles is shown in Fig. 2.1. The nine ball valves and one hand valve are used to route the refrigerant for either the once-through or the separating cycle. The liquid receiver is used only with the separating cycle and is discussed later in this chapter. Since the receiver is used only with the separating cycle, ball valves (BV) 2, 3, and 6 are closed during operation of the once-through cycle. BV 1 is opened to permit straight-through condenser flow. BV 5 and hand valve (HV) 7 are opened, and BVs 4 and 8 are closed to allow liquid coming from the condensers to proceed in series through the two refrigerant-to-refrigerant heat exchangers. After passing through the low-temperature evaporator and heat exchanger, the low-pressure refrigerant flows through BV 9 to the high-temperature evaporator and heat exchanger and then to the compressor. BV 10 is closed for the once-through cycle. The system has 60 temperature measurement points using copper-constantan thermocouples and 12 pressure measurement points as shown in Fig. 2.2.

2.1.1 Compressor and Oil Separator

The compressor is an open type-three cylinder model that is belt driven by a variable speed 7.5 hp dc dynamometer. The dynamometer is equipped with a load scale and a tachometer to measure torque and speed. An oil separator at the compressor discharge returns oil to the compressor crankcase.

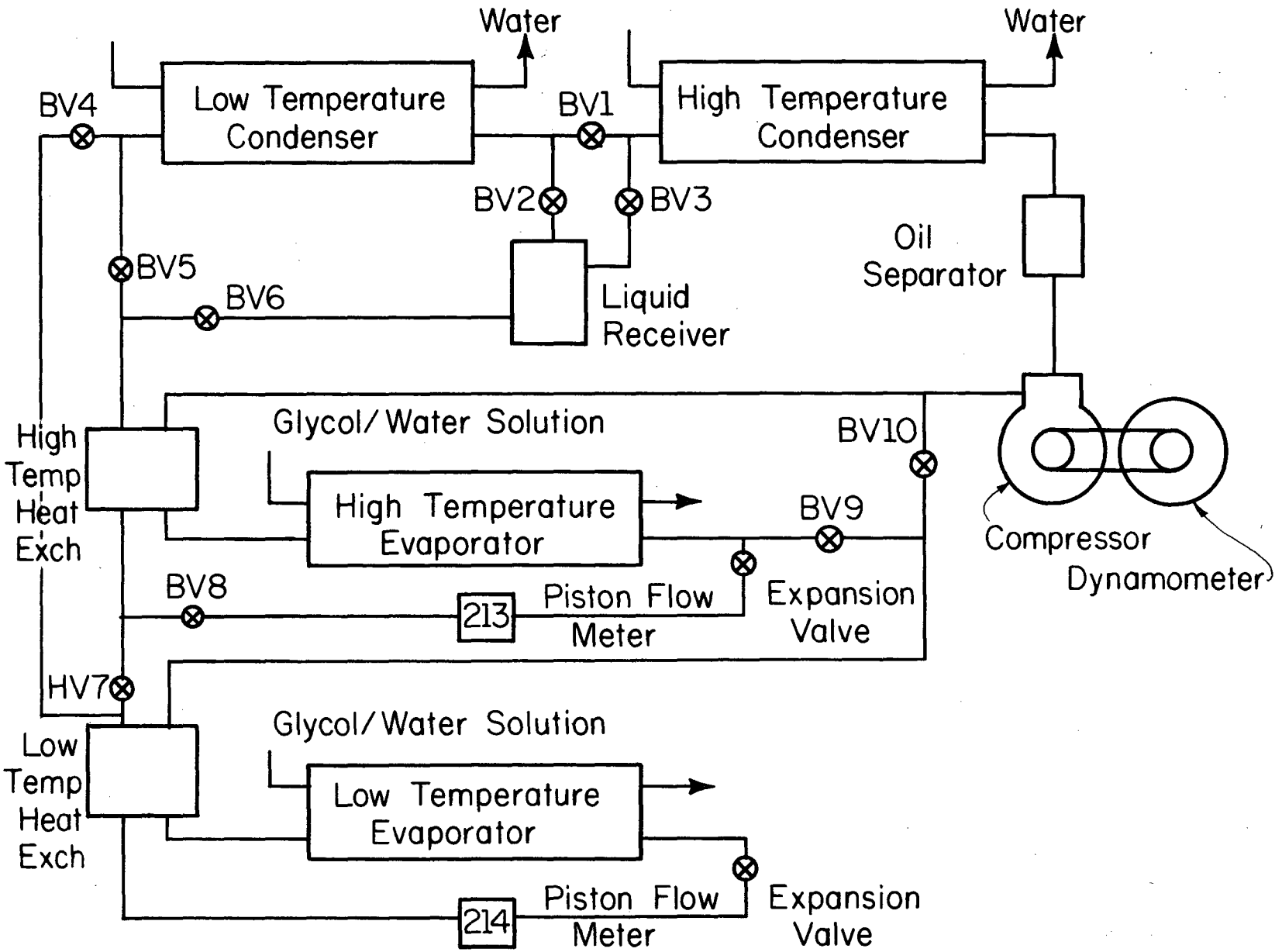

Figure 2.1 Schematic flow diagram of system

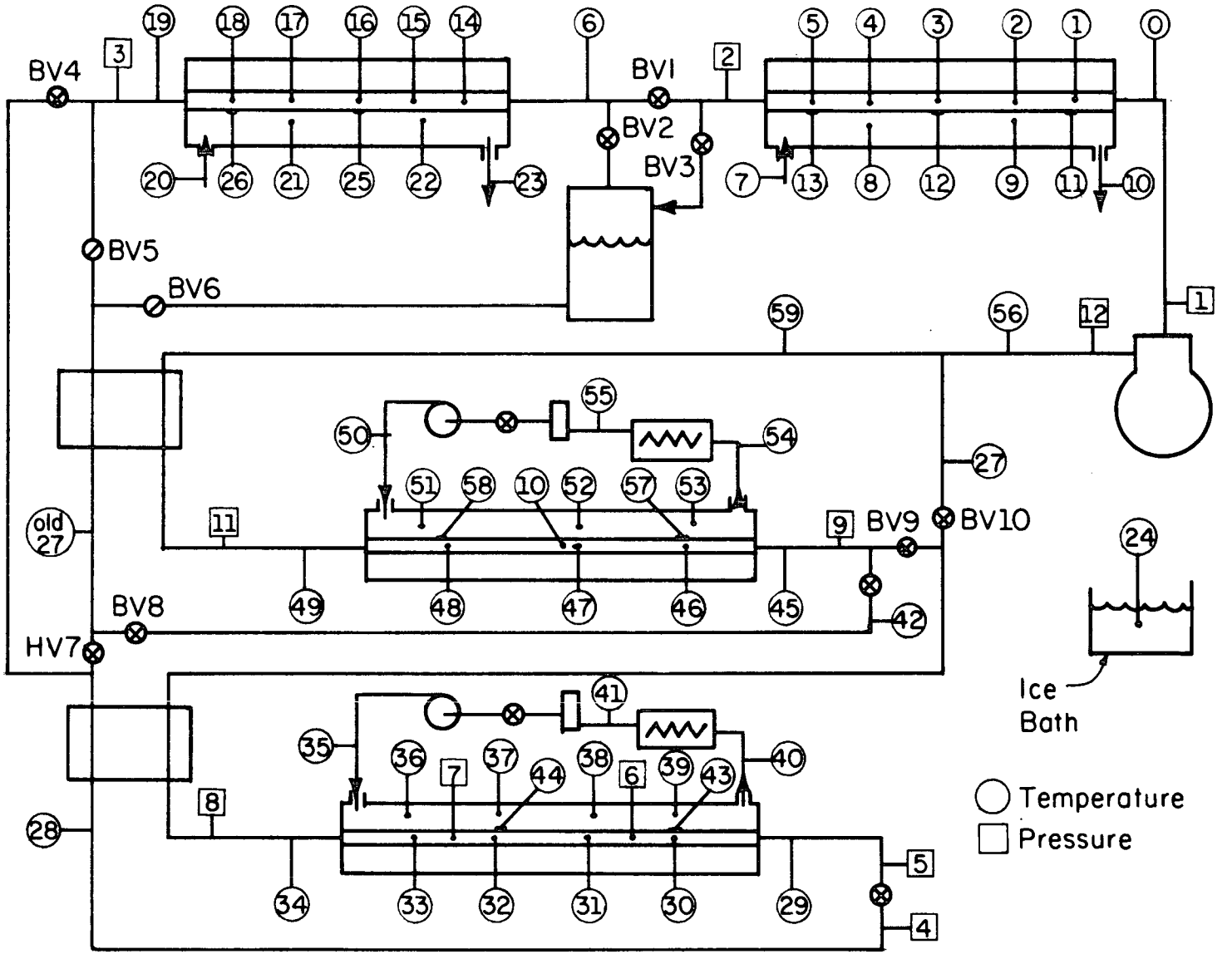

Figure 2.2 Temperature and pressure measurements

2.1.2 Condensers

The two condensers are identical tube-in-tube counterflow heat exchangers with water flowing in the annulus. Dimensions of the condensers, evaporators, and heat exchangers are given in Table 2.1. The condensers are constructed of hard copper tubing with thermocouples in the refrigerant and water streams and also on the tube wall for heat-transfer-coefficient calculations. The cooling water can be run in series or in parallel through the condensers with the flow rate through each condenser measured by a rotameter (see Fig. 2.3.). The inlet-water temperature is controlled by adjusting the bypass control valve which regulates the flow of warm water passing through the water heat exchanger.

2.1.3 Heat Exchangers

The two refrigerant-to-refrigerant heat exchangers are of counterflow tube-in-tube design. Liquid flows in the annulus and is subcooled by the low pressure refrigerant. Thermocouples measure the inlet and outlet temperatures of each stream.

Table 2.1 Specifications of Condensers, Evaporators, and Refrigerant-to-Refrigerant Heat Exchangers

Component	Number of passes	Length of refrigerant section of each pass, m	ID and OD of outer tube, mm	ID and OD of inner tube, mm	Refrigerant-side heat-transfer area m^2
Low temperature evaporator	3	1: 3.683 2: 3.683 3: 1.854	ID = 31.75 OD = 34.93	ID = 19.05 OD = 22.23	0.5518
High temperature evaporator	2	3.0734	ID = 31.75 OD = 34.93	ID = 19.05 OD = 22.23	0.3679
Low temperature condenser	3	3.1242	ID = 25.40 OD = 28.58	ID = 12.70 OD = 15.88	0.3739
High temperature condenser	3	3.1242	ID = 25.40 OD = 28.58	ID = 12.70 OD = 15.88	0.3739
Low temperature heat exchanger	1	1.549	ID = 31.75 OD = 34.93	ID = 19.05 OD = 22.22	Inner: 0.0927 Outer: 0.1082
High temperature	1	1.549	ID = 31.75 OD = 34.93	ID = 19.05 OD = 22.22	Inner: 0.0927 Outer: 0.1082

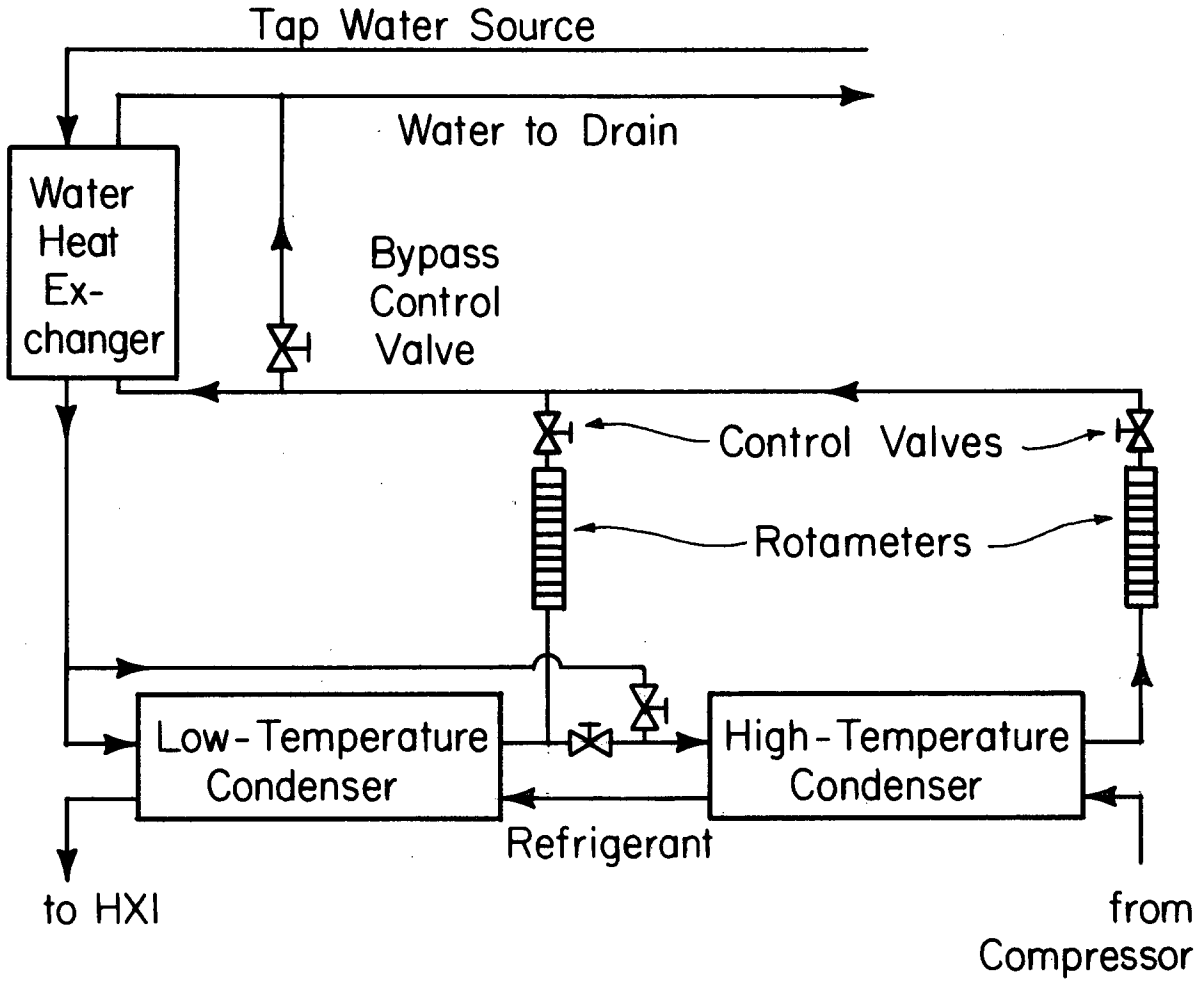

Figure 2.3 Condenser water control

2.1.4 Evaporators

The high-temperature and low-temperature evaporators are also of tube-in-tube counterflow construction. An ethylene-glycol/water solution is circulated in the annulus by a 0.5 hp centrifugal pump and is heated by an electric immersion heater. The heat input rate is controlled by a variable transformer, and the glycol flow rate is measured by a rotameter.

2.2 Upgrading the System

2.2.1 Model 214 Positive Displacement Flow Meter

In order to improve the accuracy of measuring the refrigerant flow rate, a four-piston positive-displacement meter was installed. Previously only a liquid rotameter was available for direct measurement of refrigerant flow. The rotameter was good for a quick flow-rate indication but lacked the accuracy desired. The new flow transducer at the LTE inlet, designated Model 214 and manufactured by Fluidyne Instrumentation, has a range of 10 to 6000 cc/minute. The signal output comes from a photo-optic transmitter which gives 100 pulses/revolution. The meter was calibrated by the manufacturer at 9.2343 pulses/cc. A 10 micron filter protects the meter from solid materials. The accuracy of the meter is 0.5 percent of the reading. The pulse rate was read with a frequency counter which had a resolution of 0.1 Hz when using a 10 second gate time.

2.2.2 Expansion Valve

A new expansion valve was installed in order to have more precise control over the refrigerant flow rate. The old valve was found to be slightly oversized and had a two turn stem, so that a small adjustment of the valve stem gave a large change in the flow rate. The new valve has a 10-turn stem with a 0.062 in. (1.58 mm) port which allows precise and steady flow regulation.

2.3 Changes to Allow Separating Cycle

In addition to the above changes, some modifications have been made which allow the system to be run as a separating cycle. None of the basic components such as the evaporators, condensers, and heat exchangers have been changed, just the routing to them. Ball valves are used to route the

refrigerant so that the system can operate as a once-through cycle or as a separating cycle. Ball valves were used because they have both low pressure drop and positive shut-off. Three new components used solely with the separating cycle were added, namely a liquid receiver, another refrigerant meter, and another expansion valve.

2.3.1 Liquid Receiver

A liquid receiver was added which is used only with the separating cycle. The receiver is 125 mm in diameter and 400 mm tall and is located between the HTC and the LTC, where separation of liquid and vapor occurs. The receiver has fittings welded on for a liquid sight glass. The assembly is rated from vacuum up to 3400 kPa (500 psi) working pressure.

2.3.2 Model 213 Positive Displacement Flow Meter

Another meter was installed at the inlet to the HTE and is used only with the separating cycle. This is a smaller piston meter, designated model 213 and manufactured by Fluidyne Instrumentation which has a range of 1 to 1,200 cc/minute. The output also comes from a photo-optic transmitter. This meter was calibrated by the manufacturer at 118.70 pulses/cc and has the same accuracy as the model 214 meter (0.5% of the reading).

2.3.3 Expansion Valve for Separating Cycle

An expansion valve identical to the one described in Sec. 2.2.2 was installed to regulate the refrigerant flow rate to the HTE during the separating cycle operation has been added.

2.4 Operating Procedure

The detailed operating procedure is listed in APPENDIX I.

3. SIMULATION OF THE ONCE-THROUGH CYCLE

3.1 Comparison of Simulation and Experiments

In the initial report from the UIUC to ORNL in 1978, on refrigerant mixtures, Stoecker (8) simulated some refrigeration cycles to explore the possibility of saving energy by using refrigerant mixtures. A once-through, two-evaporator system with two heat exchangers showed the most promising results for saving energy giving a 12 percent power reduction at a 50 percent mixture of R-114 and R-12 in comparison to R-12 alone. Launay (7) later refined the simulation program and optimized the distribution of heat-transfer area. Further simulation work by Stoecker and McCarthy (5) included heat-transfer coefficients and pressure drop data based on tests. However, the simulation results have not yet been compared directly with the experiments. In this phase of the work several changes have been made to the simulation program, all aimed at comparing the simulation conditions and results to the experiments. The simulation results should then help explain why the full extent of the reduction in power as predicted by the original simulation is not being seen in the experimental results.

The changes made to the simulation program fall into four categories: 1) matching the conditions that are specified for simulation to those specified when running the system, 2) using the Downing equations (9) for refrigerant property calculations, 3) sectioning the condensers and evaporators so that each section uses its own heat transfer coefficient as measured from experimental data, and 4) increasing the load in the LTE to better match what actually occurred in the experimental studies.

3.2 Matching Test Parameters

In order to compare the experimental results with the simulation results, the conditions that are specified for simulation, termed "imposed parameters," should be the same as the conditions that prevailed during the experiments. Figure 3.1 is a diagram of the system showing some of the variables with the imposed parameters enclosed in parentheses. Table 3.1 defines the abbreviations for the components and imposed parameters used in Fig. 3.1. Several changes had to be made to the list of imposed parameters used in the simulation in order to match the experimental system.

Table 3.1 Description of Components and Imposed Parameters in Fig. 3.1

Component	Description
Condensers	
DSH	Desuperheating section of high temperature condenser (HTC)
CO1	First condensing section, HTC
CO2	Second condensing section, HTC
LTC1	First section of low temperature condenser (LTC)
LTC2	Second section, LTC
LTC3	Third section, LTC
Heat Exchangers	
HX1	High temperature heat exchanger
HX2	Low temperature heat exchanger
Evaporators	
LTE1	First section of low temperature evaporator (LTE)
LTE2	Second section, LTE
LTE3	Third section, LTE
E1	First evaporating section of high temperature evaporator (HTE)
E2	Second evaporating section, HTE
SH	Superheating section, HTE

Imposed Parameter	Description
Condensers	
TCLI	Temperature of water into LTC
TCHI=TCLO	Temperature of water into HTC = temperature of water out of LTC
WLTC	Flow rate of water in LTC
WHTC	Flow rate of water in HTC
Evaporators	
TELI	Temperature of glycol into LTE
TELO	Temperature of glycol out of LTE
WGEL	Flow rate of glycol through LTE
TEHI	Temperature of glycol into HTE
TEHO	Temperature of glycol out of HTE
WGEH	Flow rate of glycol through HTE

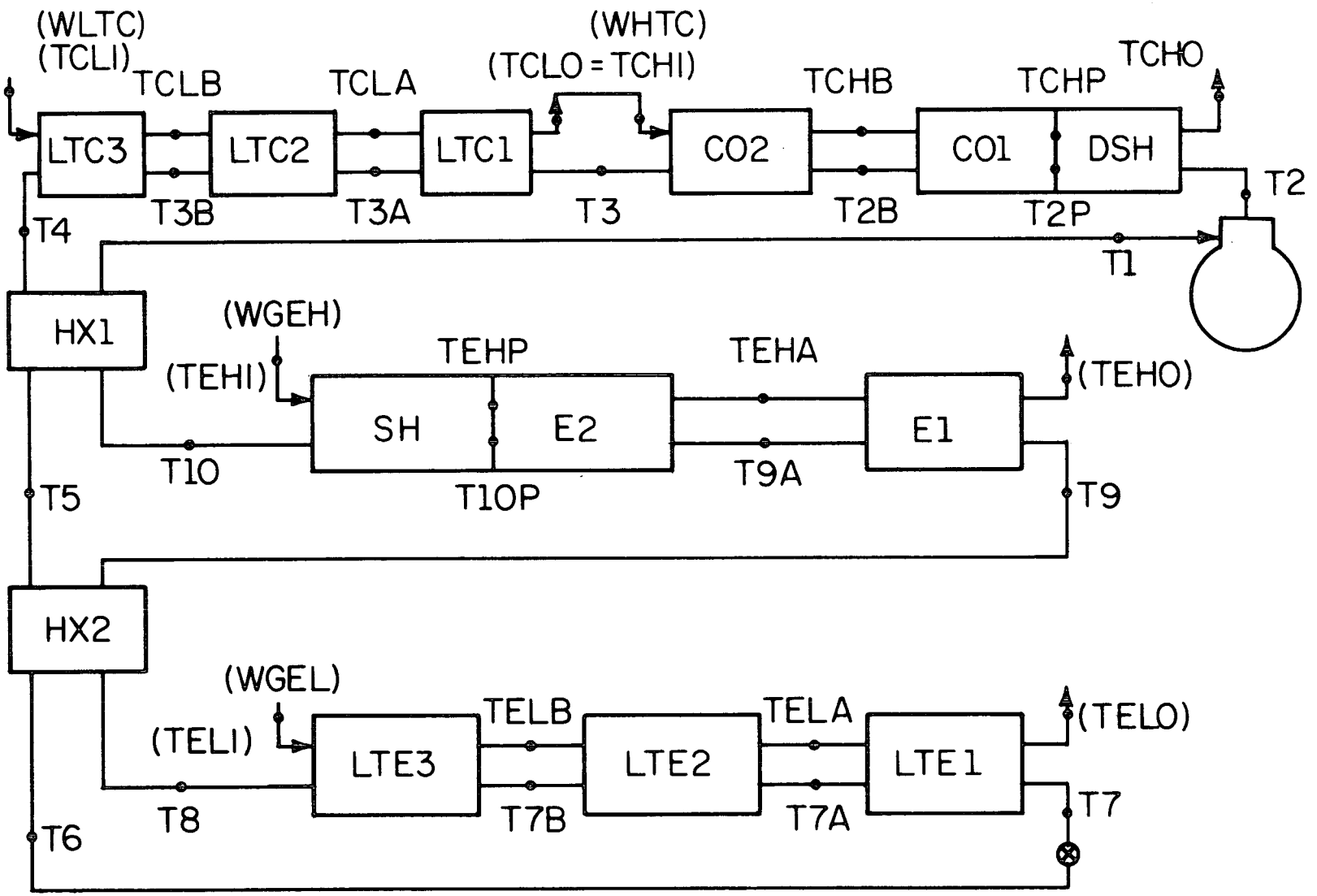

Figure 3.1 Simulation diagram with designations of components and variables. Imposed parameters in parentheses.

Several revisions were made to the simulation program for the purpose of either correcting a previous error or providing imposed parameters in the same form as experienced in the experimental tests. An error was discovered in the results shown in Fig. 6.2 of the 1984 ORNL report (5). The simulation results represented in that graph showed a drop in temperature of the superheated vapor leaving the HTE. The error was that the heat-transfer rate equation for the superheating portion of the HTE was omitted. In its place was a specification of the amount of superheat which was converging to a negative value. The correction made was to omit the superheat specification and to introduce in its place a heat-transfer rate equation for the superheating portion of the HTE.

In the second edition of the simulation program (Launay's work), the area of the HTE (AHTE) was a variable. In the third edition (McCarthy's work), it was left as a variable but an equation set AHTE to the area on the experimental system. The equation which sets the area has been removed, and AHTE is now an imposed parameter.

Another change was to specify the outlet temperatures of the chilled fluid (glycol) in the HTE (TEHO) and LTE (TELO) instead of specifying the heat input rates. The inlet temperatures of the glycol, TEHI and TELI, and the glycol flow rates were already specified. Specifying either the heat transfer rates or the glycol temperatures and flow rates determines the load on the system, but this change simply brings the simulation into conformity with the tests.

The final change was to remove the high temperature condenser (HTC) inlet water temperature (TCHI) as an imposed parameter. Because the condenser cooling water was run in series through the LTC and HTC, TCHI was equated to the outlet water temperature from the LTC.

3.3 Downing Equations

The vapor pressure, vapor enthalpy, and vapor specific volume are now calculated using the equations outlined in the Downing paper (9) instead of the equations fit from tabular data. Each equation was written into a FORTRAN function which was called every time that property was evaluated.

3.3.1 Vapor Pressure

The Downing equation for vapor pressure was in the form

$$\log_{10} P = A + \frac{B}{T} + C \log_{10} T + DT + E\left(\frac{F - T}{T}\right) \log_{10} (F - T)$$

where the constants A, B, C, D, E, and F are given for various refrigerants in the computer program in APPENDIX A. The antilog of the equation was taken to get P directly. Since the constants were given in customary U.S. units T must be in degrees R and P in psia. The conversion into S.I. units is

$$P,kPa = (P,psia) * 6.894757$$

3.3.2 Vapor Enthalpy

The Downing equation for vapor enthalpy is given as

$$H = aT + \frac{b\,T^2}{2} + \frac{c\,T^3}{3} + \frac{d\,T^4}{4} - \frac{f}{T} + JPV$$
$$+ J\left[\frac{A_2}{V-b} + \frac{A_3}{2(V-b)^3} + \frac{A_4}{3(V-b)^3} + \frac{A_5}{4(V-b)^4}\right]$$
$$+ J\,e^{-kT/T_c}\left(1 - \frac{kT}{T_c}\right)\left[\frac{C_2}{V-b} + \frac{C_3}{2(V-b)^2} + \frac{C_4}{3(V-b)^3} + \frac{C_5}{4(V-b)^4}\right] + X$$

where the constants are given for various refrigerants in Ref. 9. The conversion to S.I. units is

$$H(kJ/kg) = 2.326[H(Btu/lb) - H_f(32°F)] + 200$$

where H_f is the liquid enthalpy taken from refrigerant tables.

3.3.3 Specific Volume

The calculation of specific volume is obtained from the Downing equation of state which is written in the form

$$P = \frac{RT}{V-b} + \frac{A_2 + B_2\,T + C_2\,e^{-kT/T_c}}{(V-b)^2} + \frac{A_3 + B_3\,T + C_3\,e^{-kT/T_c}}{(V-b)^3}$$

$$+ \frac{A_4 + B_4\,T + C_4\,e^{-kT/T_c}}{(V-b)^4} + \frac{A_5 + B_5\,T + C_5\,e^{-kT/T_c}}{(V-b)^5}$$

Multiplying the whole equation by (V-b)/P gives an implicit expression for V

$$V = \frac{RT}{P} + \frac{A_2 + B_2\,T + C_2\,e^{-kT/T_c}}{P(V-b)} + \frac{A_3 + B_3\,T + C_3\,e^{-kT/T_c}}{P(V-b)^2}$$

$$+ \frac{A_4 + B_4\,T + C_4\,e^{-kT/T_c}}{P(V-b)^3} + \frac{A_5 + B_5\,T + C_5\,e^{-kT/T_c}}{P(V-b)^4} + b$$

Since the equation is implicit, an initial value of V is passed to the function, along with T and P, and V is solved for iteratively. Specific volume was left in U.S. units since it is only needed for the enthalpy function which uses it in U.S. units.

3.4 Heat-Transfer Evaporators and Condensers

In order to better match the simulation with the experimental apparatus, each pass of the evaporators and condensers was treated as a single unit. Thus, each pass can assume its own overall heat transfer coefficient, U, as determined from the experimental results, and temperatures in and out of each pass can be compared with experimental data, rather than requiring some average U-value for the entire heat exchanger.

Each condenser and evaporator pass was treated in an identical manner. Five equations described each pass and were used to compute five variables. The terms included in the simulation are shown in Fig. 3.2.

Variables determined from other equations:

$T_{1,i}$, $T_{2,i}$, W_1, W_2, $H_{1,i}$, $H_{2,i}$

Given: UA

Variables to be determined:

$T_{1,o}$, $T_{2,o}$, q, $H_{1,o}$, $H_{2,o}$

Equations:

Energy balance fluid 1 $q = w_1(H_{1,o} - H_{1,i})$

Energy balance fluid 2 $q = w_2(H_{2,i} - H_{2,o})$

Heat transfer rate $q = UA \cdot LMTD(T_{2,i}, T_{2,o}, T_{1,i}, T_{1,o})$

where LMTD is the log mean temperature difference given by

$$LMTD(T_{2,i}, T_{2,o}, T_{1,i}, T_{1,o}) = \frac{(T_{2,i} - T_{1,o}) - (T_{2,o} - T_{1,i})}{\ln(\frac{T_{2,i} - T_{1,o}}{T_{2,o} - T_{1,i}})}$$

Enthalpy 1 out $H_{1,o} = H(T_{1,o}, P_1, V_1, \text{concentration})$

Enthalpy 2 out $H_{2,o} = H(T_{2,o}, P_2, V_2, \text{concentration})$

In the cases where evaporation ends (in the HTE) or condensation begins (in the HTC), the boundaries of the sections are determined by the location of the superheat boundary. Thus, the first two sections of the HTC are described as shown in Fig. 3.3.

3.5 Enthalpy Expressions

The expression for the enthalpy of a saturated or superheated vapor composed of a mixture of R-12 and R-114, is

$$H_i = \text{conc HR114V}(T_i, PP_{4i}, V_{4i}) + (1 - \text{conc}) \text{HR12V}(T_i, PP_{2i}, V_{2i})$$

where HR114V and HR12V are the function names for the Downing enthalpy equations and

T_i = temperature, °C

PP_{4i}, PP_{2i} = partial pressures of R-114 and R-12 respectively, kPa

V_{4i}, V_{2i} = partial specific volume of R-114 and R-12, respectively, ft^3/lb

conc = R-114 concentration (mass fraction)

Similarly for a subcooled or saturated liquid, the expression for the mixture enthalpy is

$$H_i = \text{conc H114L}(T_i) + (1 - \text{conc}) \text{H12L}(T_i)$$

where H114L and H12L are the names of functions in the program listed in APPENDIX II that calculate liquid enthalpy based on a curve fit of tabular data.

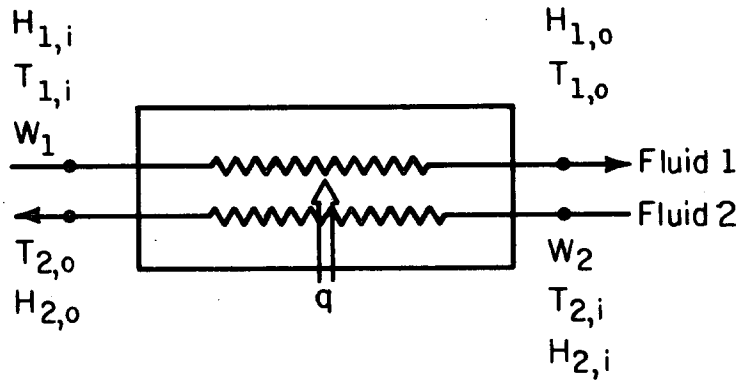

Figure 3.2 Describing a pass

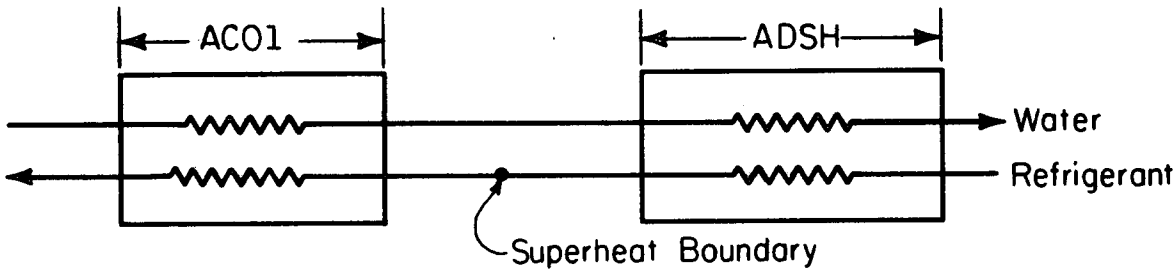

Figure 3.3 Condenser section boundaries

In the two-phase region, the property equation is

$$H_i = FRL_i\ HL_i + (1 - FRL_i)\ HV_i$$

where HL is the enthalpy of the liquid in the mixture

$$HL = XL \cdot H114L(T_i) + (1 - XL)\ H12L(T_i)$$

FRL = fraction of liquid

XL is the mole fraction of R-114 in liquid

HV is the enthalpy of the vapor in the mixture

$$HV = XV \cdot HR114V(T_i,\ PP_i,\ V_{4i}) + (1 - XV)\ HR12V(T_i,\ PP_i,\ V_{2i})$$

XV is the mole fraction of R-114 in vapor

The enthalpy changes on the glycol or water side of the evaporators and condensers were calculated using the specific heat of the glycol or water multiplied by the temperature change.

3.6 Comparison of Simulated and Experimental Results

The simulations conducted in previous phases of the project were performed using certain assumptions of component performance. Experimental data were now available to tune the simulation program, and actual component performance is used in the simulation. One of the objectives of the comparison is to gain further insight into the influence of the nonazeotropic mixtures on the energy characteristics of the two-evaporator system.

3.6.1 Heat-Transfer Coefficients

Previous simulations have assumed values for the heat-transfer coefficients in the condensers, evaporators, and refrigerant-to-refrigerant heat exchangers. Furthermore, the magnitude of the coefficients were assumed constant, regardless of the refrigerant concentration, and an overall heat-transfer coefficient was assumed for the entire heat exchanger. The overall heat-transfer coefficients, the U-value, for each pass of the heat exchangers were derived from experimental measurements and expressed as functions of the refrigerant composition. The equations were derived from curve fits, and sample graphical comparisons of the curves and the original data are shown in Figs. 3.4 through 3.9. The abbreviations are those specified in Fig. 3.1 for the components. The expressions fitted to each curve are as follows:

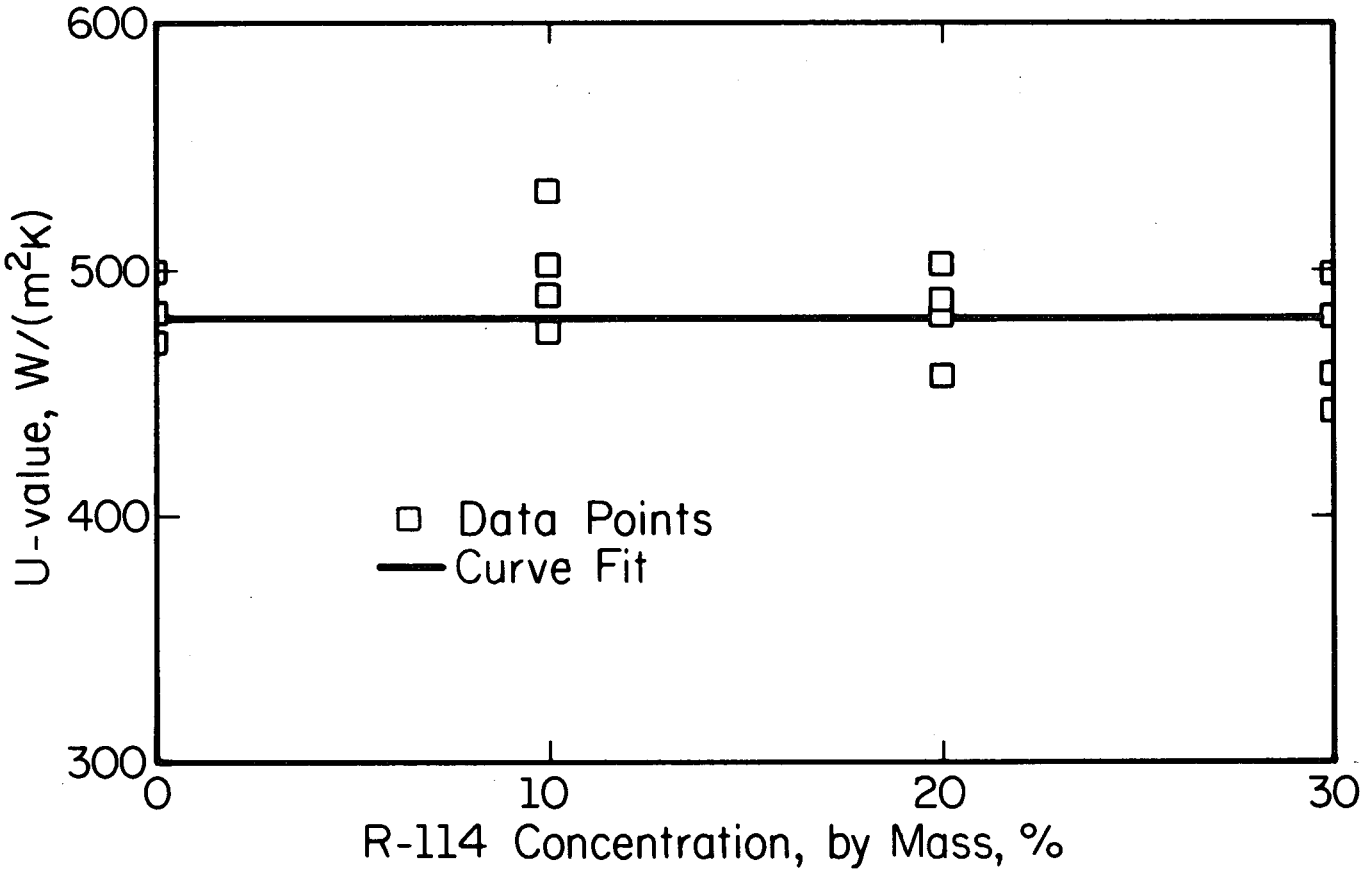

Figure 3.4 U-value of desuperheating section of condenser, UDSH

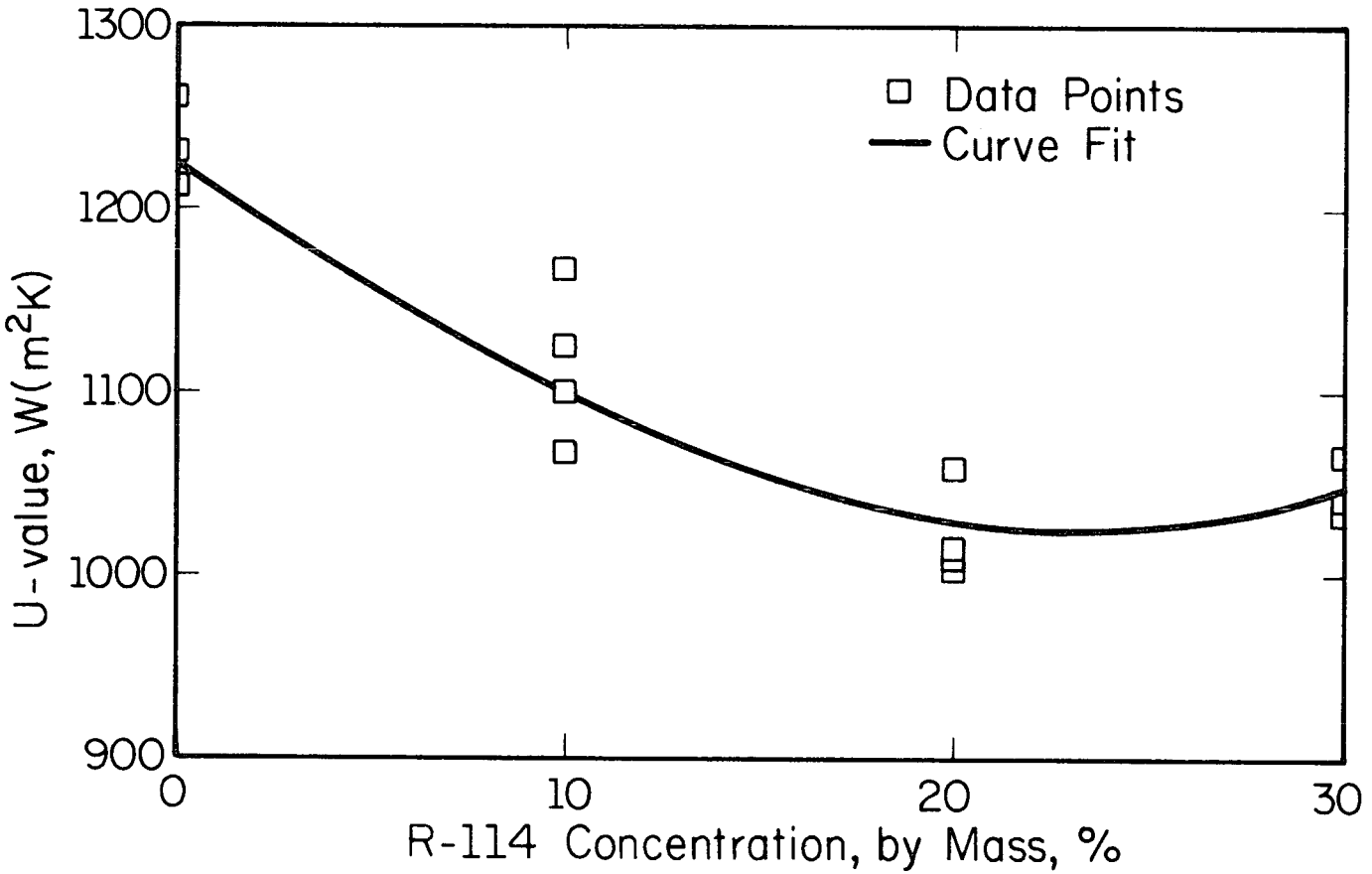

Figure 3.5 U-value of first condensing section of condenser, UC01

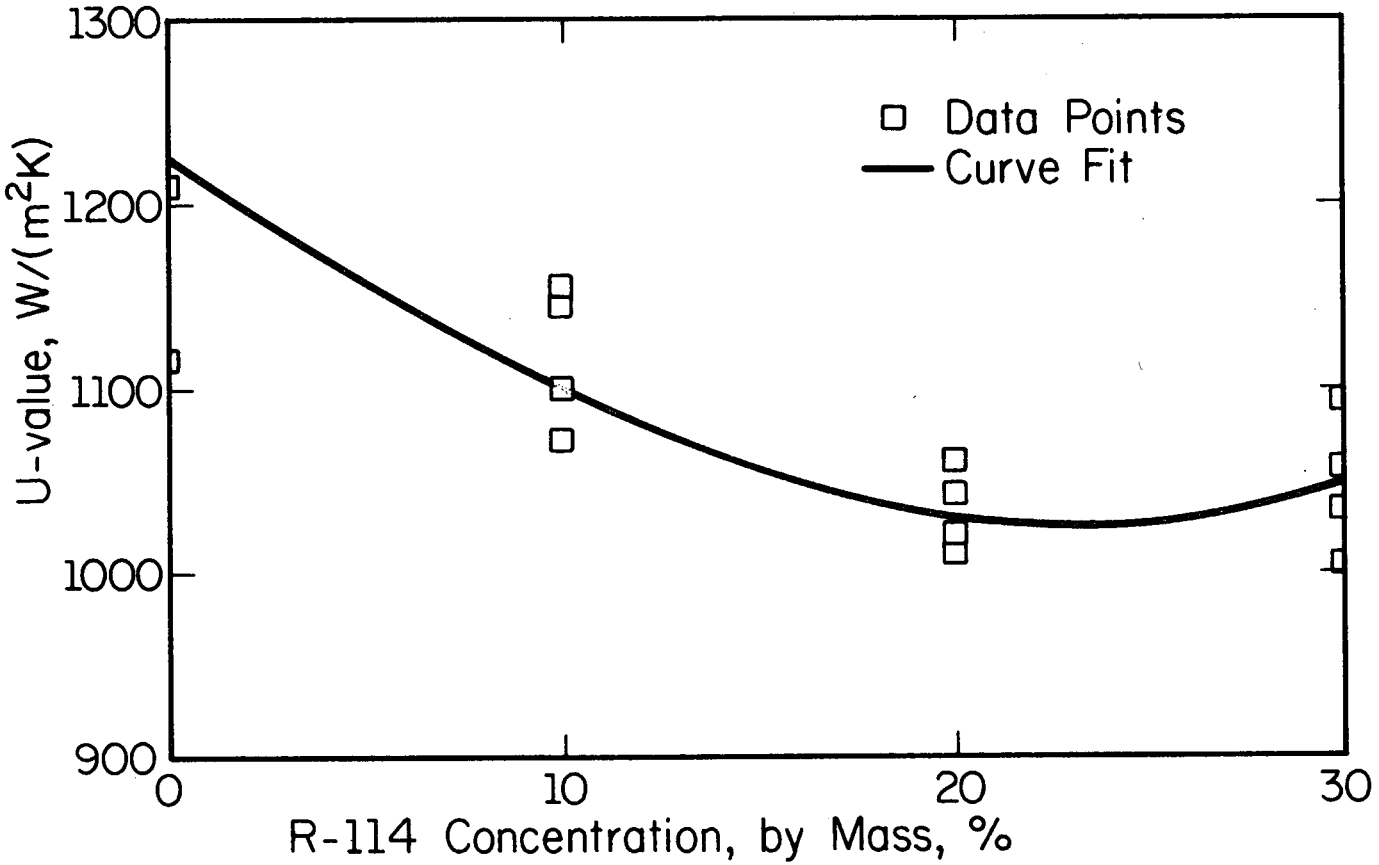

Figure 3.6 U-value of second condensing section of condenser, UC02

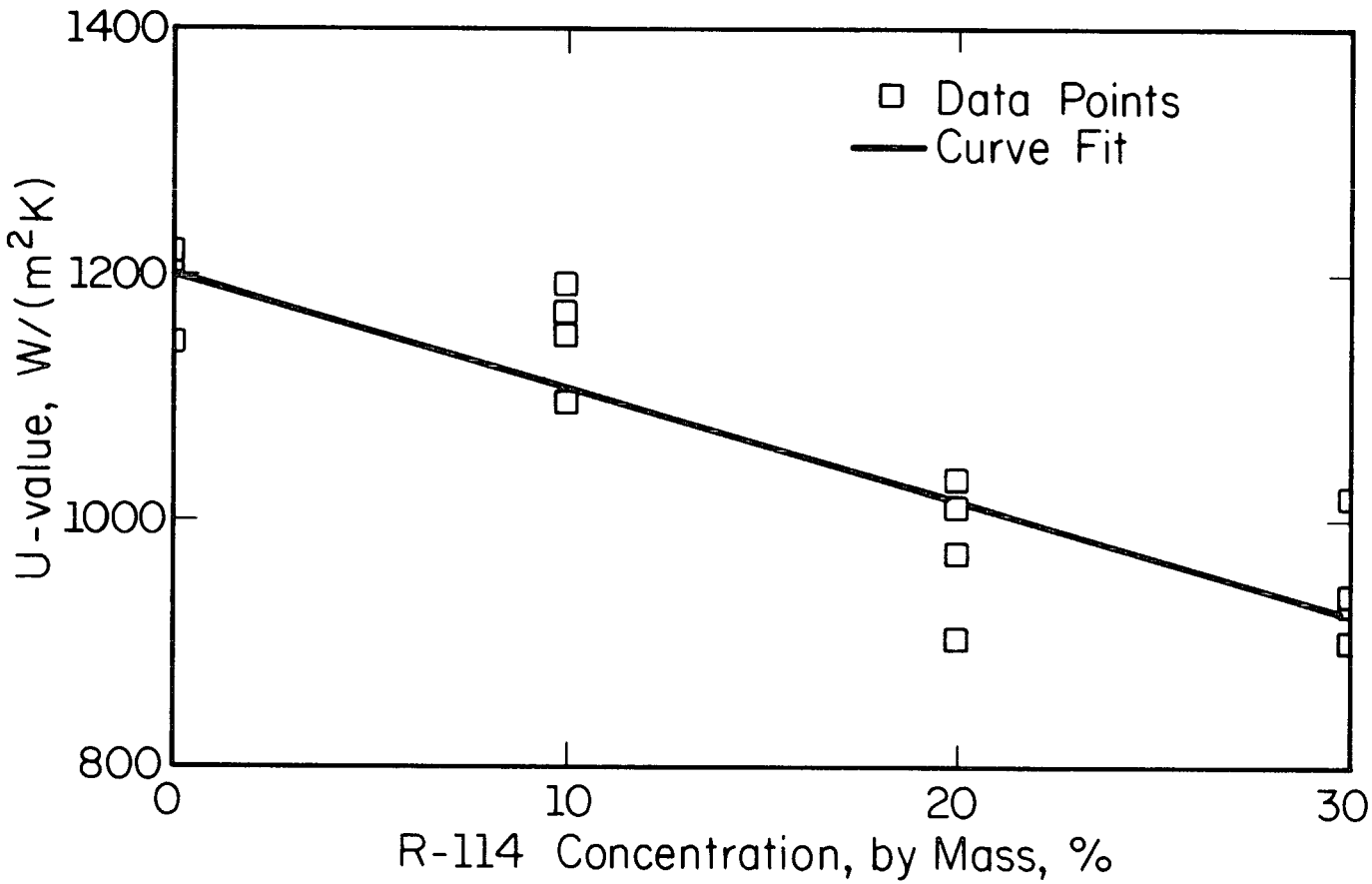

Figure 3.7 U-value of first pass of low temperature condenser, ULTC1

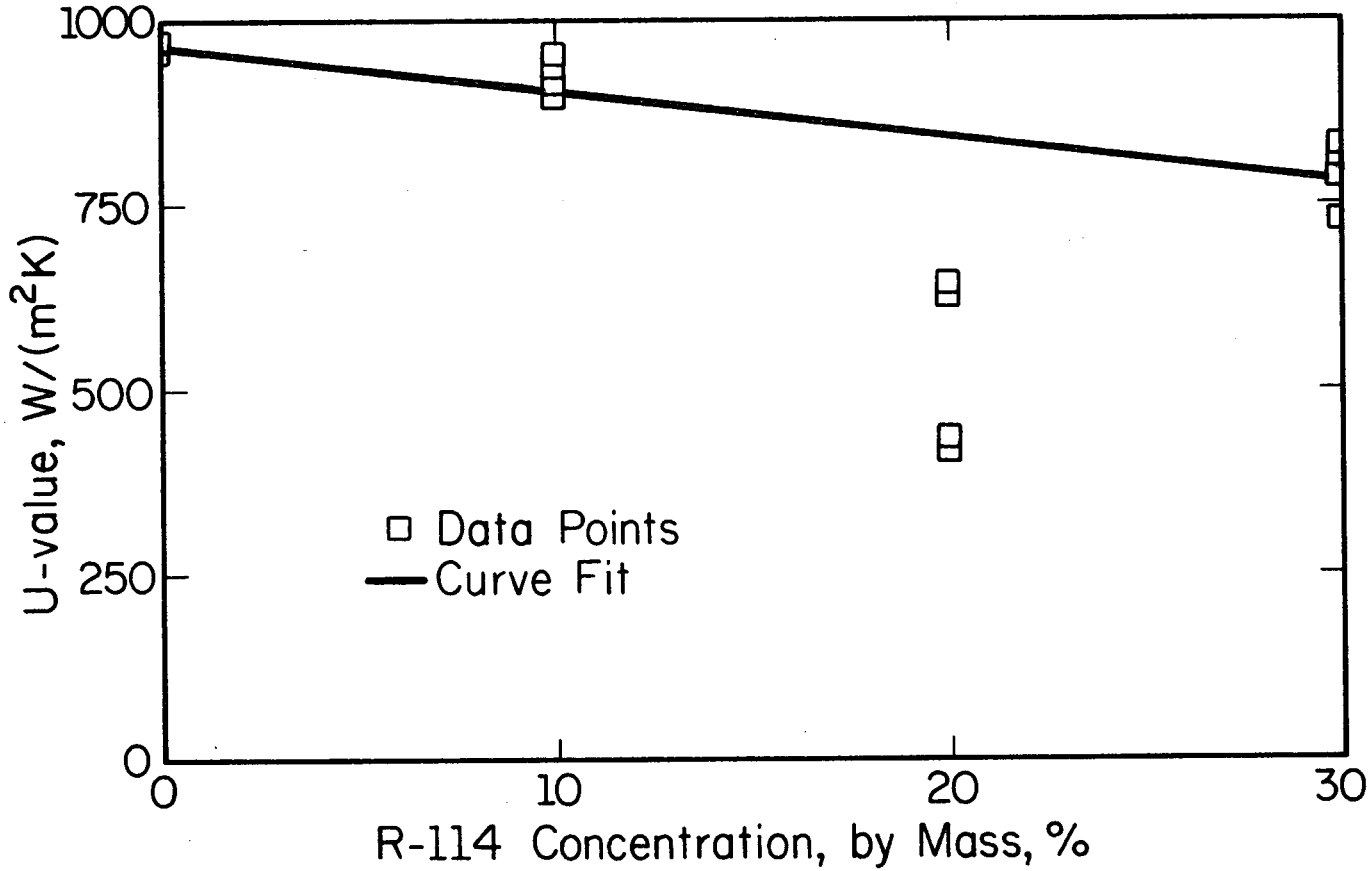

Figure 3.8 U-value of second pass of low temperature condenser, ULTC2

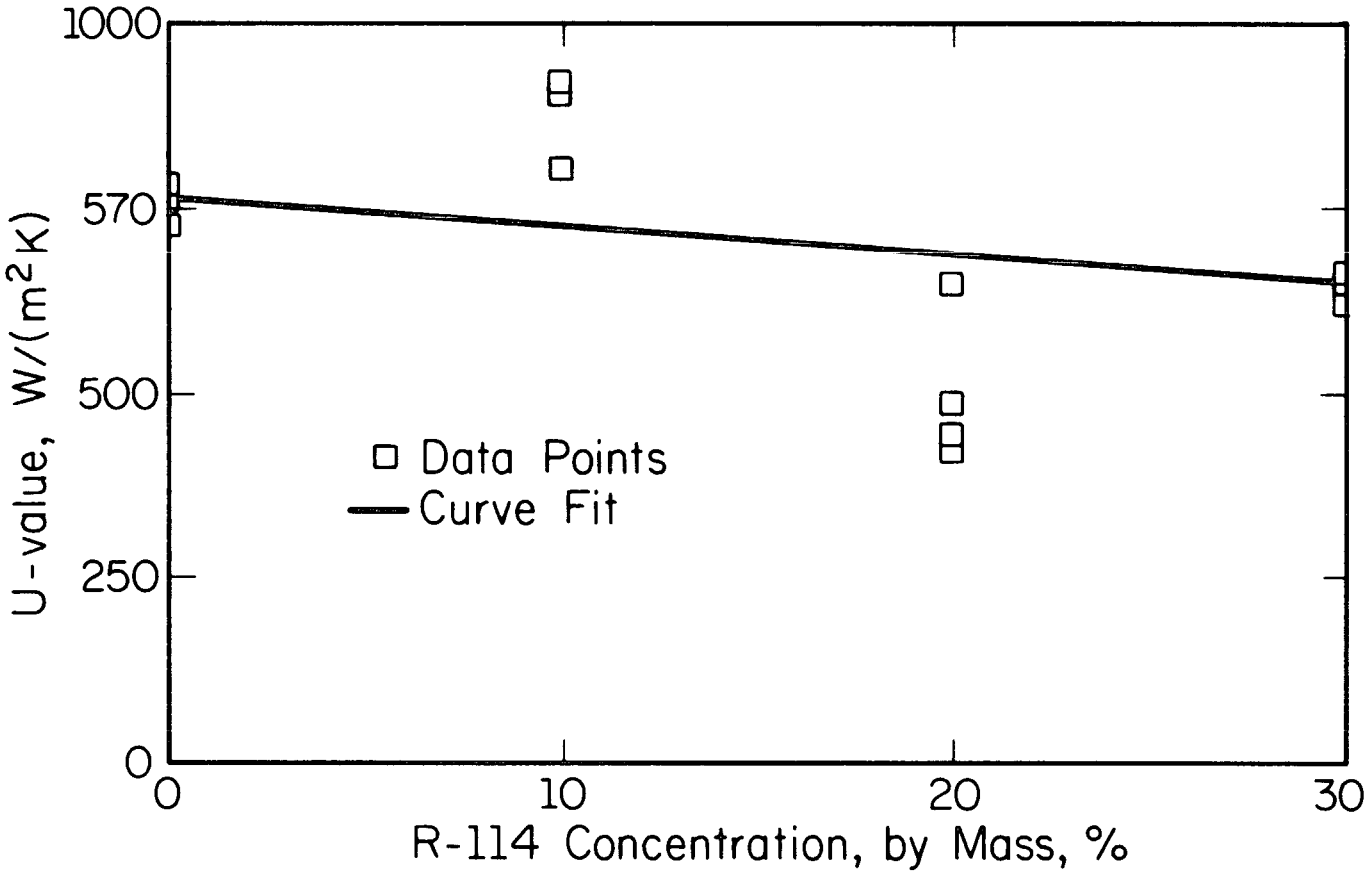

Figure 3.9 U-value of third pass of low temperature condenser, ULTC3

High Temperature Condenser

UDSH= 0.480(kW/m^2K)

$UCO1 = 1.225 - 1.41\ conc + conc^2 + 5.83\ conc^3$

$UCO2 = 1.225 - 1.41\ conc + conc^2 + 5.83\ conc^3$

Low temperature condenser

ULTC1 = 1.20 - 0.920 conc

ULTC2 = 0.965 - 0.620 conc

ULTC3 = 0.765 - 0.380 conc

Low temperature evaporator

ULTE1 = 0.165

ULTE2 = 0.190

ULTE3 = 0.245

High temperature evaporator

UE1 = 0.236

$UE2 = 0.245 + 0.325\ conc - 0.75\ conc^2$

Heat exchangers

UHX1 = 0.09

UHX2 = 0.225

3.6.2 Condensing Temperatures

Temperature profiles for the condensers are shown in Fig. 3.10. The condenser inlet temperature, which is the discharge temperature of compressor, is a function of the inlet pressure and temperature to the compressor, the discharge pressure, and the compressor characteristics. A simple model for the outlet enthalpy from the compressor is used, namely

Hout = Hin + 0.9 * isentropic work.

This equation proposes that in addition to 10 percent of the isentropic work, all of the friction occurring during the compression is lost to the ambient. The simple equation is satisfactory for R-12 alone, but with 20 percent R-114 the simulated value is lower than experimental. Addition of R-114 to R-12 would be expected to reduce the compressor discharge temperature, because R-114 inherently has low discharge temperatures. The experimental tests

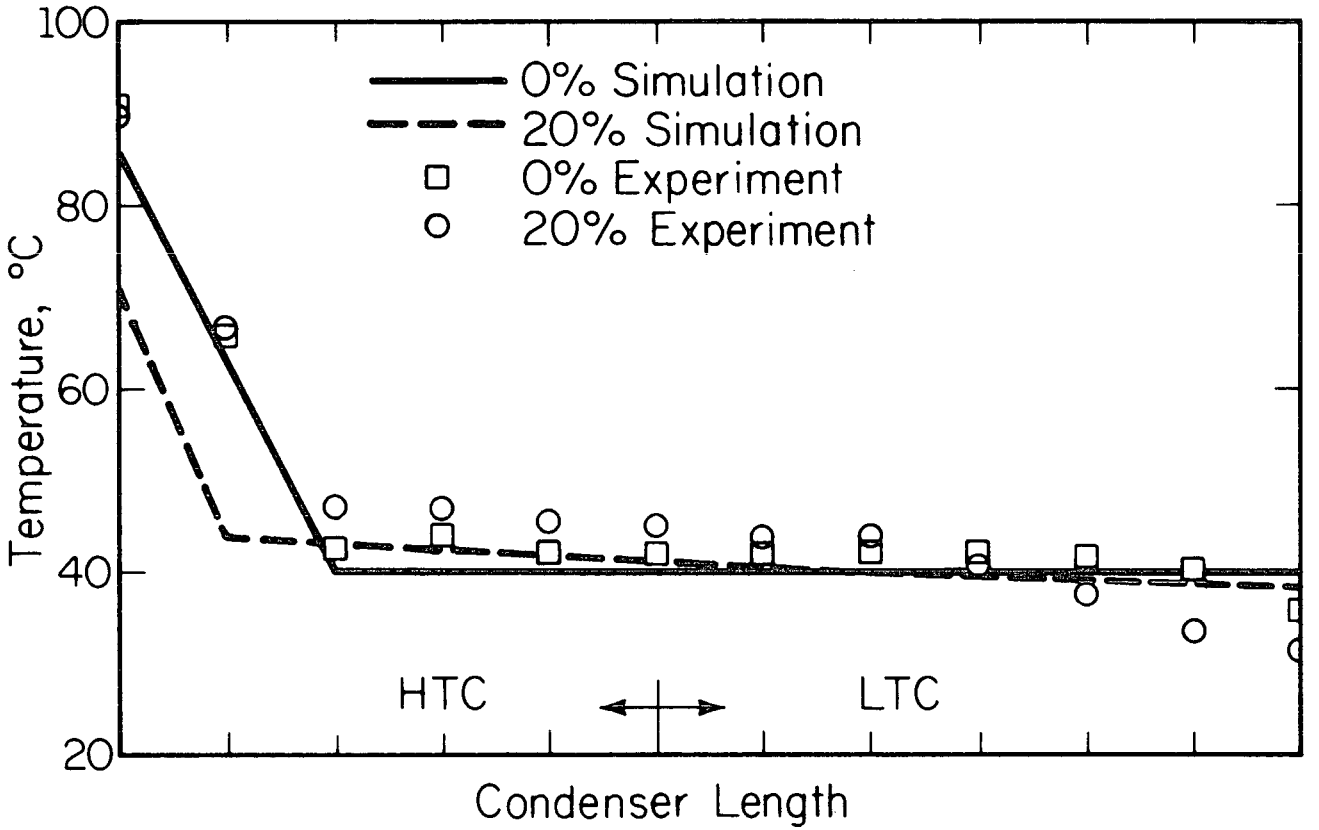

Figure 3.10 Comparison of simulated and actual refrigerant temperatures in condensers

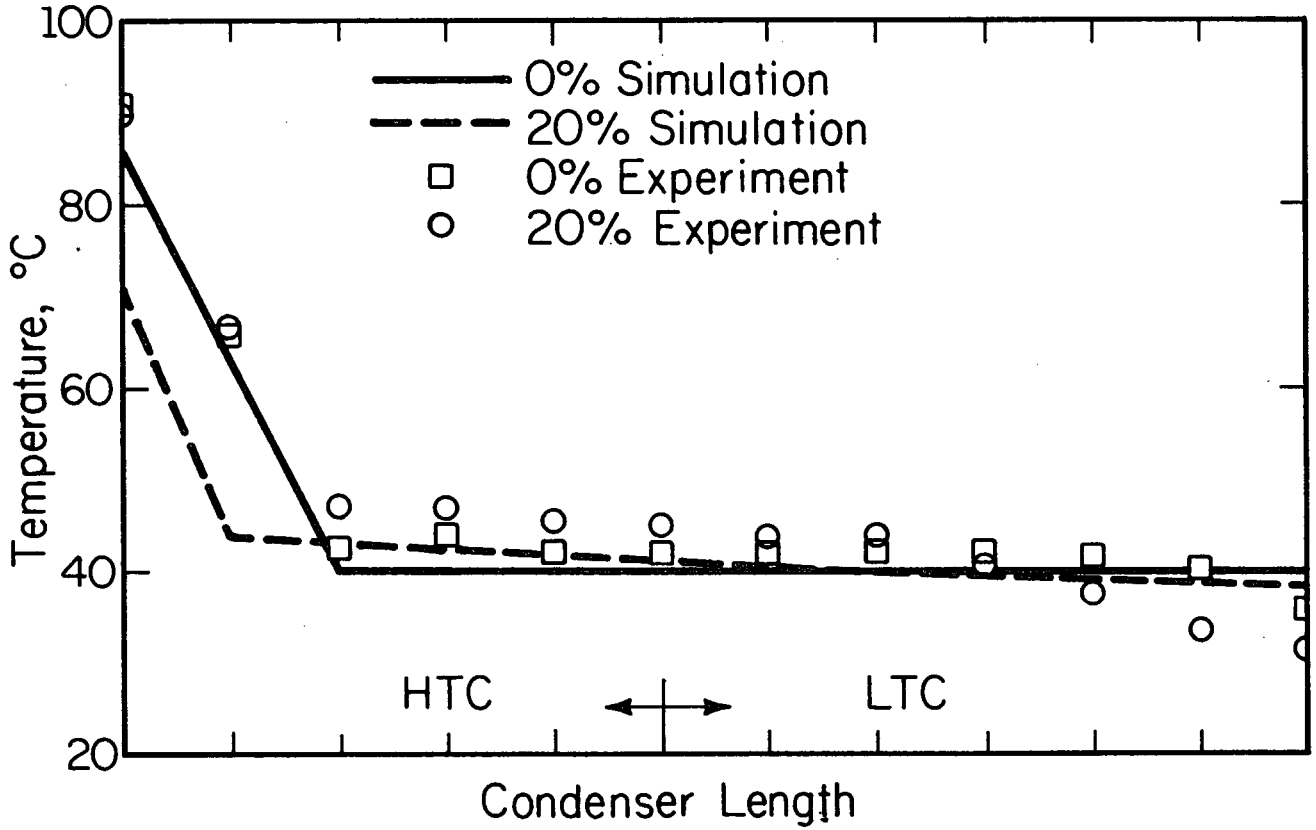

Figure 3.10 Comparison of simulated and actual refrigerant temperatures in condensers at several mass percentages of R-114

showed little difference between the discharge temperatures of 0 percent and 20 percent R-114 mixtures, probably because of the additional friction in the compressor because of the higher speed that was required.

The condensing temperatures match quite well but the simulated values are about 3°C too low. The experiments also show a small amount of subcooling, suggesting that even though it was attempted to operate with saturated liquid leaving the condenser, the liquid had to be subcooled if vapor bubbles were to be prevented from leaving the condenser.

3.6.3 Position at Which Condensation Begins

The simulation program should be able to predict the location in the condenser where desuperheating ends. Temperature profiles of the condensers show that the location of the start of condensation is between 1/6 and 1/3 of the length of the HTC. When the entering temperature to the condenser predicted by the simulation is correct the desuperheating area is also correct. At the 20 percent R-114 concentration when the simulation predicts too low an entering temperature the predicted onset of condensation is too early.

3.6.4 Evaporating Temperatures

Another parameter that the simulation should match is the evaporating temperatures. The temperature profiles for the evaporators are shown in Fig. 3.11. The simulation matches the evaporating temperature level well but predicts too much superheat leaving the evaporator at lower R-114 concentrations.

3.6.5 Superheat Boundary in the High-Temperature Evaporator

Some attempts were made to restructure the simulation program so that the point at which superheating began on the low-pressure side was in the HTHX. The simulation program would not converge with such a structure. This experience brought with it the realization that if superheating began in the HTHX the system was overspecified. With the refrigeration loads and temperature levels specified for both evaporators, each must be allowed a degree of freedom to satisfy its own heat-transfer relations. This situation was one where the simulation and the system experiments provided mutual

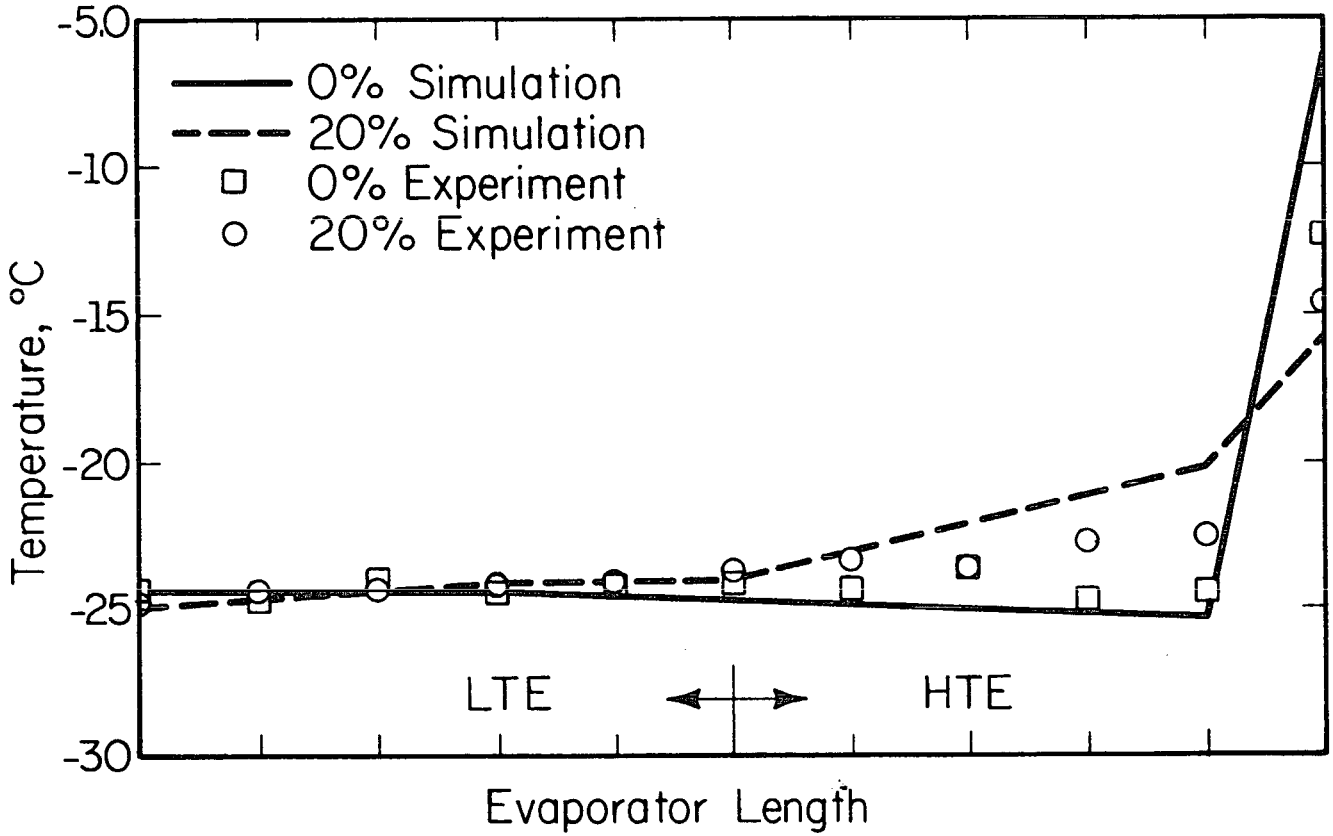

Figure 3.11 Comparison of simulated and actual refrigerant temperatures in evaporators at several mass percentages of R-114

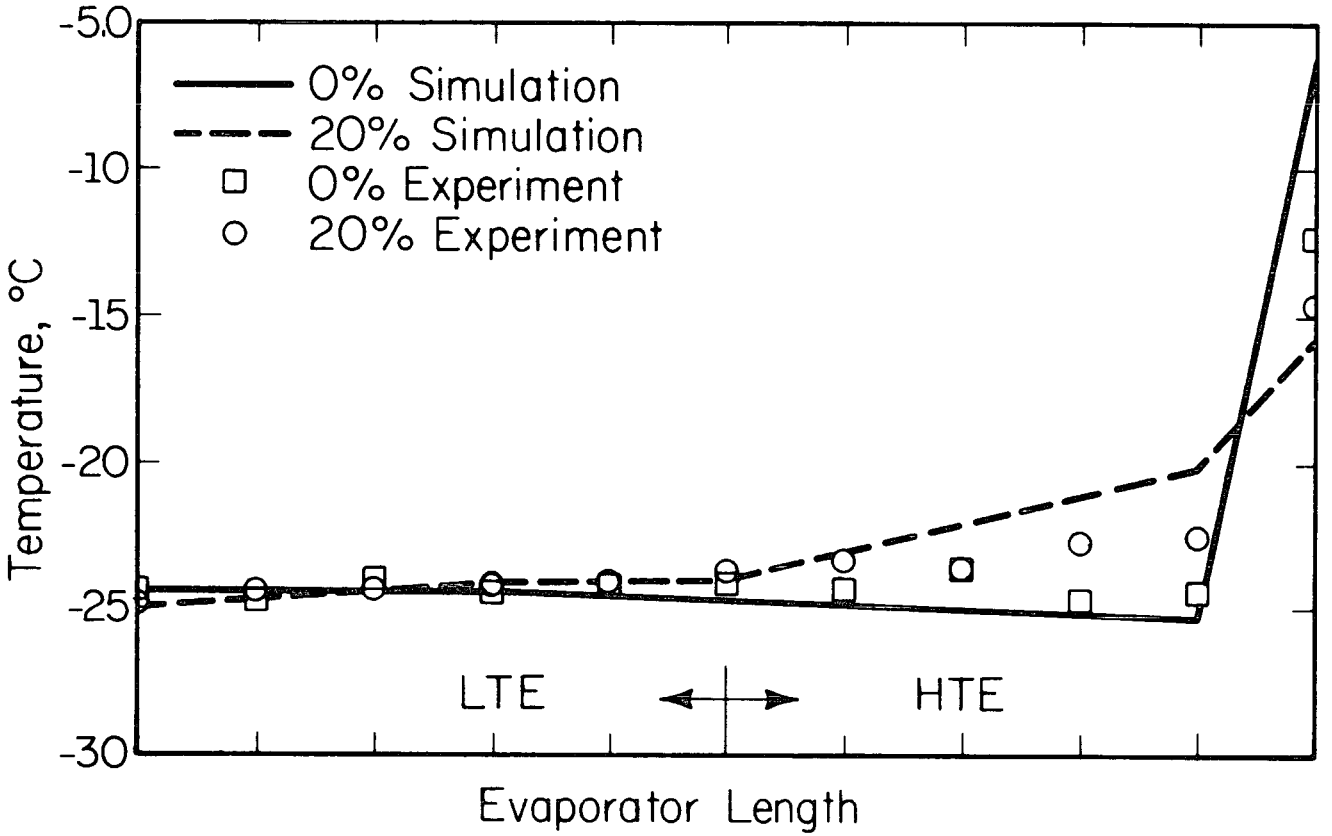

Figure 3.11 Comparison of simulated and actual refrigerant temperatures in evaporators

insight. We found early in the testing that the capacity and temperature level in the LTE was essentially controlled by the low-side pressure. The capacity of the HTE was predominantly regulated by adjusting the position of the point at which superheat began in that evaporator.

As the concentration of R-114 was increased in the mixture the refrigerant temperature level in the HTE progressively rose and to compensate for the lower mean-temperature-difference between the glycol and refrigerant, the point at which superheat began moved closer to the outlet of the evaporator. The simulation runs showed this trend, but further indicated that at a concentration of about 30% R-114 the superheat point was out of the HTE and into an impossible physical case. However, we had conducted tests above 30% R-114 concentration which we thought were valid ones. A re-examination of those tests, however, showed a slight drift in refrigeration capacity in the HTE at R-114 concentrations greater than 30%.

Further experiments have verified this observation. A sight glass was installed at the HTE outlet to allow a visual check of the refrigerant quality. With a 30 percent R-114/70 percent R-12 mixture, the superheat boundary was near the exit of the HTE, and the HTE target temperatures were difficult to maintain. With higher concentrations of R-114, these target conditions could not be met. At lower concentrations superheating began further back in the HTE and the target conditions were easily maintained.

3.6.6 Refrigerant Flow Rate

The simulated flow rate matches the experimental flow rate very well (Fig. 3.12). Both the simulated and experimentally measured flow rates increase slightly as the concentration of R-114 in the mixture increases. This trend is expected because the latent heat of R-114 is approximately 12-15% less than that of R-12, so the flow rate must increase at higher R-114 concentration to maintain a given refrigeration capacity.

3.7 Energy Savings Using Refrigerant Mixtures

One of the main purposes served by the simulation program is to provide greater insight into cycle performance. In particular, the 1978 simulation [8] predicted that a 12 percent power reduction could be achieved using a 50 percent R-114/50 percent R-12 mixture in comparison to using R-12 alone. The

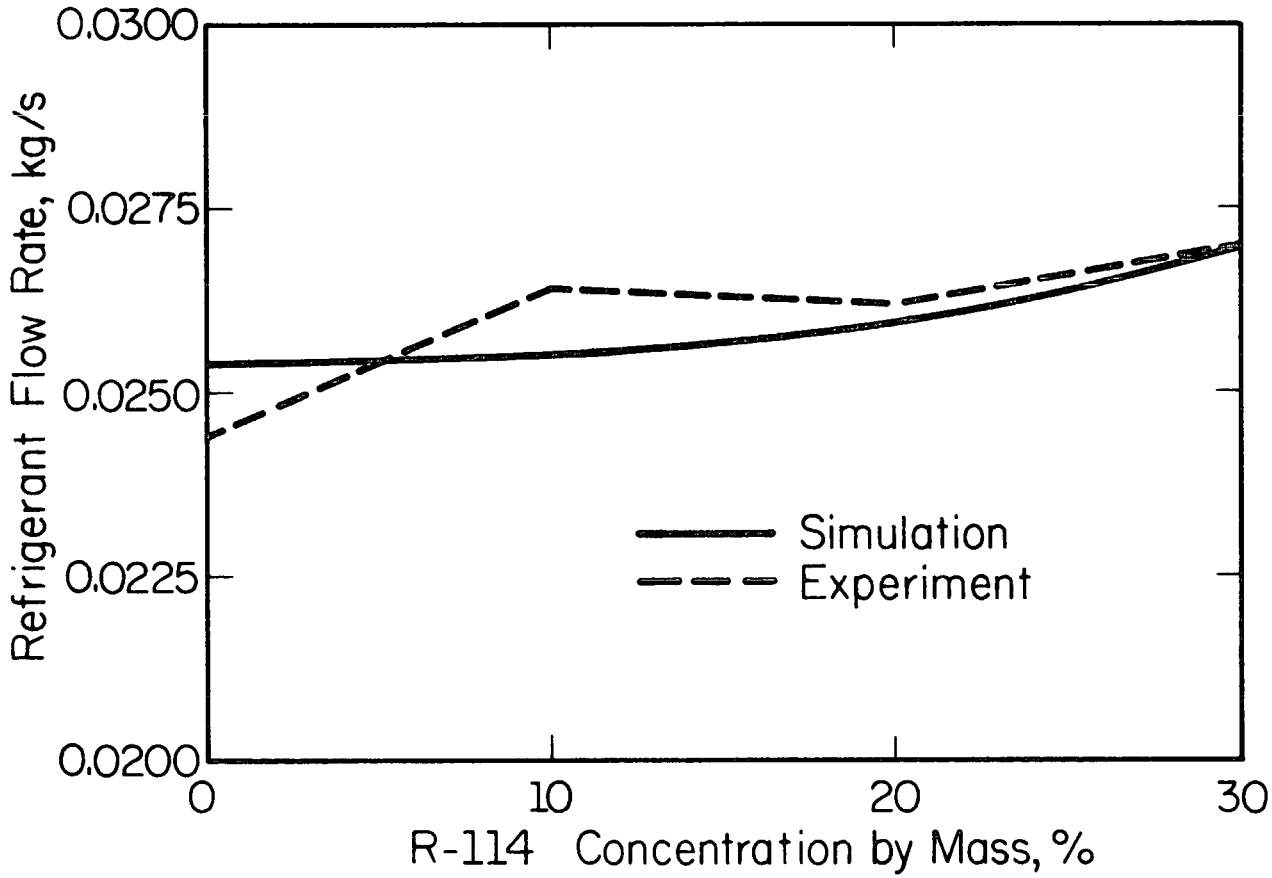

Figure 3.12 Comparison of simulated and actual refrigerant flow rate

experimental tests thus far have not attained that great a power reduction, so one of the present goals of the simulation was to explain why. An even greater benefit of the simulation program might be achieved if it could indicate directions to improve the actual amount of energy conservation.

The explanations provided by the simulation program are:

1. The impossibility of obtaining saturated vapor of the low-pressure refrigerant leaving the HTHX.
2. The reduction in heat-transfer coefficients as the concentration of R-114 increases.

The latest version of the simulation program is expected to be more accurate than previous versions because of improved refrigerant property representation and because of the more-realistic treatment of the heat-transfer performance of the condensers and evaporators. The heat transfer equations are now expressed for each pass of the condensers and evaporators, which provides a truer representation, especially for the portion of the condenser where desuperheating occurs and in the HTE and HTHX where superheating takes place. A further benefit of this partitioning is that a different heat-transfer coefficient can be used for each pass of the condenser and evaporator, substituting values derived from tests on the system.

A major reason for the reduction in the original energy savings prediction of 12 percent is that the amount of superheat in the HTE must be adjustable in order to achieve predetermined refrigeration capacities and temperature levels in both evaporators. This point was emphasized in Sec. 3.6.5. The simulation assumed saturated vapor leaving the HTHX, and the validity of the simulation was maintained by not specifying the temperature level (but only the heat-transfer rate) in the HTE. In refrigerant-mixture systems the cycle performance is improved by the use of refrigerant-to-refrigerant heat exchangers where boiling refrigerant on one side of the heat exchanger subcools liquid on the other side. Indeed, there was some subcooling of high-pressure refrigerant liquid in the experimental system because of the transfer of heat to vapor being superheated. The magnitude of subcooling was much less, however, than if the refrigerant were boiling on the low-pressure side.

Another explanation for the reduced energy conservation is because of the degradation of heat-transfer coefficients, the U-values, as the concentration

of R-114 increased in R-12. In order to determine the change in performance attributable to the reduction in heat-transfer coefficients, two simulations were made--one with constant U-values and the other with the U-values changed as a function of the refrigerant concentration. Those results are shown in Fig. 3.13. With constant condensing U-values, a 3.5 percent reduction in power is achieved at a 20 percent concentration of R-114 by mass in the R-12/R-114 mixture. With the actual U values the power reduction is 1.6 percent. The reduction in power is therefore penalized by about 2 percent due to the degredation in heat-transfer coefficients.

3.8 Summary of Equations Used in the Simulation Program

The simulation program is listed in APPENDIX II and below is a summary of the residual equations used to model the system.

	Equation number in simulation program
Fraction of liquid, FRLi	1-9
2 phase enthalpies	10-18
Vapor enthalpies	19-23
Saturation conditions	24-26
Liquid enthalpies	27-29
Heat exchanger rate equations	30-42
Refrigerant energy balances	43-56
Water or glycol energy balances	57-68
Compressor energy balance	69
Power, isentropic power	70,71
Calculation of U-value for superheating section of HTE	72
Volumetric efficiency	73
Vapor partial specific volumes	74-103
Rate equation on HTE, second pass	104
Refrigerant energy balance on HTE, second section	105
Glycol energy balance on HTE, second pass	106
Enthalpy at point 9A, in the HTE	107
Fraction of liquid at point 9A	108

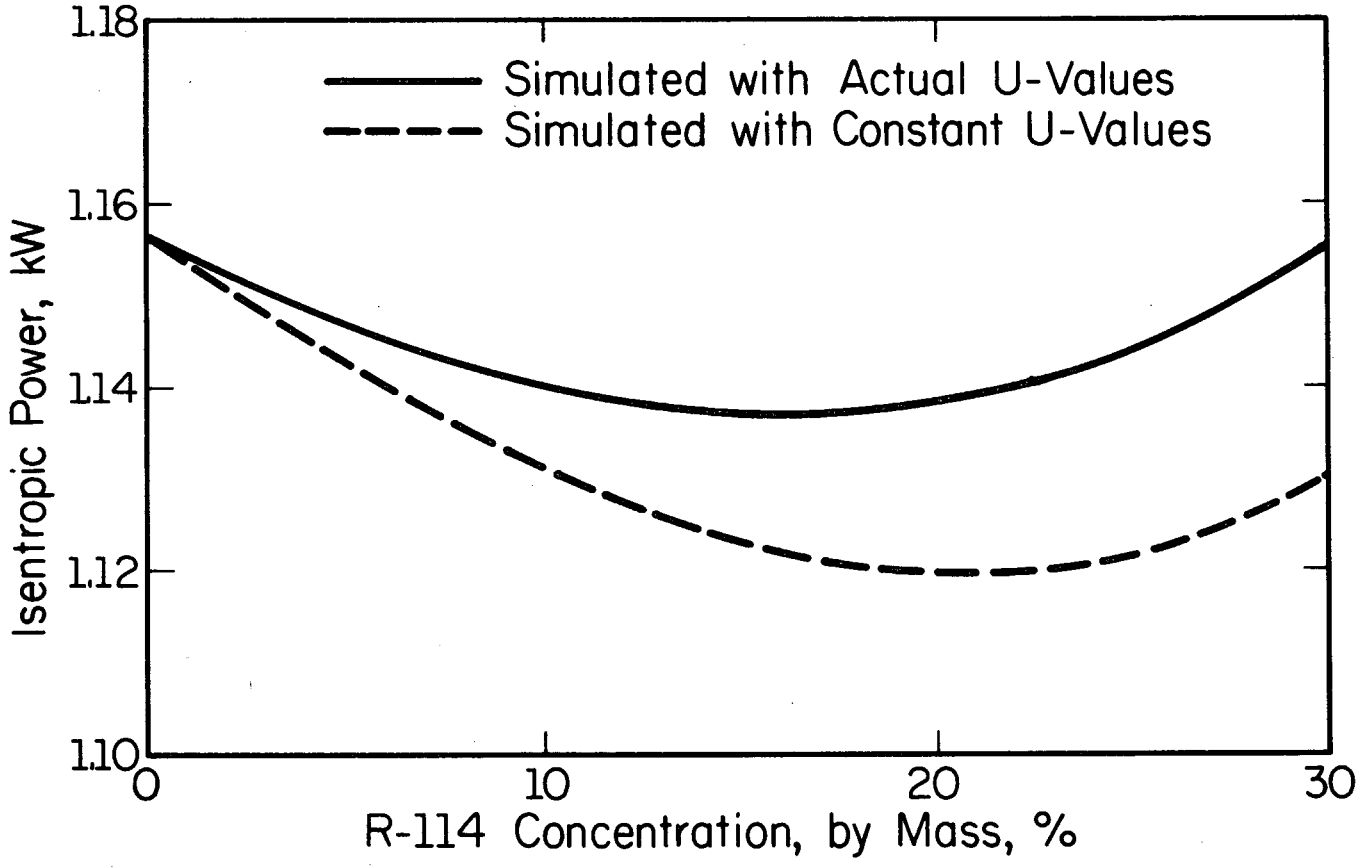

Figure 3.13 Isentropic compression power from simulation for actual U-values and constant U-values

4. PERFORMANCE OF THE ONCE-THROUGH CYCLE USING R-22/R-114 AND R-13B1/R-152a MIXTURES

4.1 Comparison of R-22/R-114 with R-12/R-114 Mixtures

In the initial phase of this project Stoecker (8) chose as working substances a mixture of R-12 and R-114. Some of the reasons for this choice were (1) the combination forms a nonazeotropic mixture, (2) the standard COP of refrigerants R-12 and R-114 when used separately are about the same, (3) there is a wide enough spread between the boiling temperatures of the two refrigerants so that the temperature change of evaporation or condensation is significant (order of magnitude of 10°C), and (4) the mixtures of R-12 and R-114 behave nearly as ideal mixtures. Reason (4) facilitated computation of mixture properties using only the properties of single substances as bases.

The standard COP of R-12 is 4.70 (page 16.9, ASHRAE Handbook of Fundamentals, 1981) at the evaporating temperature of -15°C and condensing temperature of 30°C, and R-22 and R-114 have COPs of 4.66 and 4.49, respectively. In choosing mixtures it was sought to find a combination of refrigerants with comparable COPs. Therefore, changes in concentration would have an effect due to the change in temperature through the two-phase region, and not because of the substitution of a higher COP refrigerant. The concentration of an R-22/R-114 mixture can be chosen to have the same vapor specific volume as R-12 alone, so a substitution can be made while keeping the refrigeration capacity unchanged.

A mixture that has a wide temperature spread between the boiling temperatures of the constituents at a given pressure may be advantageous. Mixtures with a wider spread between their boiling temperatures typically have a greater maximum temperature spread between the bubble point and the dew point, and mixtures of R-22 and R-114 have a wider spread than do R-12 and R-114. The temperature spread between the bubble point and dew point for a 40 percent R-22/60 percent R-114 at 500 kPa is 19°C, based on data provided by Cannon (10). In comparison, a mixture of 40 percent R-12/60 percent R-114 at the same pressure has a temperature spread is 8°C.

4.2 R-22/R-114 Properties

The dew point and bubble point temperatures for a 40 percent R-22/60 percent R-114 mixture at 500 kPa were determined assuming ideal mixing and also from Reference 10 which uses the Redlich-Kwong-Soave (RKS) equation of state. Table 4.1 shows the comparison.

Table 4.1 Dew-Point and Bubble-Point Temperatures for a 40 Percent by Mass R-22/60 percent R-114 mixture at 500 kPa using different mixing rules.

	Bubble point (°C)	Dew point (°C)	ΔT = DP-BP (°C)
Ideal mixing	14.1	33.3	19.2
DuPont table	11.6	30.6	19.0

The assumption of ideal mixing gave temperatures about 2.5°C higher than Reference 10 which is considered to be more accurate than the ideal mixture calculation.

4.3 R-22/R-114 Test Conditions and Results

The following conditions were specified for all R-22/R-114 tests.

Low-Temperature Evaporator

T40 = temperature of glycol out of LTE = -20°C
T35 = temperature of glycol into LTE = -15°C
glycol flow rate = 0.0639 kg/s

High-Temperature Evaporator

T54 = temperature of glycol out of HTE = -5°C
T50 = temperature of glycol into HTE = 0°C
glycol flow rate = 0.0637 kg/s
These conditions gave a load of 1 kW on each evaporator.

Condenser

Series flow of cooling water
T20 = temperature of inlet water = 30°C
cooling water flow rate = 0.0911 kg/s

To achieve these target conditions three parameters were varied: the compressor speed, the hand expansion valve setting, and the refrigerant charge to achieve saturated liquid at the outlet of the condenser.

4.4 Comparison of Temperature Profiles of R-22/R-114 and R-12/R-114 Mixtures

The maximum spread of temperatures between liquid and vapor at a given pressure occurs at 50% concentrations for both of these mixtures. A comparison of the maximum calculated change of temperatures and the experimentally measured changes in the LTE-LTHX-HTE are shown in Table 4.2.

Table 4.2 Maximum calculated and experimentally measured changes in temperature of 50% mixtures.

	R-12/R-114	R-22/R-114
Calculated	10	19
Experimentally measured	6	12

The rise in temperature from the inlet of the LTE to the estimated point where superheating began in the HTE was for both the R-12/R-114 and the R-22/R-114 mixture approximately half of the maximum predicted from the property equations. Two reasons for the lower temperature rise experimentally are (1) the pressure drop through the evaporators and LTHX, and (2) the fact that the liquid-vapor mixture was already partially vaporized after it left the expansion valve and entered the LTE. The actual rise in temperature with the R-22/R-114 mixture was almost twice that of the R-12/R-114 mixture, as the property calculations predicted.

There are two positions in the experimental system where the temperatures can be compared with calculated temperatures. The condition at the outlet of the condenser is slightly subcooled liquid, so the temperature there should be slightly below the bubble point temperature. Because of the nonequilibrium of

vapor/liquid temperatures in the condenser, some subcooling is needed in order to have a vapor-free liquid. The experimental temperature at the condenser outlet during the R-22/R-114 tests averaged 34°C. The bubble point temperature from the RKS equations was 36.1°C, indicating approximately 2°C of subcooling which is reasonable.

The condition at the outlet of the expansion valve should be slightly above the bubble point at the low-side pressure. The experimental temperature there averaged -33°C. The calculated temperature was -33.8°C which provides a good check.

4.5 Comparison of Compressor Power

The 50/50 mixture of R-22/R-114 was chosen for comparison with pure R-12 because the compressor speed was approximately the same for each case. With nearly equal compressor speed in our test facility a comparison of measured power is more meaningful because the power lost to mechanical friction is nearly constant, so the power measured on the dynamometer in the two cases can be compared directly. Table 4.3 shows the average speed, dynamometer load, and actual compressor power for R-12 alone and for the 50/50 mixture of R-22/R-114. The glycol temperatures and flow rates and condenser flow rates and inlet temperature were the same in all tests.

Table 4.3 Comparison of Compressor Power

	Speed (RPM)	Dynamometer load (lb)	Dynamometer power (kW)
R-12 Alone	613	11.7	1.33
R-22/R-114	633	12.0	1.42

The power determined from dynamometer measurements with the R-22/R-114 mixture was 7 percent higher than with R-12 alone, and some explanation must be sought for the lack of improvement when using the mixture. One of the explanations is that the condensing and boiling heat-transfer coefficients with the R-22/R-114 mixture are less than those of R-12 alone. The overall U-values of the condenser when applying R-22/R-114 were approximately 65 percent of those R-12 alone. The U-values of the mixture in the evaporators were from

60 to 80 percent of the of R-12 values. A different optimum mass flux may be warranted with R-22/R-114 compared to the system using R-12.

Another explanation may lie in the increased mixture temperature rise in the evaporators (drop in the condenser) compared to R-12 alone. The change of temperature in Table 4-2 which occurs during the phase change of R-22/R-114 in the condensers and evaporators is rather close to the temperature change of the external fluid--water for the condensers and glycol for the evaporators. The classic objective is to match changes of temperature of the refrigerant and the external fluid. When the superheating of refrigerant in the evaporator and desuperheating in the condenser are considered, however, it may be that there is increased irreversibility because the refrigerant temperature is now changing more than the external fluid.

Some comparative performance parameters are shown in Table 4.4.

Table 4.4 Comparison of Parameters Affecting Compressor Performance

	R-22/R-114	R-12 Alone
Suction pressure	104 kPa	105 kPa
Discharge pressure	1075 kPa	950 kPa
Pressure ratio	10.3	9.0
Mass flow rate of refrigerant	0.0177 kg/s	0.0177 kg/s
Specific volume at suction pressure	0.165 m^3/kg	0.152 m^3/kg
Volumetric efficiency	47%	45%

The suction pressures were nearly identical but the R-22/R-114 mixture had a higher head pressure so the pressure ratio was 14 percent higher with the mixture.

The mass flow rate for the mixture was the same as for R-12. However, the specific volume of the R-22/R-114 mixture was higher than that of R-12, and the volumetric efficiencies were almost the same, so the compressor speed with the mixture was 3 percent higher with the R-22/R-114 than with R-12.

4.6 Tests with R-13B1/R-152a Mixture

Cooper and Borchardt (4) chose a mixture of R-13B1 and R-152a as a combination possessing favorable characteristics for air-to-air heat pumps. A 70 percent R-13B1/30 percent R-152a mixture closely approximates the

refrigerating and heating capacity of R-22 and was therefore of particular interest, although Cooper and Borchardt conducted tests with compositions varying from 50/50 to 70/30 mass percent mixtures of R-13B1 and R-152a, respectively.

We charged the experimental facility with a 70 percent/30 percent mixture of R-13B1 and R-152a, respectively, and conducted several tests. The compressor and variable-speed dynamometer had been selected for R-12 and for the even-less-dense mixtures of R-12/R-114, so the torque with which the compressor loaded the motor was quite high. The speed was reduced in order to reduce the torque, but at too low a speed the motor would overheat. The facility thus permitted only a narrow band in which the dynamometer could be kept in operation. Any attempts to match refrigeration capacity and temperatures of tests with other refrigerants was not successful.

Some experimentally-measured temperatures could, however, be compared with property tables provided by the refrigerant manufacturer. Table 4.5 shows for the stated condensing and evaporating pressures the saturated vapor and saturated liquid temperatures from the property tables. These values may be compared with the measured temperatures into the LTE and at the estimated point where superheat begins in the HTE. Also shown is the estimated temperature where condensation begins and the temperature leaving the condenser. Because the mixture entering the LTE already has begun to vaporize, the measured temperature of -32°C is two degrees higher than that of saturated liquid, -34°C. The temperature estimated from the measured temperature profiles for the beginning of superheat checks with the tabular value. The estimated temperature where condensation begins is 37°C, which is close to the tabular value of 39°C. No doubt there was subcooling leaving the condenser, because the measured temperature of 26°C is lower than the value from the table for saturated liquid.

The change in temperatures in the evaporators and condensers with the 70 percent R13B1/30 percent R-152a is of the order of 7 to 9°C which is approximately the same as that experienced with the 50 percent R-12/50 percent R-114 mixture.

Table 4.5 Experimentally-Measured Temperatures and Temperatures from Property Tables of R-13B1/R-152a at the Evaporator and Condenser Pressures

Position	Pressure kPa abs.	Temperature, °C Measured	Tables
Entering LTE	223	-32	-34
Begin superheat in HTE	207	-23	-23
Begin condensation in HTC	1549	37	39
Leaving LTC	1519	26	32

5. SEPARATING CYCLE

5.1 Description of Separating Cycle

A separating cycle is one in which the nonazeotropic working fluid is separated into two branches that have different refrigerant concentrations. Because the two streams have different concentrations, they will evaporate at different temperatures, given the same pressure. In a domestic refrigerator, for example, the low temperature stream would feed the freezer compartment evaporator and the high temperature stream would feed the fresh food compartment evaporator. The separating cycle should be explored as a means of accomplishing the refrigeration duty with less energy than by a standard once-through cycle. The separating cycle is also a convenient cycle for exploring capacity modulation. Liquid may be stored in vessels of one or the other of the two branches to alter the concentration of the circulating mixture. Changing the concentration will change the mass-flow capacity of the compressor and thus change the system capacity.

The cycle used in the experiments is shown in Fig. 5.1 with the corresponding points shown on a T-x diagram in Fig. 5.2. Starting with superheated vapor at the compressor outlet, point 1, the HTC desuperheats the vapor and performs partial condensation to point 2. The fluid at point 2 is composed of a vapor, 2v, which is rich in R-12 and a liquid, 2L, which is rich in R-114. At point 2 the mixture enters the liquid receiver where the vapor and the liquid separate. The vapor stream condenses in the LTC to point 3 and then subcools in the LTHX to point 4. This liquid stream then passes through the LTE expansion valve to point 5, partially evaporates in the LTE to point 6, and completes its evaporation in the LTHX to point 7. The liquid stream at point 2L is subcooled in the HTHX to point 8 and then drops in pressure to point 9. Complete evaporation and some superheating occur in the HTE to point 10. The vapor is superheated further in the HTHX to point 11. The two vapor streams meet again at point 12 from which it is compressed to point 1.

5.2 Operating The Test Facility on Separating Cycle

The test facility was originally built to operate on a once-through cycle, but was modified during this phase of the project so that it would also operate on the separating cycle shown in Fig. 5.1. There are a few important

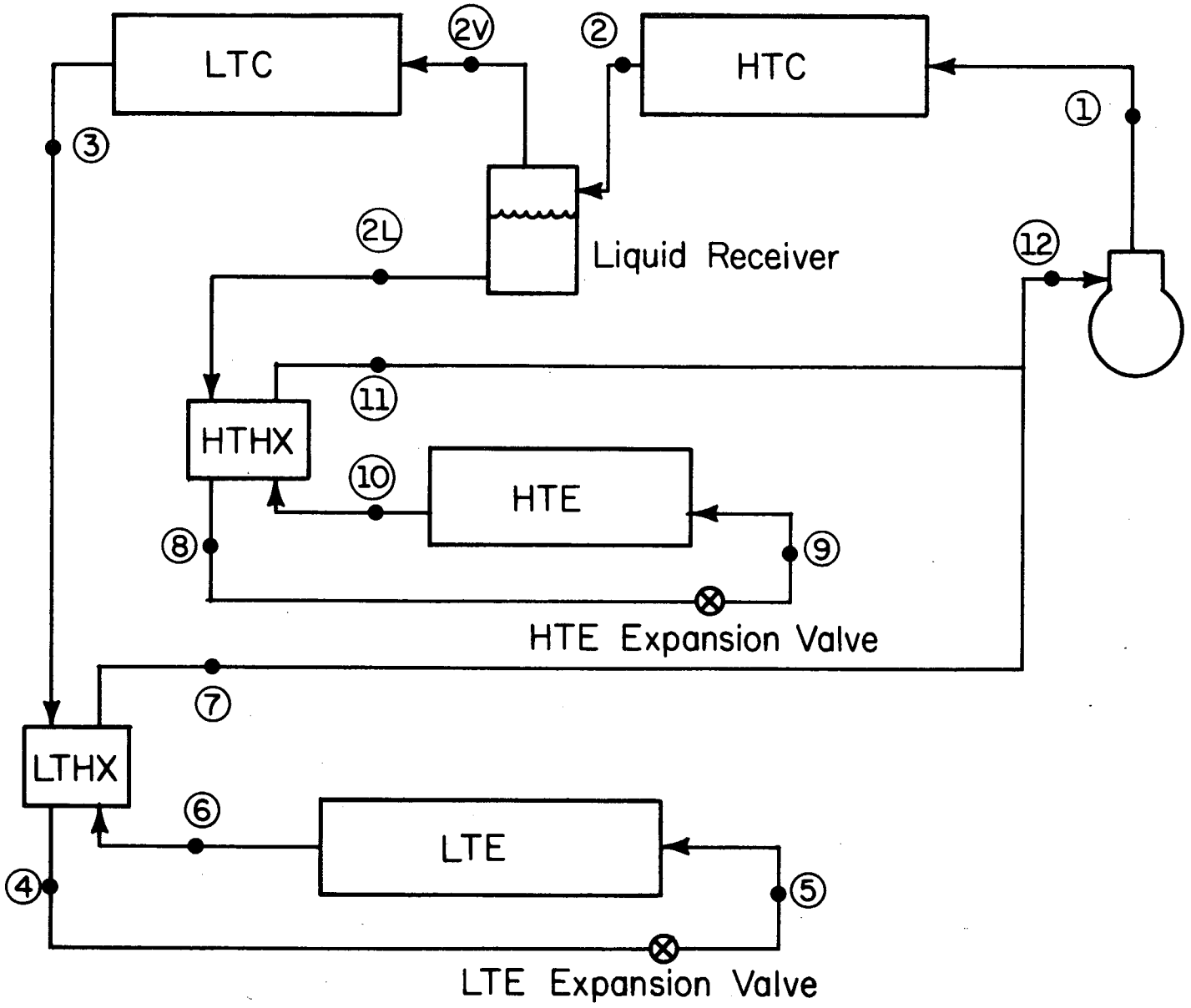

Figure 5.1 Diagram of separating cycle

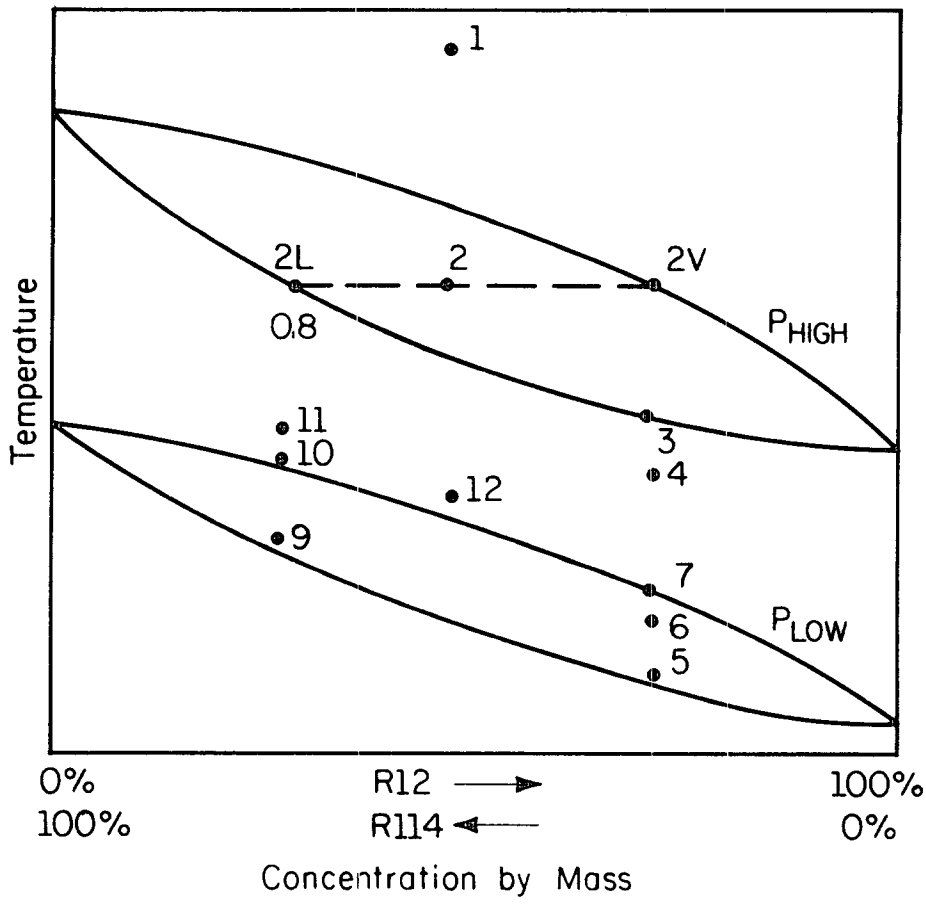

Figure 5.2 Temperature-concentration diagram for separating cycle

differences between operating the test facility on the separating cycle and operating on the once-through cycle.

5.2.1 Specifying Saturated Vapor Point

There is an additional degree of freedom with the separating cycle in comparison to the once-through cycle, because there are two expansion valves instead of one. Each expansion valve controls the location of the superheat boundary in the evaporator which it is feeding. In the once-through cycle which has only one expansion valve, the LTE was always flooded and superheating began somewhere in the HTE. The HTE glycol temperatures constrained the location where superheating began. In the separating cycle, the LTE and HTE refrigerant streams are controlled independently, so an additional condition must be specified in order to have a unique operating state. In the tests run so far we have specified the condition of saturated vapor at the outlet of the LTHX, point 7 in Fig. 5.1. In order to be able to specify the HTE glycol temperatures, specified superheating must begin in the HTE, as it did with the once-through cycle.

5.2.2 Condenser Water Flow

A problem encountered with the separating cycle was that if the temperature level of the water entering the LTC was not sufficiently lower than the HTC water temperature level, there would not be complete condensation in the LTC. As shown in Fig. 5.3, the refrigerant condensing temperature drops lower after separation occurs (2'-3') than with the once-through cycle where condensation proceeds straight through (2-3). In order to get complete condensation in the LTC, the tests were run with a high water flow rate through the LTC and a low flow rate through the HTC. In this manner the mean temperature of the water was kept low in the LTC and permitted the temperature of the water in the HTC to be higher.

There are other ways to meet the requirement of a wide range of temperature of condenser cooling fluid. If a system were designed to be used solely as a separating cycle, the LTC would have more area than the HTC, which would allow series coolant flow. Shifting condenser area has the same affect as having different flow rates. Another approach proposed by Kazacki (11) and Labochnik and Ceonov (12) is to expand part of the liquid from the liquid

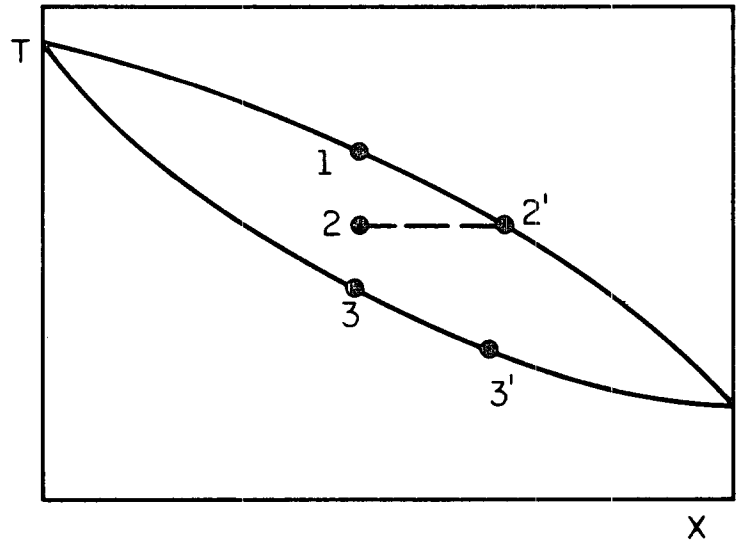

Figure 5.3 Temperature-concentration diagram showing condensation processes

receiver in the low temperature condenser which completes the condensation of vapor coming off the top of the liquid receiver.

5.3 Test Data

The data from three tests using the separating cycle with refrigerant mixtures are shown in APPENDIX III. Two of the tests were conducted with 50 percent R-114/50 percent R-12 and one with 25 percent R-114/75 percent R-12. The target conditions for these three tests were:

Condensers

T20 = 25°C = inlet water temperature
Water flow rate, LTC = 0.0909 kg/s
Water flow rate, HTC = 0.0261 kg/s
T7 = inlet to HTC = T23 = outlet of LTC
Water flow rate drained after passing through LTC = 0.0648 kg/s

Evaporators

LTE

T35 = -15°C = glycol temperature in
T40 = -20°C = glycol temperature out
Glycol flow rate = 0.0640 kg/s

HTE

T50 = 0°C = glycol temperature in
T54 = -5°C = glycol temperature out
Glycol flow rate = 0.0640 kg/s

Refrigerant-to-refrigerant heat exchanger

Small amount of suction gas superheat after LTHX, (T27 = T34 + 5°C)

These target conditions result in the same refrigeration duty (heat-transfer rate and temperatures) as for one series of once-through cycle tests. The condenser water flow rates are different, however, for the separating and once-through cycles. In the separating cycle 0.0909 kg/s is passed through the LTC, but only 0.0261 kg/s continues through the HTC. Furthermore, in the separating cycle tests the entering condenser-water temperature was 25°C rather than 30°C, in order to achieve full condensation in the LTC.

5.4 Temperature Profiles

For convenience, the temperatures measured in one of the tests (Test 97) are displayed on the cycle diagram, Fig. 5.4. For the temperatures and pressures measured in the test, the R-114 concentration in the vapor leaving the liquid receiver was computed to be 33 percent. The liquid had an R-114 concentration of 58 percent. These conditions are shown in Fig. 5.5. Evaporator temperatures, plotted in Fig. 5.6, cover a range of -35.0°C to -29.1°C in the LTE and -27.6°C to -7.7°C in the HTE with superheating beginning at approximately -20°C. Because of the characteristics of the separating cycle, there is a greater temperature rise from the inlet of the LTE to the saturated vapor point in the HTE than there is in the once-through cycle. In Test 97 there was a 15°C rise while the rise in the typical once-through cycle with 50 percent R-114 was 8°C. The condensing temperatures are plotted in Fig. 5.7. The profile shows that there is an 18°C drop through the condensing region, whereas a typical 50/50 percent mixture in the once-through cycle shows a 10°C drop.

The temperatures of the 50/50 percent mixture in Table 5.1 may be compared with those of the 25/75 percent mixture. The refrigerant temperature levels in the LTE are comparable with both mixtures as are the temperatures in the HTE. This situation is expected, because the same rate of heat transfer to glycol at identical temperatures is required. It is observed, however, that the rise in refrigerant temperature in the LTE is less with the 25/75 percent mixture than with the 50/50 percent mixture. The reason is because of the overall concentration shift as shown in Fig. 5.1. As the concentration shifts to the right the vapor, which is the source of the LTE refrigerant, will have a low concentration of R-114. Having a high concentration of R-12 results in a small temperature change between the bubble-point and dew-point lines.

The 25/75 percent mixture experiences higher superheat leaving the compressor, which is probably attributable to two causes. One is that the essential characteristic of R-114 is that its lines of constant entropy do not bend as far into the superheat region as R-12. Another observation is that the compression ratio is less with the 50/50 mixture--11.6 vs. 13.1 for the 25/75 percent mixture. The significance of this observation is that the separating cycle can achieve a given refrigeration duty with a lower

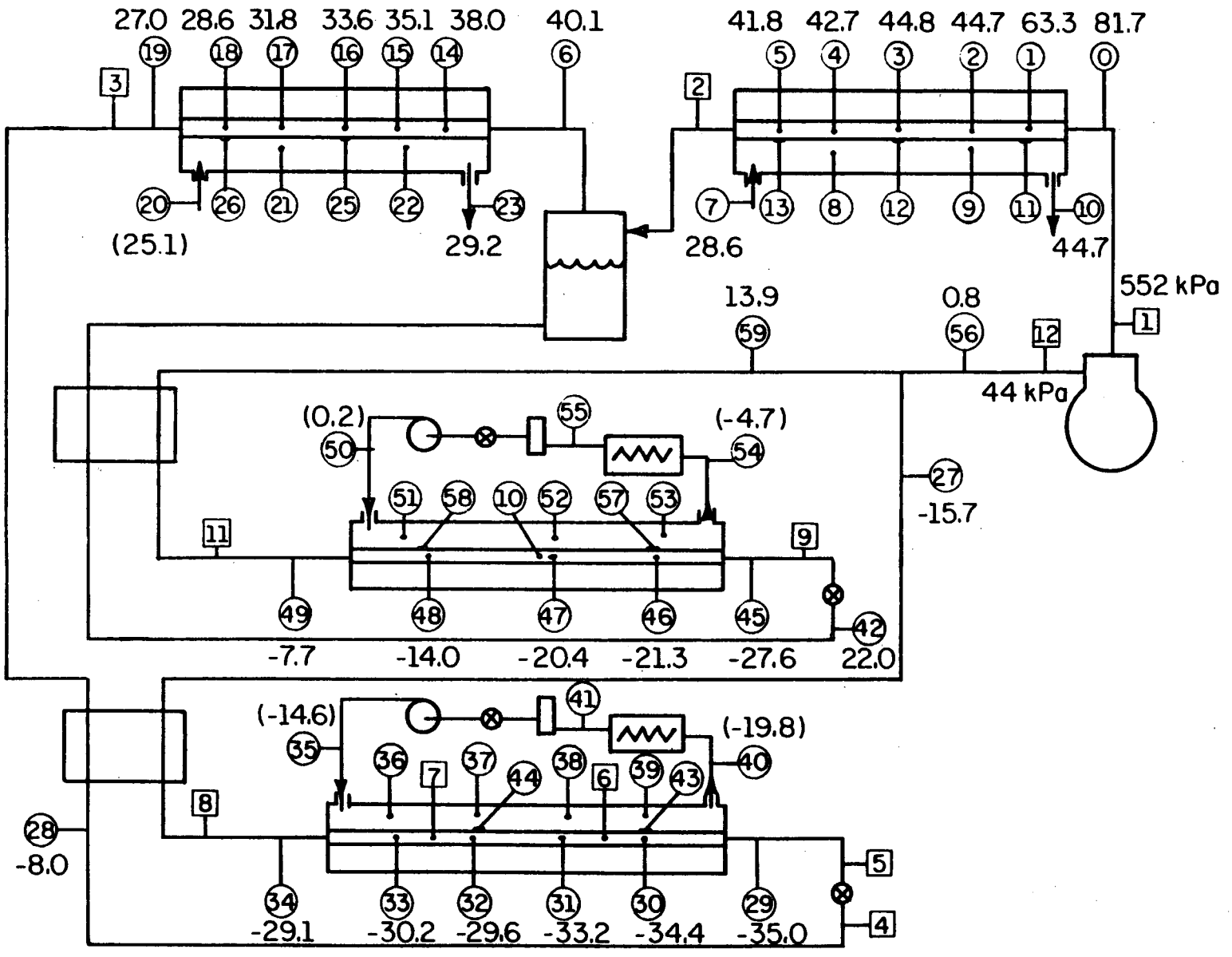

Figure 5.4 Separating cycle showing temperatures (°C) from Test 97

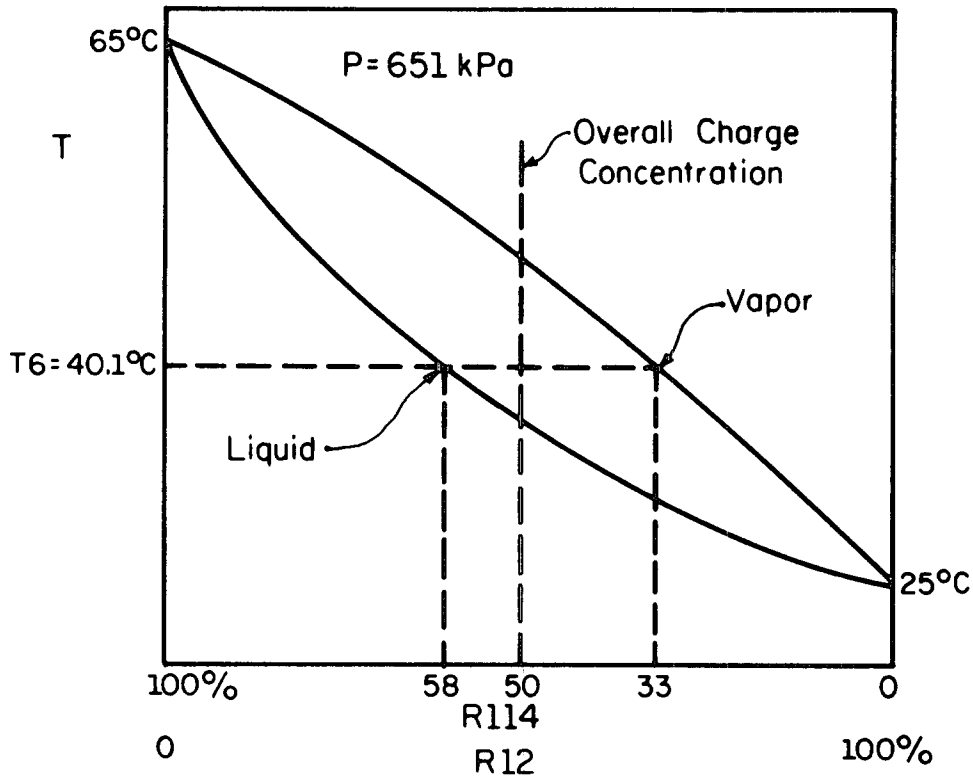

Figure 5.5 Temperature concentration diagram showing separation in condenser

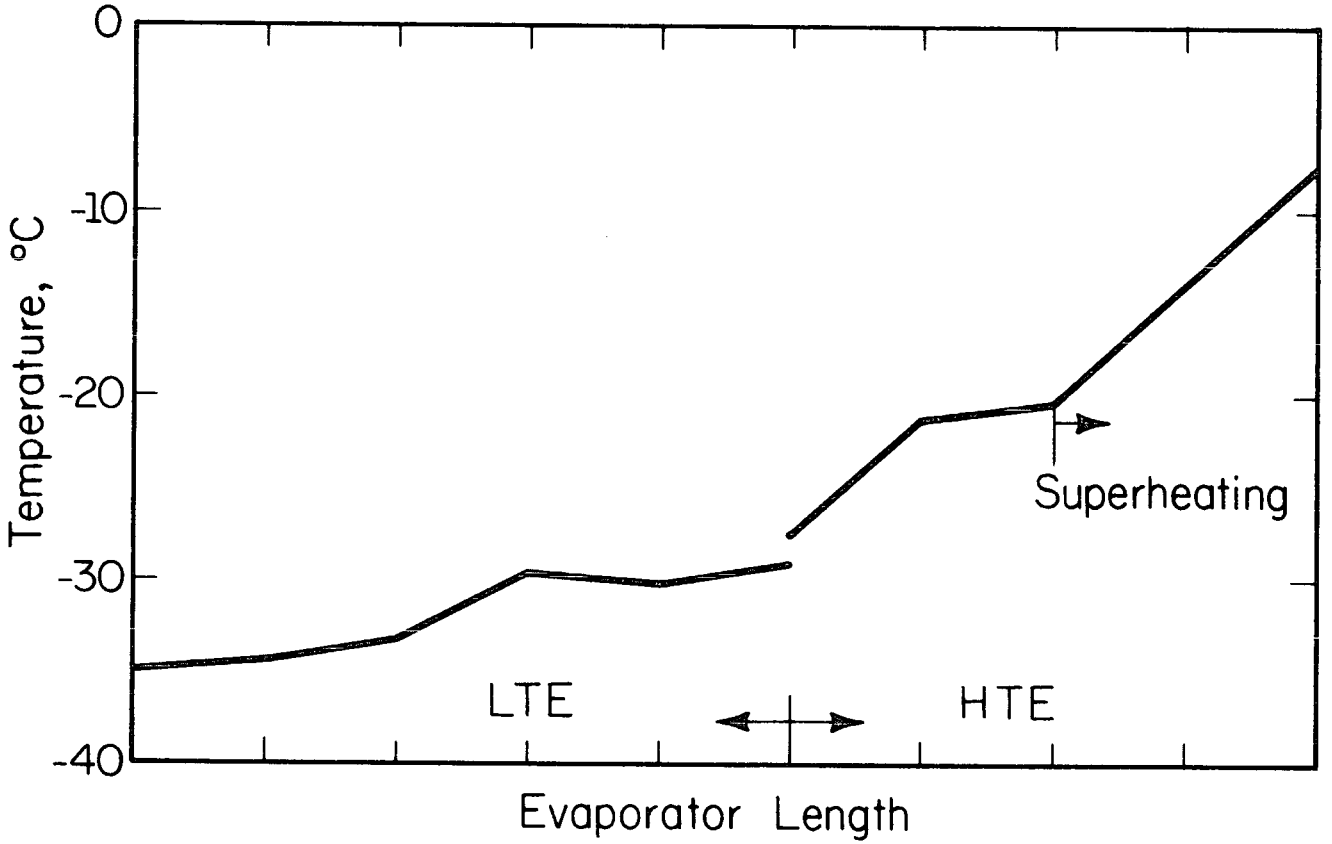

Figure 5.6 Evaporator temperature profile for separating cycle

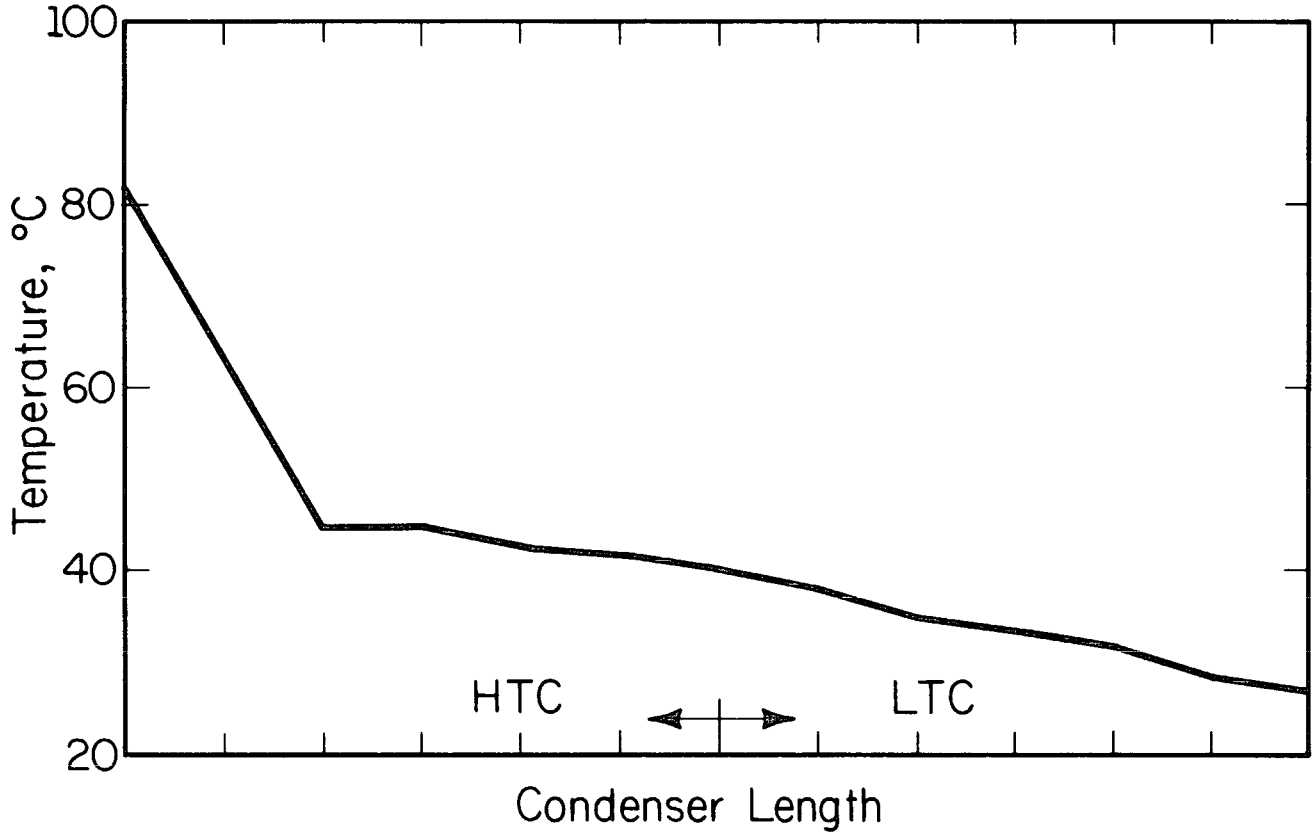

Figure 5.7 Condensing temperatures in the separating cycle

compression ratio than a nonseparating cycle. This property may be important for systems using reciprocating compressors.

5.5 Compressor Power Comparisons

The greater temperature rise in the evaporator is advantageous thermodynamically, but this cycle has not proven that it will save energy over a once-through cycle using R-12. The isentropic power for the separating cycle using 50 percent R-12/50 percent R-114 was 3 percent higher than for the once-through cycle with pure R-12. The isentropic power for the once-through cycle tests was 0.73 kW compared to 0.75 kW for the 50/50 separating cycle tests. The refrigerant mass rate of flow through the compressor was 8 percent higher in the separating cycle but the enthalpy rise across the compressor was lower. However, caution is urged when comparing this set of separating cycle tests with the once-through cycle tests. Even though the duty was identical, the condenser water flow was different. The inlet water was 5°C cooler for the separating cycle but the full flow was used only in the LTC.

6. CONCLUSIONS

6.1 Scope of this Study

The research covered in this report addresses three main topics: (1) refinement of a simulation program to match the experimentally-measured behavior of a once-through, two-evaporator refrigeration system, (2) exploration of two additional refrigerant pairs, R-22/R-114 and R-13B1/R-152a, and (3) experimental study of the operation of nonazeotropic mixtures in a separating cycle. The underlying theme of the entire project is the achievement of energy-savings by using refrigerant mixtures in refrigeration systems. The experimental results thus far have not demonstrated substantial savings that could be attributed to the thermodynamics of nonazeotropic mixtures. The most attractive energy-conserving potential provided by refrigerant mixtures continues to be enhancing heating capacity in a heat pump at low ambient temperatures. The work described on the separating cycle in this report is a contribution to that continuing development.

6.2 Comparison of Experimental and Simulated Results with a Once-Through, Two-Evaporator System

Simulation is the prediction of the operating variables of a system (temperatures, pressures, mass and energy flow rates, etc.) when the component performance, properties of working substances, and values of the imposed parameters are known. Simulation is often used in the design stage when not all of the above conditions are accurately known. In this study, however, the experimental system was in place and measurements of the operating variables are available. With such an advantage the component performance can be refined until the simulated results match the experimental behavior. Further insight was obtained about this particular cycle during the comparison. Deciding which variables can be specified in the simulation and which should be free to float has its counterpart in operating the system. Specifically, the fact was reinforced that the refrigeration capacity and the temperature levels of the fluid being chilled in both evaporators could be controlled only if there was some superheating in the HTE. The failure of the simulation program when superheat did not exist led to a re-examination of experimental data, which confirmed this observation.

The need for a certain amount of superheating in the HTE has further significance in explaining why the energy savings are in the range of 2-to-4 percent rather than the 12 percent predicted in the initial phase of this project. With some superheat required in the HTE, the HTHX could only provide superheating of the refrigerant on the low-pressure side. The early simulation postulated saturated vapor at the outlet of the low-pressure side of the HTHX.

Because of the different regimes of boiling in the evaporator and condensation in the condenser, it was necessary to simulate these two heat exchangers as a series of heat exchangers, each with its own heat-transfer coefficient. Having refined the simulation program to incorporate partitioned heat exchangers, it was then possible to introduce the experimentally-measured heat-transfer coefficients, which are a function of the refrigerant concentration. The simulation program is then able to identify the magnitude of the cycle efficiency reduction due to the degradation of heat-transfer coefficients with mixtures in comparison to single refrigerants. Were it possible to maintain constant heat-transfer coefficients in the condensers and evaporators, there would be a 3.5 percent energy saving using an R-12/R-114 mixture in comparison to R-12 alone. Because of the reduction in heat-transfer coefficients when shifting to a mixture, the energy saving realized is of 2 percent.

6.3 Other Combinations of Refrigerants

Two other combinations of refrigerants in addition to the R-12/R-114 mixture were explored in this phase, R-22/R-114 and R-13B1/R-152a. Because R-22 and R-114 have a wide spread of boiling temperatures at a given pressure, they can form mixtures with changes of temperature during boiling or condensation as large as 19-20°C. R-22 is a polar and R-114 a nonpolar refrigerant, so equations of state using ideal mixing are not adequate to describe their behavior. While the test system was not designed to make or confirm property measurements, there was a closer agreement between experimentally measured T-x-p points and properties computed from the Redlich-Kwong-Soave equation than to properties determined from ideal relations.

The rise in temperature of the boiling refrigerant in the evaporators closely matched the drop in temperatures of the glycol being chilled. This

condition is favorable, because it should result in the minimum thermodynamic irreversibility. Experimental power measurements, however, showed no efficiency improvement of the R-22/R-114 mixture over R-12 alone. Two reasons are advanced -- one is that the heat-transfer coefficients measured with the R-22/R-114 mixture were less than those using either R-12 alone or the R-12/R-114 mixture. A second possibility is that when the superheating in the HTE and HTHX are considered, the rise in temperature of the refrigerant was much greater than the drop in the glycol temperature. The matching of temperature changes of refrigerant and glycol, then, may not have occurred at all.

6.4 Separating Cycle

The experimental facility was revised to convert the once-through cycle to a separating cycle with two branches, each operating with a different mixture concentration. One characteristic of the separating cycle feeding two evaporators is that there is a large temperature spread between the refrigerant temperatures in the two evaporators. There may be application for this wide spread of temperature. Another inherent characteristic of the separating cycle is that the temperature between the dew-point in the HTC and the bubble point in the LTC is so great that complete condensation in the LTC may be difficult. This problem can be solved by permitting the entire high-side pressure to rise, but with the attendant energy penalty. The problem can possibly be solved by proper design of condensers for the separating cycle, or by performing the final stage of condensation in a heat exchanger with evaporating refrigerant on the other side.

6.5 Capacity Modulation Using the Separating Cycle

The study of the separating cycle was preliminary and may offer energy advantages attributable to the thermodynamics of the cycle. An extension of the separating cycle may suggest another concept for changing the refrigerant concentration to adjust capacity. Figure 6.1 shows a reservoir installed on the low-pressure side, and the active mixture concentration could be changed by shifting would be to shift liquid from the separator to the reservoir or vice versa. Liquid collected in the separator is rich in R-114, while liquid collected in the reservoir is richer in R-12 than the liquid in the

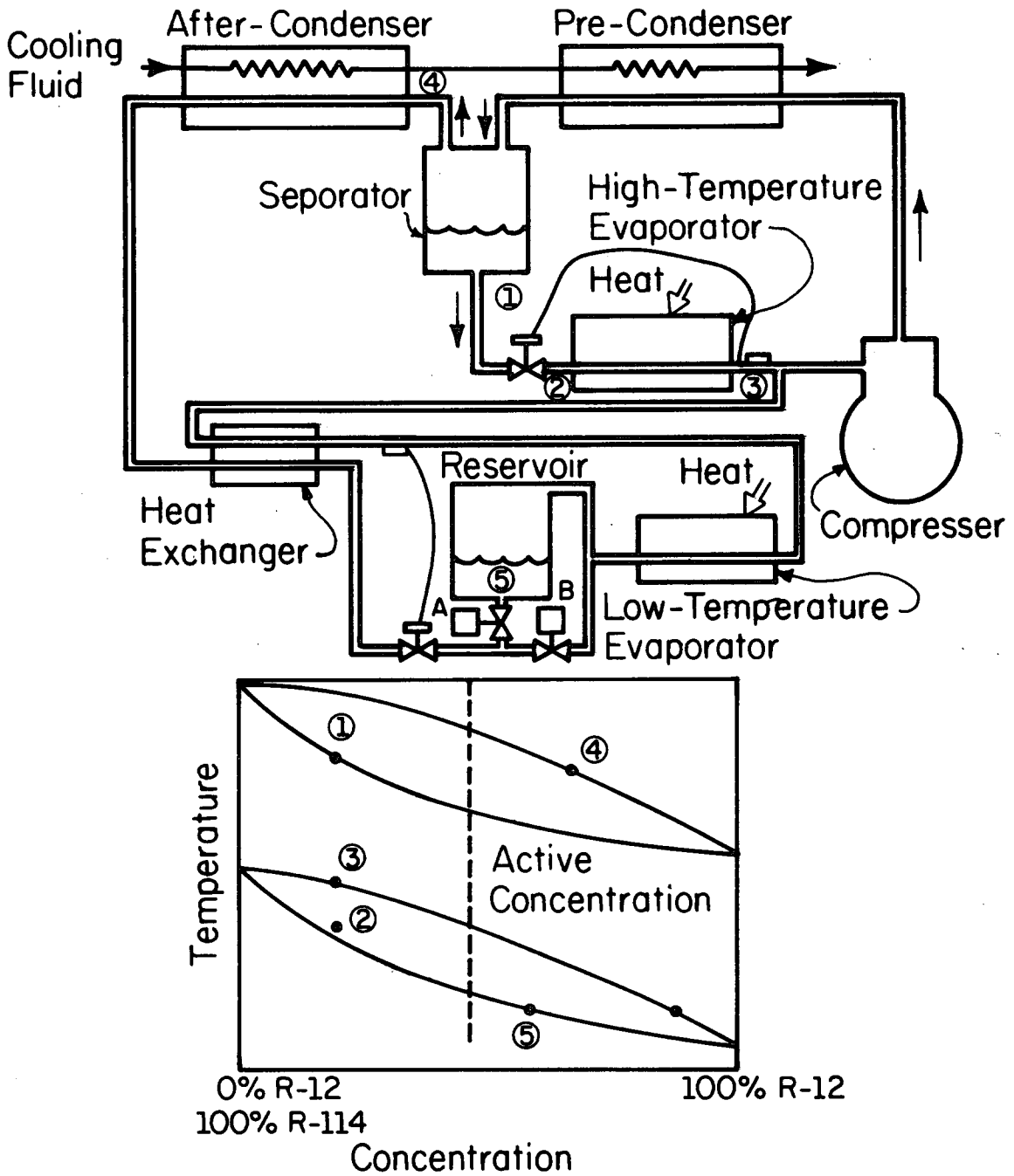

Figure 6.1 Separating cycle used for capacity modulation--two evaporators

separator. Shifting liquid to the separator increases the refrigeration capacity, because the mixture circulating through the compressor is richer in R-12 than before. Shifting liquid to the reservoir decreases capacity. Figure 6.1 is a two-evaporator system, while the capacity-modulating method might be possible for a single-evaporator system, such as a heat pump, by using a cycle similar to that shown in Fig. 6.2. The final condensation in this cycle is performed by an evaporator that boils a mixture of high R-114 concentration. The concept of shifting liquid between the separator and reservoir can provide a rapid means of adjusting the capacity.

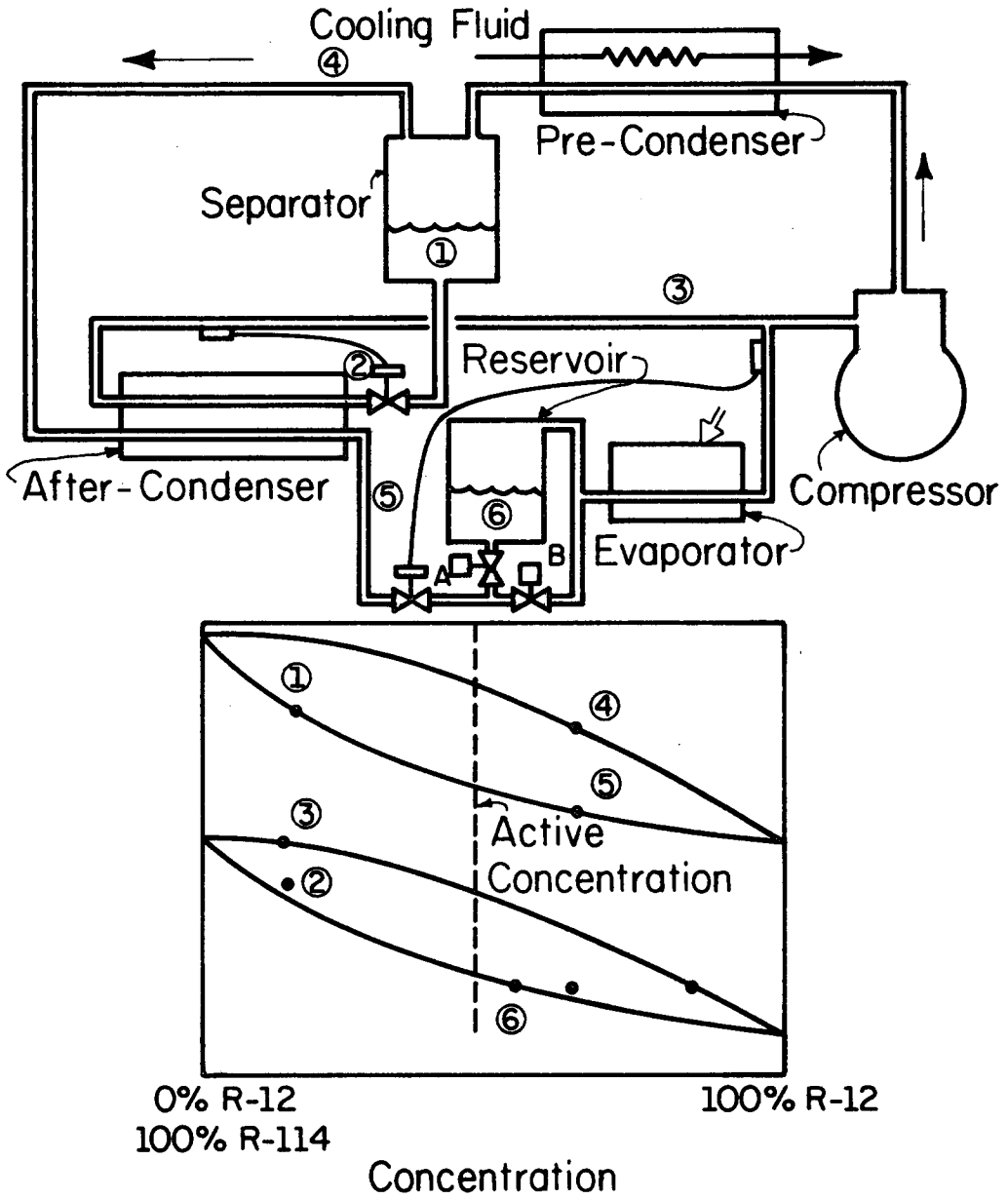

Figure 6.2 Separating cycle used for capacity modulation--single evaporator

APPENDIX 1. OPERATING PROCEDURE

The following operating procedure was used to conduct the tests on the two system:

Startup

1. Draw brine sample from each evaporator and record specific gravity and temperature.
2. Connect the six isothermal input cards to the datalogger.
3. Check that all ball valves are in the proper position for either the separating cycle or the once-through cycle, see check list.
4. Close both compressor bypass hand valves.
5. Open condenser water inlet valve.
6. For separating cycle, open HTE flow meter bypass valve and close the valve in series with the flow meter.
7. For separating cycle, open LTC water flow valve and set flow rate. Open preheater bypass completely. Leave HTC water flow valve closed for now.
8. For once-through cycle, open just HTC water flow valve for series condenser flow and set to target value.
9. Turn on glycol pumps and set desired flow rates.
10. Close both expansion valves.
11. Start dc generator set and compressor. Set speed to approximately 500 rpm.
12. Weigh out R-114 on scale.
13. Set scale to level after correct amount has been added.
14. Open charging valve and add refrigerant until balance levels.
15. Repeat steps 12 through 14 for R-12 or R-22.

Running

16. Prepare ice bath for T-24.
17. Connect frequency counter and power supplies to flow meters.

Separating Cycle

(This section pertains only to running the separating cycle. See next section for once-through cycle.)

18. Open HTE expansion valve enough to flood HTE but not compressor.
19. Initially open the LTE expansion valve two or three turns.

20. When liquid to LTE is subcooled, slowly open HTC water valve to desired flow rate.
21. After HTC has water flow, close the water preheater bypass part way to raise the inlet water to target temperature.
22. When liquid to HTE is subcooled, first open the valve in series with the HTE flow meter and then slowly close the flow meter bypass valve. (The 213 meter should not be operated with a two-phase flow, especially in the plug flow regime. The meter may be damaged if the liquid contains vapor.)
23. When glycol temperatures are near target values, turn on the heater and adjust the variable transforms so the desired temperature spread is maintained.
24. Adjust LTE expansion valve so that LTHX is almost flooded (i.e. T27 = T34 + 5°C.)
25. Adjust compressor speed to achieve LTE glycol target temperatures.
26. Adjust HTE expansion valve to achieve HTE glycol target temperatures. The action taken in one of the three previous steps will influence the conditions in the other two so all three must be worked together to achieve all target conditions.
27. Monitor condenser conditions and keep at target values.

Once-Through Cycle

(Skip this section if running the separating cycle.)

28. Open the expansion valve to get the flow rate near the expected value. It will take time for the liquid to flood through the LTE and into the HTE.
29. When glycol temperatures get near target values, turn on the heater and adjust the variable transformer so the desired temperature spread is maintained.
30. When LTE is flooded, adjust compressor speed to bring down LTE glycol temperatures to target values.
31. When HTE glycol temperatures pull down near target values, adjust expansion valve to attain HTE glycol target temperatures. (Superheating should begin in the HTE.) The action taken in one of the two previous steps will influence the conditions in the other so both steps must be worked together to achieve all target conditions.
32. Monitor condenser conditions and keep at target values.

Shutdown

33. Close expansion valve(s).
34. Reduce compressor speed to minimum and then stop. Turn off dc generator set.
35. Keep glycol pumps running and heaters on until glycol warms above 0°C to prevent local freezing.
36. Shut off condenser water inlet valve.
37. Shut off condenser water flow valve(s).
38. Turn variable transformer on heater down to minimum, then shut off power to the variable transformer.
39. Turn off glycol pumps. Disconnect datalogger, frequency counter, and power supply.

Valve Positions

	Separating Cycle	Single-Train Cycle
BV1	closed	open
BV2	open	closed
BV3	open	closed
BV4	open	closed
BV5	closed	open
BV6	open	closed
HV7	closed	open
BV8	open	closed
BV9	closed	open
BV10	open	closed

APPENDIX II.
LISTING OF SIMULATION PROGRAM

APPENDIX

Simulation Program Listing

```
PROGRAM OAK84 -- EXTENSION OF SIMUL7

 PROGRAM SIMUL7(TAPE1,OUTPUT,TAPE6=OUTPUT)
 ****************************************

 LATEST REVISIONS MADE: FEB,84

 THIS PROGRAM SIMULATES THE PERFORMANCE OF A 2-CONDENSER,
 2-EVAPORATOR, 2-HEAT EXCHANGER VAPOR COMPRESSION REFRIGERATION
 SYSTEM USING MIXTURES OF R-114 AND R-12.  IT IS BASED ON WORK
 DONE BY PHILIPPE LAUNAY DURING COMPLETION OF HIS MASTERS THESIS
 AT THE UNIVERSITY OF ILLINOIS IN 1980. THIS VERSION INCLUDES
 VARIABLE HEAT TRANSFER COEFFICIENTS, VARIABLE PRESSURE DROP,
 AND THE HEAT EXCHANGERS HAVE BEEN BROKEN INTO PASSES.
  FOR FLOW DIAGRAM OF SIMULATED SYSTEM INCLUDING VARIABLE
 DEFINITIONS, SEE "PERFORMANCE OF NON-AZEOTROPIC MIXTURES OF
 DICHLORODIFLUOROMETHANE (R-12) AND DICHLOROTETRAFLUOROETHANE
 (R-114) IN A VAPOR COMPRESSION REFRIGERATION SYSTEM"
 C. I. MCCARTHY, MASTERS THESIS, UNIVERSITY OF ILLINOIS 1983

   GLOSSARY OF TERMS USED IN SIMUL7
   --------------------------------

 V()=SYSTEM VARIABLE
 DSE()=DESIGNATION OF VARIABLE
 R()=RESIDUAL EQUATION
 PD(X,Y)=PARTIAL DERIVATIVE OF X WRT Y
 VCORR()= CORRECTION IN THE VARIABLE DURING THIS ITERATION
 VD()=V+DELTA V
 RD()=R EVALUATED AT VD
 DAT()=DATA PARAMETER (IMPOSED TEST CONDITION)
 DATNAME()=NAME OF DATA PARAMETER
 DATUNIT()= UNITS  "   "      "
 UNITV()=    UNIS OF VARIABLE
 NVAR= NUMBER OF VARIABLES
 TLRNCE=LIMIT OF THE MAX CHANGE IN A VARIABLE BETWEEN
    ITERATIONS TO TEST FOR CONVERGENCE
 ITMAX=MAX NUMBER OF ITERATIONS

 ********************************************

 DIMENSION V(110),DES(110),R(110),PD(110,110),VCORR(110),VD(110),
*  RD(110),DAT(18),DATNAME(18),DATUNIT(18),UNITV(110)

 INTEGER DAMPING,FOPTION
 COMMON DAT


  NVAR=108
  TLRNCE=0.001
  ITMAX =10

 THESE NEXT VARIABLES ARE REQUIRED BY SUBROUTINE SIMUL.
  DAMPING = 0
  FOPTION=0
  ITER=0

C     READING THE TRIAL VALUES STORED IN INPUT FILE (WHEN RUNNING
C     ON CYBER "/LGO,INPUTFILENAME,OUTPUTFILENAME")
```

```
      REWIND 1
      READ (1,10)
      READ (1,12) (DATNAME(I),DAT(I),DATUNIT(I),I=1,16)
      READ (1,10)
      READ (1,11) (DES(I),V(I),UNITV(I),I=1,NVAR)

*****OPTIONAL PRINTOUT OF INPUT FILE INFORMATION
      PRINT 19,(K,DATNAME(K),DAT(K),DATUNIT(K),K=1,18)
      PRINT 17,(I,DES(I),V(I),UNITV(I),I=1,NVAR)


      LOOP REPUNS SIMULATION STEPPING UP CONCENTRATION (DAT(1)) 5%
      EACH TIME. TRIAL VALUES FOR THE NEXT RUN ARE THE CONVERGED
      VALUES FOR THE PREVIOUS RUN.

      DO 30 L=1,11
      CALL SIMUL(NVAR,TIRNCE,ITMAX,V,DES,R,PD,VCORR,VD,RD,DAMPING,
     *  PCETION,ITER)
      PRINT 20,ITER,(K,DATNAME(K),DAT(K),DATUNIT(K),K=1,16)
      PRINT 17,(I,DES(I),V(I),UNITV(I),I=1,NVAR)
      IF(ITER.EQ.10) GOTO 77
      DAT(1)=DAT(1)+.050
0     CONTINUE

77    STOP
   10 FORMAT (/)
   11 FORMAT (9X,A5,2X,F21.5,3X,A5)
   12 FORMAT(20X,A5,2X,F8.4,3X,A5)
   17 FORMAT(108(3X,"V(",I3,") = ",A5," = ",F21.5,3X,A5,/)/)
   19 FORMAT(/,"1",4X,"VALUES FROM INPUT FILE",/,5X,27(**),/)
     * /,16(10X,"DAT(",I2,") = ",A4," = ",F8.4,3X,A5,/))
   20 FORMAT(/,10X,"AFTER",I3," ITERATIONS SOLUTION IS:",/
     * 10X,32(**)/16(12X,"DAT(",I2,") = ",A5," = ",F8.4,3X,A5/)/)
      END


      SUBROUTINE EQNS(NVAR,V,R)
      *************************
      THIS SUBROUTINE CONTAINS ALL OF THE EQUATIONS THAT DESCRIBE THE
      SYSTEM.

      GLOSSARY OF TERMS USED IN SUBROUTINE EQUATIONS
      ----------------------------------------------

      HTE= HIGH TEMP EVAPORATOR
      LTE= LOW TEMP EVAPORATOR
      HTC= HIGH TEMP CONDENSOR
      LTC= LOW TEMP CONDENSOR
      HX1= REFRIGERANT TO REFRIGERANT HEAT EXCHANGER NO 1
      HX2=      "        "        "        "      "      NO 2


      W= REFRIGERANT FLOW RATE        (KG/S)
      PHI=PRESSURE AT COMPRESSOR DISCHARGE     (KPA)
      PLC=     "     "     "       SUCTION      (KPA)
      T1=TEMP AT POINT 1            (C)
      T2= "    "   "   2            (C)
      T2P= "   "   "   2P (SUPERHEAT BOUNDARY IN HTC)    (C)
      TN=  "   "   "   N            (C)
      HN=ENTHALPY AT POINT N        (KJ/KG)
```

```
FRLN=FRACTION OF LIQUID AT POINT N

QLTC= HEAT TRANSFER RATE IN LTC    (KW)
QHTC=   "      "        "   " HTC    (KW)

TCHP= TEMP OF WATER OPPOSITE POINT 2P   (C)

AHTE= HEAT TRANSFER AREA OF HTE    (M**2)

TELO= TEMP OF GLYCOL LEAVING LTE   (C)
TEHE=   "   "   "    OPPOSITE 10F   (C)
TEHO=   "   "   "    LEAVING HTE    (C)
TCLC=   "   " WATER      "     LTC   (C)
TCHO=   "   "  "         "     HTC   (C)

POWR= POWER REQUIRED BY COMPRESSOR     (KW)

V2N= PARTIAL VOLUME OF R-12 AT POINT N    (M**3/KG)
V4N=    "        "    "  R-114 "   "   N    (M**3/KG)

ETAV=        "      VOLUMETRIC EFFIENCY

E12= WORK OF ISENTROPIC COMPRESSION FOR R-12     (KW)
E114=  "   "   "                    "      "  R-114    (KW)

TELAVG= AVERAGE TEMP IN LTE    (C)
TEHAVG=    "        "   " HTE    (C)

CPGL= SPECIFIC HEAT OF GLYCOL IN LTE    (KJ/KG-C)
CPGH=    "        "   "    "     " HTE    (KJ/KG-C)
CPWA=    "        "   " WATER            (KJ/KG-C)

ACC= AREA OF HTC THAT IS CONDENSING  (M**2)
ADSH=  "   "  "    "   " DE-SUPERHEATING  (M**2)

U--- = OVERALL HEAT TRANSFER COEFFICIENT FOR ---   (KW/M**2-K)
UA--- = PRODUCT OF U AND A FOR ---     (KW/K)

AEHTE= AREA OF HTE THAT IS EVAPORATING    (M**2)
ASH=     "   "  "    "   " SUPERHEATING   (M**2)

*****************************************************

    IMPOSED PARAMETERS
   ------------------

CONC= CONCENTRATION OF R-114 IN R-12  (MASS FRACTION)

ALTE= HEAT TRANSFER AREA OF LTE     (M**2)
AHX1=   "      "        "   " HX1     (M**2)
AHX2=   "      "        "   " HX2     (M**2)
ALTC=   "      "        "   " LTC     (M**2)
AHTC=   "      "        "   " HTC     (M**2)
AHTE=   "      "        "   " HTE      (M**2)

WGEL= FLOW RATE OF GLYCOL IN LTE     (KG/S)
WGEE=   "     "   "     "     " HTE    (KG/S)
WLTC=   "     "   " WATER IN LTC      (KG/S)
WHTC=   "     "   "   "     " HTC     (KG/S)
```

```
TCLI= TEMP OF INLET WATER TO LTC    (C)
TEII=   "   "   "   GLYCOL TO LTE   (C)
TEHI=   "   "   "     "     " HTE   (C)
TEHC=   "   " OUTLET  "     " HTE   (C)
TELC=   "   " OUTLET  "     " LTE   (C)
*************************************************

  VARIABLES
 -----------

PN= PRESSURE AT POINT N    (KPA)

X= DUMMY VARIABLE (MOLE FRACTION OR MASS FRACTION)

XCLN= MOLE CONCENTRATION OF LIQUID R-114 AT POINT N

XLN= MASS FRACTION OF LIQUID R-114 AT POINT N
XVN=   "      "      " VAPOR    "   "   "   N

XCV10P= MOLE CONCENTRATION OF VAPOR AT POINT 10P
XCV2P=    "        "        "   "   "   "   2P

HLN= ENTHALPY OF LIQUID AT POINT N (IN 2 PHASE REGION)   (KJ/KG)
HVN=    "     " VAPOR   "   "   N (IN 2 PHASE REGION)   (KJ/KG)

PP4H= PARTIAL PRESSURE OF R-114 ON HIGH SIDE      (KPA)
PP2H=    "        "    "  R-12   "   "   "       (KPA)
PP4L=    "        "    "  R-114  " LOW SIDE      (KPA)
PP2L=    "        "    "  R-12   "   "   "       (KPA)
PP4L10=  "        "    "  R-14   AT POINT 10     (KPA)
PP2L10=  "        "    "  R-12   "   "   10      (KPA)

PLC2PSI= "        "    "  R-12 ENTERING COMPRESSOR    (PSI)
PLC4PSI= "        "    "  R-114   "            "      (PSI)
*************************************************************

   INLINE FUNCTIONS
 ----------------------

H12L(T)=     "     " R-12  LIQUID    (KJ/KG)
H114L(T)=    "     " R-114    "      (KJ/KG)

MOLFRAC(X)= MOLE FRACTION OF X
MASFRAC(X)= MASS FRACTION OF X

XCL(P,T)= MOLE FRACTION OF LIQUID R-114 IN 2 PHASE REGION
XCV(P,T)=   "      "       " VAPOR  R-114  " "   "    "

C2N1(T,P) , C2N2(T,P)  FUNCTIONS USED TO CALCULATE ISENTROPIC
                       WORK FOR R-12- DERIVED FROM TABLES
WIR12= ISENTROPIC WORK OF COMPRESSION FOR R-12

C4N1(T,P) , C4N2(T,P)  FUNCTIONS USED TO CALCULATE ISENTROPIC
                       WORK FOR R-114 - DERIVED FROM TABLES
WIR114= ISENTROPIC WORK OF COMPRESSION FOR R-114
****************************************

END OF GLOSSARY
```

```
      ***************************************************
      IMPLICIT REAL (A-Z)
      INTEGER NVAR,I
      DIMENSION  V(NVAR),R(NVAR),DAT(18)


      COMMON DAT
-----INLINE FUNCTIONS
C     LIQUID ENTHALPIES
      P. LAUNAY 1980.

      H12L(T) =200. + .9251*(T) + .00081*(T)**2 + .0000048*(T)**3
      H114L(T)=200. + .9545*(T) + .00116*(T)**2 + .000003*(T)**3
C     MASS FRACTION AND MOLE FRACTION

      MOLFRAC(X)=(X)/(1.4135 - 0.4135*(X))
      MASFRAC(X)=1.4135*X/(1.+0.4135*X)
C     CONCENTRATION IN LIQUID AND VAPOR PHASES

      XCL(P,T)=(P-PSAT12(T)) / (PSAT114(T)-PSAT12(T))
      XCV(P,T,X)=PSAT114(T)*X/P
-----WORK OF ISENTROPIC COMPRESSION FOR R12 & R114
      P. LAUNAY 1980.

      C2N1(T,P)=(T + 273.15)*((.6933E-1 + .232E-4*T) +
     *          (-.2019E-4 + .757E-7*T)*P)
      C2N2(T,P)=(T + 273.15)*((.414E-2 - .148E-4*T) +
     *          (-.876E-5 + .231E-6*T)*P)
      WIR12(T,P1,P2)=(C2N1(T,P1) + C2N2(T,P1)*ALOG(P2/P1))*ALOG(P2/P1)
      C4N1(T,P)=(T + 273.15)*((.4949E-1 + .36E-5*T) +
     *          (-.3024E-4 + .4083E-6*T)*P)
      C4N2(T,P)=(T + 273.15)*((.75E-3 + .285E-4*T) +
     *          (.428E-5 + .365E-6*T)*P)
      WIR114(T,P1,P2)=(C4N1(T,P1) + C4N2(T,P1)*ALOG(P2/P1))*ALOG(P2/P1)

C      REDEFINING V(I) TO MAKE EQUATIONS EASIER TO UNDERSTAND

      W    =V(1)
      PHI  =V(2)
      PLO  =V(3)
      CDHTC=V(4)
      CCC1=V(5)
      CCC2=V(6)
      CLTC1=V(7)
      CLTC2=V(8)
      CLTC3=V(9)
      CLTE1=V(10)
      CLTE2=V(11)
      CE1=V(12)
      CSH=V(13)
      ACC1=V(14)
      AE2=V(15)
```

```
FOWR=V(16)
IPCWR=V(17)
BPM=V(18)
PTAV=V(19)
FRI2E=V(20)
FRI3=V(21)
FRI3A=V(22)
FRI3E=V(23)
FRI7=V(24)
FRI7A=V(25)
FRI7E=V(26)
FRI8=V(27)
FRI9=V(28)
T1=V(29)
T2=V(30)
T2P=V(31)
T2E=V(32)
T3=V(33)

T3A=V(34)
T3E=V(35)
T4=V(36)
T5=V(37)
T6=V(38)
T7=V(39)
T7A=V(40)
T7E=V(41)
T8=V(42)
T9=V(43)
T10=V(44)
T10E=V(45)
TCHE=V(46)
TCHP=V(47)
TCHC=V(48)
TCIP=V(49)
TCLA=V(50)
TCIC=V(51)
TEIP=V(52)
TELA=V(53)
CITE=V(54)
TEHP=V(55)
CHTE=V(56)
H1=V(57)
H2=V(58)
H2P=V(59)
H2B=V(60)
H3=V(61)
H3A=V(62)
H3P=V(63)
H4=V(64)
H5=V(65)
H6=V(66)
H7=V(67)
H7A=V(68)
H7P=V(69)
H8=V(70)
H9=V(71)
H10=V(72)
H10E=V(73)
V21=V(74)
V41=V(75)
```

```
      V22=V(76)
      V42=V(77)
      V22E=V(78)
      V42E=V(79)
      V22B=V(80)
      V42B=V(81)
      V23=V(82)
      V43=V(83)
      V23A=V(84)
      V43A=V(85)
      V23E=V(86)
      V43E=V(87)
      V27=V(88)
      V47=V(89)
      V27A=V(90)
      V47A=V(91)
      V27E=V(92)
      V47E=V(93)
      V28=V(94)
      V48=V(95)
      V29=V(96)
      V49=V(97)
      V210=V(98)
      V410=V(99)
      V210E=V(100)
      V41CE=V(101)
      V29A=V(102)
      V49A=V(103)
      T9A=V(104)
      H9A=V(105)
      TEHA=V(106)
      FBI9A=V(107)
      CE2=V(108)
C     IMPOSED PARAMETERS
      CONC=DAT(1)
      ALTE=DAT(2)
      AHX1=DAT(3)
      AHX2=DAT(4)
      ALTC=DAT(5)
      AHTC=DAT(6)
      AHTE=DAT(7)
      WGEI=DAT(8)
      WGEH=DAT(9)
      WLTC=DAT(10)
      WHTC=DAT(11)
      TEHC=DAT(12)
      TELC=DAT(13)
      TCLI=DAT(14)
      TCHI=TCLO
      TELI=DAT(15)
      TEHI=DAT(16)

      INCLUSION OF PRESSURE DROPS BASED ON TEST DATA.  (MCCARTHY 9-16-82)

      P2   = PHI -   1.0
      P3   = PHI -   2.0
      P4   = PHI -   5.0
      P7   = PLO + 7.9 + 14.1*CONC + 1.4*CONC**2
```

```
      P8  = PLC + 6.8 + 11.8*CONC + 1.4*CONC**2
      P9  = PLO + 6.3 + 11.6*CONC + 1.4*CONC**2
      P10 = PLC + 3.4 +  5.4*CONC + 0.3*CONC**2

C     PRELIMINARY COMPUTATIONS -THESE ARE USED FOR THE RESIDUAL EQUATIONS
      BUT ARE KEPT OUT OF THE RESIDUALS FOR CLARITY.

-----MASS CONCENTRATION OF R114 IN LIQ. & VAP.
      XCL7=XCL(P7,T7)
      XCL7A=XCL(P7,T7A)
      XCL7B=XCL(P7,T7B)
      XCL8=XCL(P8,T8)
      XCL9=XCL(P9,T9)
      XCL9A=XCL(P9,T9A)
      XCL3=XCL(P3,T3)
       XCL3A=XCL(P3,T3A)
      XCL3B=XCL(P3,T3B)
      XCL2B=XCL(P2,T2B)
      XL7 =MASFRAC(XCL7)
       XL7A=MASFRAC(XCL7A)
      XL7B=MASFRAC(XCL7B)
      XL8 =MASFRAC(XCL8)
      XL9 =MASFRAC(XCL9)
      XL9A=MASFRAC(XCL9A)
      XL3 =MASFRAC(XCL3)
      XL3A=MASFRAC(XCL3A)
      XL3B=MASFRAC(XCL3B)
      XL2B=MASFRAC(XCL2B)
      XV7 =MASFRAC(XCV(P7,T7,XCL7))
      XV7A=MASFRAC(XCV(P7,T7A,XCL7A))
      XV7B=MASFRAC(XCV(P7,T7B,XCL7B))
      XV8 =MASFRAC(XCV(P8,T8,XCL8))
      XV9 =MASFRAC(XCV(P9,T9,XCL9))
      XV9A=MASFRAC(XCV(P9,T9A,XCL9A))
      XV3 =MASFRAC(XCV(P3,T3,XCL3))
      XV3A=MASFRAC(XCV(P3,T3A,XCL3A))
      XV3B =MASFRAC(XCV(P3,T3B,XCL3B))
      XV2B=MASFRAC(XCV(P3,T2B,XCL2B))

-----MOLE CONCENTRATION OF R114 IN VAP. AT 10P,2P & LIQ. AT 4
      XCV10P=XCV(P10,T10P,XCL(P10,T10B))
      XCL4 =XCL(P4,T4)
      XCV2B=XCV(P2,T2P,XCL(P2,T2P))

-----PARTIAL PRESSURES OF R12 & R114 IN SUPERHEATED REGION
      PP4H    = MOLFRAC(CONC)*PHI
      PP2H    = PHI - PP4H
      PP4L    = MOLFRAC(CONC)*PLO
      PP2L    = PLO - PP4L
      PP4L10  = MOLFRAC(CONC)*P10
      PP2L10  = P10 - PP4L10
      PP4H2=MOLFRAC(CONC)*P2
      PP2H2=P2-PP4H2
      PP4H3=MOLFRAC(CONC)*P3
      PP2H3=P3-PP4H3
      PP4L7=MOLFRAC(CONC)*P7
      PP2L7=P7-PP4L7
      PP4L8=MOLFRAC(CONC)*P8
      PP2L8=P8-PP4L8
      PP4L9=MOLFRAC(CONC)*P9
```

```
      PP2L9=P9-PP4L9

-----ENTHALPIES OF LIQ. & VAP. IN 2-PHASE REGION
      HL7 =XL7*H114L(T7)  + (1.-XL7)*H12L(T7)
      HL7A=XL7A*H114L(T7A)  + (1.-XL7A)*H12L(T7A)
      HL7B=XL7B*H114L(T7B)  + (1.-XL7B)*H12L(T7B)
      HL8 =XL8*H114L(T8)  + (1.-XL8)*H12L(T8)
      HL9 =XL9*H114L(T9)  + (1.-XL9)*H12L(T9)
      HL9A=XL9A*H114L(T9A)  + (1.-XL9A)*H12L(T9A)
      HL3 =XL3*H114L(T3)  + (1.-XL3)*H12L(T3)
      HL3A=XL3A*H114L(T3A)  + (1.-XL3A)*H12L(T3A)
      HL3B =XL3B*H114L(T3B)  + (1.-XL3B)*H12L(T3B)
      HL2B=XL2B*H114L(T2B)  + (1.-XL2B)*H12L(T2B)
      HV7 =XV7*HR114V(T7,PP4L7,V47)+(1.-XV7)*HR12V(T7,PP2L7,V27)
      HV7A=XV7A*HR114V(T7A,PP4L7,V47A)+(1.-XV7A)*HR12V(T7A,PP2L7,V27A)
      HV7B=  XV7B*HR114V(T7B,PP4L7,V47B)+(1.-XV7B)*HR12V(T7B,PP2L7,V27B)
      HV8 =XV8*HR114V(T8,PP4L8,V48)+(1.-XV8)*HR12V(T8,PP2L8,V28)
      HV9 =XV9*HR114V(T9,PP4L9,V49)+(1.-XV9)*HR12V(T9,PP2L9,V29)
      HV9A=XV9A*HR114V(T9A,PP4L9,V49A)+(1.-XV9A)*HR12V(T9A,PP2L9,V29A)
      HV3 =XV3*HR114V(T3,PP4H3,V43)+(1.-XV3)*HR12V(T3,PP2H3,V23)
      HV3A=XV3A*HR114V(T3A,PP4H3,V43A)+(1.-XV3A)*HR12V(T3A,PP2H3,V23A)
      HV3B =XV3B*HR114V(T3B,PP4H3,V43B)+(1.-XV3B)*HR12V(T3B,PP2H3,V23B)
      HV2B=XV2B*HR114V(T2B,PP4H2,V42B)+(1.-XV2B)*HR12V(T2B,PP2H2,V22B)

-----SATURATION ENTHALPIES

      HR4V10P=HR114V(T10P,PP4L10,V410P)
      HR2V10P=HR12V(T10P,PP2L10,V210P)

      HR4V2P=HR114V(T2P,PP4H2,V42P)
      HR2V2P=HR12V(T2P,PP2H2,V22P)

-----WORK OF ISENTROPIC COMPRESSION  (P.LAUNAY)
      E12  = WIR12(T1,PP2L,PP2H)
      E114 = WIR114(T1,PP4L,PP4H)

-----CP'S OF LIQUIDS KJ/KG K (LTE 40% GLYCOL, HTE 30% GLYCOL)
      THESE GLYCOL EQUATIONS WERE OBTAINED BY FITTING A LEAST SQUARES
      CURVE TO GRAPHICAL DATA.  (MCCARTHY NOV 82)

      TEL1AV =  (TELO+TELA)/2.
      TEL2AV =  (TELA+TELB)/2.
      TEL3AV =  (TELB+TELI)/2.
      TEH1 =  (TEHA+TEHC)/2.
      TEH2 =  (TEHA+TEHB)/2.
      TEH3=(TEHI+TEHP)/2.
      CPGL1   = 3.397 + .0045*TEL1AV - 2.03E-5*TEL1AV**2
      CPGL2 = 3.397 + .0045*TEL2AV - 2.03E-5*TEL2AV**2
      CPGL3 = 3.397 + .0045*TEL3AV - 2.03E-5*TEL3AV**2
      CPGH1  = 3.703 + .00234*TEH1 + 4.05E-5*TEH1**2
      CPGH2  = 3.703 + .00234*TEH2 + 4.05E-5*TEH2**2
      CPGH3  = 3.703 + .00234*TEH3 + 4.05E-5*TEH3**2
      CPWA   = 4.19

-----UA VALUES (KW/K) BASED ON ACTUAL TEST RESULTS.  (MCCARTHY NOV 82)
      UPDATED JAN. 84

      HTC
      ADSH  =2./3.*AHTC-ACC1
      ACC2=AHTC/3.
      UCO1 =  1.225- 1.410*CONC + CONC**2 + 5.83*CONC**3
```

```
      UCO2 = 1.225- 1.410*CONC + CONC**2 + 5.83*CONC**3
      UCO1=1.225
      UCC2=1.225
      UDSH  = 0.48
      UACC1 = UCO1 * ACO1
      UACO2 = UCO2 * ACC2
      UADSH = UDSH * ADSH

      LTC
      ULTC1 = 1.20 - 0.92*CONC
      ULTC2 = 0.965-0.62*CONC
      ULTC3 = 0.765 - .38*CONC
      ULTC2=.965
      ULTC3=.765
      ULTC1=1.20
      UALTC1= ULTC1*(ALTC/3.)
      UALTC2= ULTC2*(ALTC/3.)
      UALTC3=ULTC3*(ALTC/3.)

      HEAT EXCHANGERS
      UHX1  = 0.09
      UHX2  = 0.225
      UAHX1 = UHX1 * AHX1
      UAHX2 = UHX2 * AHX2

       LTE
      ULTE1 = 0.165
      ULTE2 = 0.190
      ULTE3 = 0.245
      UALTE1= ULTE1*(ALTE*2./5.)
      UALTE2= ULTE2*(ALTE*2./5.)
      UALTE3= ULTE3*(ALTE/5.)

       HTE
      AE1=.5*AHTE
      ASH=.5*AHTE - AE2
      UE1 = 0.245
      UAE1 = UE1 * AE1
      UE2   = 0.245 + .325*CONC - .75*CONC**2
      UE2=0.245 + .325*CONC
      USH=0.220
      UAE2 = AE2 * UE2
      UASH  = USH * ASH

-----DEFINING QLTE3 IN TERMS OF VARIABLES QLTE1 AND  QLTE2
      QLTE3=QLTE-QLTE1-QLTE2

C     COMPUTING RESIDUALS

      THESE EQUATIONS HAVE BEEN REVISED TO MOVE THE
      SUPERHEAT POINT FROM INSIDE HX1 TO INSIDE THE HIGH TEMP EVAPORATOR
      (HTE) WHICH MODELS THE PHYSICAL APPARATUS.

-----FRACTION OF LIQ. IN 2 PHASE REGIONS

      R(1)= -CONC + FRL2B*XL2B + (1.-FRL2B)*XV2B

      R(2) = -CONC + FRL3*XL3 + (1.-FRL3)*XV3
```

```
      R(3)= -CONC + FRL3A*XL3A + (1.-FRL3A)*XV3A
      R(4)= -CONC + FRL3B*XL3B + (1.-FRL3B)*XV3B
      R(5) = -CONC + FRL7*XL7 + (1.-FRL7)*XV7
      R(6)= -CONC +FRL7A*XL7A + (1.-FRL7A)*XV7A
      R(7)= -CONC + FRL7B*XL7B +(1.-FRL7B)*XV7B
      R(8) = -CONC + FRL8*XL8 + (1.-FRL8)*XV8
      R(9) = -CONC + FRL9*XL9 + (1.-FRL9)*XV9
-----ENTHALPIES IN 2 PHASE REGION
      R(10)= -H2B + FRL2B*HL2B + (1.-FRL2B)*HV2B
      R(11) = -H3 + FRL3*HL3 + (1.-FRL3)*HV3
      R(12)= -H3A + FRL3A*HL3A + (1.-FRL3A)*HV3A
      R(13)= -H3B + FRL3B*HL3 + (1.-FRL3B)*HV3B
      R(14) = -H7 + FRL7*HL7 + (1.-FRL7)*HV7
      R(15)= -H7A + FRL7A*HL7A + (1.-FRL7A)*HV7A
      R(16)= - H7B + FRL7B*HL7B + (1.-FRL7B)*HV7B
      R(17) = -H8 + FRL8*HL8 + (1.-FRL8)*HV8
      R(18) = -H9 + FRL9*HL9 + (1.-FRL9)*HV9
-----SATURATED VAPOR ENTHALPY
      R(19)= -H2P + CONC*HR4V2P +(1.-CONC)*HR2V2P
      R(20)= -H10P + CONC*HR4V10P + (1.-CONC)*HR2V10P
-----VAPOR ENTHALPY
      R(21)=-H1 +CONC*HR114V(T1,PP4L,V41)+(1.-CONC)*HR12V(T1,PP2L,V21)
      R(22)= -H2 +CONC*HR114V(T2,PP4H2,V42)
     *          +(1.-CONC)*HR12V(T2,PP2H2,V22)
      R(23) = -H10 + CONC*HR114V(T10,PP4L10,V410) +
     *          (1.-CONC)*HR12V(T10,PP2L10,V210)
-----SATURATION CONDITIONS
      R(24)= -MOLFRAC(CONC) + XCV10P
      R(25)= -MOLFRAC(CONC) + XCL4
      R(26)= -MOLFRAC(CONC) + XCV2P
-----ENTHALPIES AT 4,5,6
```

```
      R(27)= -H5 + CONC*H114L(T5) + (1.-CONC)*H12L(T5)
      R(28)= -H6 + CONC*H114L(T6) + (1.-CONC)*H12L(T6)
      R(29)= -H4 + CONC*H114L(T4) + (1.-CONC)*H12L(T4)
-----HEAT EXCHANGER RATE EQUATIONS
-----HTC
      R(30)= -(T2-TCHO)/(T2P-TCHP) + EXP(UADSH*((T2-TCHO)
     *        -(T2P-TCHP))/CDHTC)
      R(31)= -QCO1 + UACO1*LMTD(T2P,T2B,TCHB,TCHP)
      R(32)= -QCO2 + UACO2*LMTD(T2P,T3,TCHI,TCHB)
-----LTC
      R(33)= -QLTC1+ UALTC1*LMTD(T3,T3A,TCLA,TCLO)
      R(34)= -QLTC2 + UALTC2*LMTD(T3A,T3B,TCLB,TCLA)
      R(35)= -QLTC3 + UALTC3*LMTD(T3B,T4,TCLI,TCLB)
-----HX1 & HX2
      R(36)= -W*(H1-H10) + UAHX1*LMTD(T4,T5,T10,T1)
      R(37)= -W*(H9-H8) + UAHX2*LMTD(T5,T6,T8,T9)
-----LTE
      R(38)= -QLTE1+ UALTE1*LMTD(TELO,TELA,T7A,T7)
      R(39)= - QLTE2 + UALTE2*LMTD(TELA,TELB,T7B,T7A)
      R(40)= -QLTE3 + UALTE3*LMTD(TELB,TELI,T8,T7B)
----- HTE
      R(41)= -QE1 + UAE1*LMTD(TEHA,TEHO,T9,T9A)
      R(42)= -QSH + UASH*LMTD(TEHI,TEHP,T10P,T10)
-----REFRIGERANT ENERGY BALANCES
----- HTC
      R(43)= -QDHTC + W*(H2-H2P)
      R(44)= -QCO1 + W*(H2P-H2B)
      R(45)= -QCO2 + W*(H2B-H3)
-----LTC
      R(46)= -QLTC1+ W*(H3-H3A)
      R(47)= -QLTC2 + W*(H3A-H3B)
```

```
     R(48)= -QLTC3 + W*(H3B - H4)
-----HX1 & HX2
     R(49)= -(H1-H10) + (H4-H5)
     R(50)= -(H5-H6) + (H9-H8)
-----VALVE
     R(51)= -H6 + H7
-----LTE
     R(52)= -QLTE1 + W*(H7A-H7)
     R(53)= - QLTE2 + W*(H7B-H7A)
     R(54)= -QLTE3 + W*(H8-H7B)
-----HTE
     R(55)= -QE1 + W*(H9A-H9)
     R(56)= -QSH + W*(H10-H10P)
------WATER OR GLYCOL ENERGY BALANCES
-----HTC
     R(57)= -QDHTC  + WHTC*CPWA*(TCHO-TCHP)
     R(58)= -QCO1 + WHTC*CPWA*(TCHP-TCHB)
     R(59)= -QCO2 + WHTC*CPWA*(TCHB-TCHI)
-----LTC
     R(60)= -QLTC1+ WLTC*CPWA*(TCIO-TCLA)
     R(61)= -QLTC2 + WLTC*CPWA*(TCLA-TCLB)
     R(62)= -QLTC3 + WLTC*CPWA*(TCLB - TCII)
-----LTE
     R(63)= -QLTE1+ WGEL*CPGL1*(TELA-TELO)
     R(64)= - QLTE2 + WGEL*CPGL2*(TELB-TELA)
     R(65)= -QLTE3 + WGEL*CPGL3*(TELI-TELB)
-----HTE
     R(66)= -QE1 + WGEH*CPGH1*(TEEA-TEHO)
     R(67)= -QSH+WGEH*CPGH3*(TEHI-TEHP)
     R(68)= -QHTE + QE1 + QSH + QE2
-----COMPRESSOR ENERGY BALANCE (A COMPRESSION EFFICIENCY OF .9 IS USED)
```

```
      R(69)= - H2 + H1 + (IPOWR/W)*.9
-----POWER  (ISENTROPIC EFFICIENCY = .75)
      R(70)= -POWR + IPOWR/.75
----- ISENTROPIC POWER
      R(71)= -IPOWR + W*(CONC*F114 + (1.-CONC)*E12)
-----COMPRESSOR - THESE EQUATIONS ARE NOT USED
      R(72)= -RPM +5.0
      R(73)= -ETAV +.5
-----SPECIFIC VOLUMES-VOL2 AND VOL4 ARE THE FUNCTIONS WHICH CALCULATE
      SPECIFIC VOLUME FOR R-12 AND R-114 FROM THE DOWNING EQUATIONS
      R(74)= -V21+VOL2(T1,PP2L,V21)
      R(75)= -V41+VOL4(T1,PP4L,V41)
      R(76)= -V22+VOL2(T2,PP2H2,V22)
      R(77)= -V42+VOL4(T2,PP4H2,V42)
      R(78)= -V22P+VOL2(T2P,PP2H2,V22P)
      R(79)= -V42P+VOL4(T2P,PP4H2,V42P)
      R(80)= -V22P + VOL2(T2B,PP2H2,V22B)
      R(81)= -V42B + VOL4(T2B,PP4H2,V42B)
      R(82)=-V23+VOL2(T3,PP2H3,V23)
      R(83)=-V43+VOL4(T3,PP4H3,V43)
      R(84)= -V23A + VOL2(T3A,PP2H3,V23A)
      R(85)= -V43A + VOL4(T3A,PP4H3,V43A)
      R(86)= -V23B + VOL2(T3B,PP2H3,V23B)
      R(87)= -V43B + VOL4(T3B,PP4H3,V43B)
      R(88)=-V27+VOL2(T7,PP2L7,V27)
      R(89)=-V47+VOL4(T7,PP4L7,V47)
      R(90)= -V27A + VOL2(T7A,PP2L7,V27A)
      R(91)= -V47A + VOL4(T7A,PP4L7,V47A)
      R(92)= -V27B+VOL2(T7B,PP2L7,V27B)
      R(93)= -V47B+VOL4(T7B,PP4L7,V47B)
      R(94)=-V28+VOL2(T8,PP2L8,V28)
```

```
      R(95)=-V48+VOL4(T8,PP4L8,V48)
      R(96)=-V29+VOL2(T9,PP2L9,V29)
      R(97)=-V49+VOL4(T9,PP4L9,V49)
      R(98)= -V210+VOL2(T10,PP2L10,V210)
      R(99)= -V410+VOL4(T10,PP4L10,V410)
      R(100)= -V210P+VOL2(T10P,PP2L10,V210P)
      R(101)= -V410P+VOL4(T10P,PP4L10,V410P)
      R(102)= -V29A + VOL2(T9A,PP2L9,V29A)
      R(103)= -V49A + VOL4(T9A,PP4L9,V49A)
-----RATE EQUATION FOR HTE SECTION 2
      R(104)= -QE2 + UAE2*LMTD(TEHE,TEHA,T9A,T10P)
-----REFRIGERANT ENERGY BALANCE ON HTE SECTION 2
      R(105)= -QE2 + W*(H10P-H9A)
-----GLYCOL ENERGY BALANCE ON HTE SECTION 2
      R(106)= -QE2 + WGEH*CPGH2*(TEHP-TEHA)
-----ENTHALPY AT 9A
      R(107)= -H9A + FRL9A*HL9A + (1.-FRL9A)*HV9A
-----FRACTION OF LIQUID AT 9A
      R(108)= -CONC + FRL9A*XL9A + (1.-FRL9A)*XV9A

      RETURN
      END

      SUBROUTINE SIMUL(NVAR,TLRNCE,ITMAX,V,DES,R,PD,VCORR,VD,RD,
     *   DAMPING,POPTION,ITER)

     THIS IS THE NEWTON-RAPHSON SUBROUTINE WHICH IS COMBINED WITH
        THE PARDIF AND GAUSSY SUBROUTINES

      USER MUST PROVIDE THE MAIN PROGRAM AND THE EQUATION SUBROUTINE

      GLOSSARY OF TERMS USED

      ITER      = NUMBER OF ITERATIONS
      ITMAX     = MAXIMUM NUMBER OF ITERATIONS TO BE PERMITTED
      NVAR      = NUMBER OF UNKNOWNS = NUMBER OF EQUATIONS
      PD(I,J)   = PARTIAL DERIVATIVE OF FUNCTION I WITH RESP TO VARIABLE J
      R( )      = RESIDUAL OF EQUATION
      TLRNCE    = MAXIMUM FRACTION OF VALUE OF VARIABLES PERMITTED BEFORE
                  ITERATION COMPLETE.  THUS TLRNCE = 0.01 REQUIRES CHANGE OF
                  ALL VARIABLES TO BE LESS THAN 1 PERCENT FOR CONVERGENCE
```

```
V( )       = VALUE OF THE VARIABLE
VCORR( )   = CORRECTION IN THE VARIABLE DURING THIS ITERATION
DES( )     = DESIGNATION OF VARIABLE IN A4 FIELDS
DAMPING      IS THE FACTOR BY WHICH ITERATIONS ARE DAMPED IN STATEMENT
             NUMBER 43  (SET DAMPING=0 IF NO DAMPING IS DESIRED)
POPTION      IS A NUMBER REPRESENTING THE FOLLOWING PRINTING OPTIONS
             CORRESPONDING TO THE VALUE OF POPTION:
         0 = NO PRINTING DESIRED FROM THIS SUBROUTINE
         1 = PRINT LAST ITERATION ONLY
         2 = PRINT ALL ITERATIONS
         3 = PRINT PARTIAL DERIVATIVES ONLY
         4 = PRINT LAST ITERATION PLUS PARTIALS
         5 = PRINT ALL ITERATIONS PLUS PARTIALS

      DIMENSION VD(NVAR), BD(NVAR)
      DIMENSION V(NVAR),B(NVAR),PD(NVAR,NVAR),VCORR(NVAR), DES(NVAR)
      INTEGER DAMPING,POPTION

 WRITING OUT THE INPUT DATA

      IF (POPTION.EQ.0) GO TO 24
      WRITE(6,20) NVAR
   20 FORMAT(1H1,///," NUMBER OF VARIABLES = ", I4)
      WRITE(6,21) TIRNCE
   21 FORMAT(" MAXIMUM FRACTION CHANGE FOR CONVERGENCE =", F10.4, //)
      WRITE(6,22)
   22 FORMAT("0VARIABLE NUMBER AND ITS TRIAL VALUE")
      WRITE (6,23)  (J, DES(J), V(J), J = 1, NVAR)
   23 FORMAT (" V(", I2, ") = ", A4, " = ", F15.5)

 INITIALIZING THE ITERATION COUNTER
   24 ITER = 1
 CALLING SUBROUTINES TO CALCULATE VALUES OF RESIDUALS, PARTIAL
       DERIVATIVES AND CHANGES IN VALUES OF VARIABLES

   30 CALL EQNS(NVAR, V, B)
      IF (POPTION.NE.2.AND.POPTION.NE.5) GO TO 25
      WRITE (6,33)
   33 FORMAT("0EQUATION NUMBER       RESIDUAL")
      WRITE (6,35)  (I  B(I),  I = 1,NVAR)
   35 FORMAT (I10, F20.5)
   25 CALL PARDIF(NVAR, V, B, PD, VD, BD)

  PRINTING OUT NON-ZERO VALUES OF PARTIAL DERIVATIVES

      IF (POPTION.LT.3) GO TO 55
      DO 54  I = 1, NVAR
      DO 53  J = 1, NVAR
      Z = ABS(PD(I,J))
      IF(Z - 0.00000001) 53, 53, 51
   51 WRITE(6,52) I, J, PD(I,J)
   52 FORMAT(" PD(",I2,",",I2,") =", F20.10)
   53 CONTINUE
   54 CONTINUE
   55 CALL GAUSSY(PD, B, VCORR, NVAR)
      CORRECTING THE VALUES OF THE VARIABLES
      DO 44  L = 1,NVAR
      IF (DAMPING.EQ.0) GO TO 44
   43 VCORR(L) = VCORR(L)/(1.0+FLOAT(DAMPING-1)/(FLOAT(ITER)**2))
```

```
44 V(I) = V(I) - VCORR(I)
 WRITING OUT RESULTS OF THIS ITERATION
   IF (FOPTION.NE.2.AND.FOPTION.NE.5) GO TO 37
   WRITE (6,32) ITER
32 FORMAT("0RESULTS AFTER", I4, "  ITERATIONS")
   WRITE(6,34)
34 FORMAT("0",4X,"VARIABLE",16X,"VALUE",9X,"CHANGE FROM PREVIOUS")
   WRITE (6,36)  (I, DES(I), V(I), VCORR(I), I = 1,NVAR)
36 FORMAT (" V(", I2, ") = ", A4," = ", 2F21.5)
 TERMINATING IF MAXIMUM NUMBER OF ITERATIONS REACHED OR OTHERWISE
      INCREMENTING THE ITERATION COUNTER
37 IF(ITER - ITMAX) 38, 99, 99
38 ITER = ITER + 1
 CHECK TO SEE IF CHANGE OF VARIABLE IS LESS THAN SPECIFIED TOLERANCE
   K = 1
40 VAL = ABS(VCORR(K)) - ABS(TLRNCE*V(K))
   IF(VAL) 41, 30, 30
41 IF(K - NVAR) 42, 99, 99
42 K = K + 1
   GO TO 40
99 IF (FOPTION.NE.1.AND.FOPTION.NE.4) RETURN
   WRITE (6,32) ITER
   WRITE (6,34)
   WRITE (6,36)   (I,DES(I),V(I),VCORR(I),I=1,NVAR)
   RETURN
   END

   SUBROUTINE PARDIF (NVAR, V, R, PD, VD, RD)
   DIMENSION VD(NVAR), RD(NVAR)
   DIMENSION V(NVAR), R(NVAR), PD(NVAR,NVAR)
 GLOSSARY FOR SUBROUTINE PARDIF
   DV = FRACTION OF VARIABLE CHANGE USED IN TAKING PARTIAL
   VD =  V + DELTA V  =  V + V*DV
   RD = R EVALUATED AT VD
   THE PARTIAL DERIVATIVE IS  (RD - R)/(V*DV)
   DV = 0.001
   SETTING ALL VD = V
   DO 550  K = 1,NVAR
550 VD(K) = V(K)
   DO 560  J = 1, NVAR
   ADDING DELTA TO VD(J)
  CIRCUMVENT CASE OF V(J) = 0
   IF(ABS(V(J)) - 10.**(-30)) 551, 551, 552
551 VD(J) = V(J) + 0.001
   GO TO 553
552 VD(J) =(1. + DV)*V(J)
553 CALL FCNS(NVAR, VD, RD)
   DO 558 I = 1, NVAR
   IF(ABS(V(J)) - 10.**(-30)) 555, 555, 556
555 PD(I,J) = (RD(I) - R(I))/0.001
   GO TO 558
556 PD(I,J) = (RD(I) - R(I))/(V(J)*DV)
558 CONTINUE
```

```
      RETURNING VD(J) TO V(J) VALUE
      VD(J) = V(J)
  560 CONTINUE
      RETURN
      END


      SUBROUTINE GAUSSY (A, B, X, N)

      SOLUTION OF SIMULTANEOUS EQUATIONS BY GAUSS ELIMINATION

      DIMENSION A(N,N), X(N), B(N)
      BEGINNING OF ELIMINATION PROCESS
      DO 28  K = 1,N
      MOVING LARGEST COEFFICIENT INTO DIAGONAL POSITION
      AMAX = 0.
      DO 4  I = K,N
      IF(ABS(A(I,K)) - ABS(AMAX)) 4, 4, 2
    2 AMAX = A(I,K)
      IMAX = I
    4 CONTINUE
     TESTING FOR INDEPENDENCE OF EQUATIONS
      IF(ABS(AMAX) - 0.1E-15) 10, 10, 14
   10 WRITE (6,12)
   12 FORMAT ("0 EQUATIONS ARE NOT INDEPENDENT")
      RETURN
       EXCHANGING ROW IMAX AND ROW K
   14 BTEMP = B(K)
      B(K) = B(IMAX)
      B(IMAX) = BTEMP
      DO 18  J = K,N
      ATEMP = A(K,J)
      A(K,J) = A(IMAX, J)
   18 A(IMAX,J) = ATEMP
      SUBTRACTING A(I,K)/A(K,K) TIMES TERM IN FIRST EQ FROM OTHERS
      KPLUS = K + 1
      IF(K - N) 22, 28, 28
   22 DO 24  I = KPLUS,N
      B(I) = B(I) - B(K)*A(I,K)/A(K,K)
      ACON = A(I,K)
      DO 24  J = K,N
   24 A(I,J) = A(I,J) - A(K,J)*ACON/A(K,K)
   28 CONTINUE
       BACK SUBSTITUTION
      I = N
   32 SUM = 0.0
      IF(I - N) 34, 38, 38
   34 IPLUS = I + 1
      DO 36  J = IPLUS, N
   36 SUM = SUM + A(I,J)*X(J)
   38 CONTINUE
      X(I) = (B(I) - SUM)/A(I,I)
      IF(I - 1) 42, 42, 40
   40 I = I - 1
      GO TO 32
   42 RETURN
      END
```

```
THIS FUNCTION SAFELY CALCULATES LOG MEAN TEMPERATURE DIFFERENCE
MCCABTHY NOV 82.

REAL FUNCTION LMTD(T1I,T1O,T2I,T2O)
DT1  = T1I - T2O
DT2  = T1O - T2I
IF(ABS(DT1-DT2).LE.0.1) GO TO 2
IF((DT1/DT2).LE.0.0) GO TO 2
LMTD = (DT1-DT2)/ALOG(DT1/DT2)
RETURN
2 LMTD = 0.5*(DT1+DT2)
RETURN
END

  CALCULATE SATURATION PRESSURE OF R-12 FROM DOWNING EQNS

FUNCTION PSAT12(T)
DATA A12/39.88381727/
DATA B12/-3436.632228/
DATA C12/-12.47152228/
DATA D12/4.73044244E-3/
DATA PCONV/ 6.894757/
PS12E(T)= 10**(A12 + B12/TR12(T) + C12*ALOG10(TR12(T))
*   + D12*TR12(T))
PSAT12 = PS12E(T) * PCONV
RETURN
END

CALCULATE SATURATION PRESSURE OF R-114 FROM DOWNING EQNS

FUNCTION PSAT114(T)
DATA A114/27.071306/
DATA B114/ -5113.7021/
DATA C114/ -6.3086761/
DATA D114/ 6.913003E-4/
DATA E114/ .78142111/
DATA F114/ 768.35/
DATA PCONV/ 6.894757/
PS114E(T)= 10**( A114 + B114/TR114(T) + C114*
*   ALOG10(TR114(T)) + D114*TR114(T) + E114*((F114-TR114(T))/
*   TR114(T)) * ALOG10(F114 - TR114(T)))
PSAT114 = PS114E(T) * PCONV
RETURN
END

CONVERT TEMPERATURE DEGREES C INTO DEGREES R FOR USE IN DOWNING EQNS

FUNCTION TR12(T)
TR12 = T*1.8 +32. +459.7
RETURN
END

FUNCTION TR114(T)
TR114= T*1.8 +32. +459.69
RETURN
END
```

R-12 VAPOR ENTHALPY FUNCTION (DOWNING EQUATIONS)

```
      FUNCTION HR12V(T,P,V2)
      DIMENSION A2(5),C2(5)
      REAL J,K2
      DATA AV2/8.0945E-3/
      DATA BV2/3.32662E-4/
      DATA CV2/-2.413896E-7/
      DATA DV2/6.72363E-11/
      DATA J/.185053/
      DATA A2/0.0,-3.40972713,0.0602394465,-5.4873701E-4,0.0/
      DATA C2/0.0,-56.7627671,1.31139908,0.0,-2.54390678E-5/
      DATA X2/39.556551/
      DATA TC2/693.3/
      DATA K2/5.475/
      DATA SB2/.00650938866/
      FUNCA(T)= AV2*TR12(T) + BV2/2.0*TR12(T)**2 + CV2/3.0*TR12(T)**3
     *          +DV2/4.0*TR12(T)**4
      FUNCB(P,V2)=(P/6.894757)*V2+A2(2)/(V2-SB2)+A2(3)/
     *       (2.* (V2-SB2)**2)+A2(4)/(3.*(V2-SB2)**3)
      FUNCC(T)= EXP(-K2*TR12(T)/TC2)*(1.0 + K2*TR12(T)/TC2)
      FUNCD(V2)= C2(2)/(V2-SB2) + C2(3)/(2.0*(V2-SB2)
     *            **2 )+ C2(5)/(4.0*(V2-SB2)**4)
      HR12(T,P,V2)= FUNCA(T) + J*(FUNCB(P,V2)+ FUNCC(T)
     *            *FUNCD(V2)) + X2
      NEED TO CONVERT TO SI UNITS

      HR12V=(4.1868/1.8)*(HR12(T,P,V2)-15.500) + 200.
      RETURN
      END
```

R-114 VAPOR ENTHALPY FUNCTION (DOWNING EQUATIONS)

```
      FUNCTION HR114V(T,P,V4)
      DIMENSION A4(5),C4(5)
      REAL J,K4
      DATA AV4/.0175/
      DATA BV4/3.49000E-4/
      DATA CV4/-1.670000E-7/
      DATA DV4/0.0/
      DATA J/.185053/
      DATA A4/0.0,-2.3856704,0.034055687,-3.857481E-4,1.6017659E-6/
      DATA C4/0.0,-6.5643648,0.16366057,0.0,-1.0165314E-5/
      DATA X4/25.3396621/
      DATA TC4/753.95/
      DATA K4/3.0/
      DATA SB4/.005914907/
      FUNCA(T)= AV4*TR114(T) + BV4/2.0*TR114(T)**2 + CV4/3.0*
     *          TR114(T)**3+DV4/4.0*TR114(T)**4
      FUNCB(P,V4)=(P/6.894757)*V4+A4(2)/(V4-SB4)+A4(3)/
     *       (2.*(V4-SB4)**2)+A4(4)/(3.*(V4-SB4)**3)
      FUNCC(T)= EXP(-K4*TR114(T)/TC4)*(1.0 + K4*TR114(T)/TC4)
      FUNCD(V4)=C4(2)/(V4-SB4)+C4(3)/(2.0*(V4-SB4)
     *          **2 )+ C4(5)/(4.0*(V4-SB4)**4)
      HR114(T,P,V4)= FUNCA(T) + J*(FUNCB(P,V4)+ FUNCC(T)
     *            *FUNCD(V4)) + X4
      NEED TO CONVERT TO SI UNITS

      HR114V=(4.1868/1.8)*(HR114(T,P,V4)-15.541) + 200.
      RETURN
```

```
      END
THESE FUNCTIONS CALCULATE THE
SPECIFIC VOLUME OF THE TWO REFRIGERANTS IN THE MIXTURE (R12,R114).
SOURCE: R.C. DOWNING, ASHRAE TRANSACTIONS, VOL. 80, PART II, 1974.

      CONST2= THE SUM OF TERMS IN DOWNING SPECIFIC VOLUME EQN
      CONST4=  "    "   "   "    "    "     "     "    "
       NOTE: EQUATION HAS BEEN REARRANGED FROM
             P=RT/(V-SB) + F1(T)/(V-SB)**2 + F2(T)/(V-SB)**3 + ...
             TO
             V-SB = RT/P + F1(T)/P(V-SB) + F2(T)/P(V-SB)**2 + ...
             AND DENOTES
             CONST(2,4)= F1(T)/P(V-SB) + ... + F4(T)/P(V-SB)**4

      R-12 SPECIFIC VOLUME FUNCTION

      FUNCTION VOL2(T,P,V2)
      DIMENSION A2(5),B2(5),C2(5)
      REAL K2
      DATA A2/0.0,-3.40972713,0.0602394465,-5.4873701E-4,0.0/
      DATA B2/0.0,1.59434848E-3,-1.87961843E-5,0.0,3.468834E-9/
      DATA C2/0.0,-56.7627671,1.31139908,0.0,-2.54390678E-5/
      DATA K2/5.475/
      DATA TC2/693.3/
      DATA SB2/.00650938866/
      DATA R2/.088734/

      TE=TR12(T)
      EE=EXP(-K2*TR12(T)/TC2)
      PE=P/6.892757
      VE=V2-SB2

      CONST2=  (A2(2)+B2(2)*TE+C2(2)*EE)/(PE*VE)
     *        +(A2(3)+B2(3)*TE+C2(3)*EE)/(PE*VE**2)
     *        +(A2(4)+B2(4)*TE+C2(4)*EE)/(PE*VE**3)
     *        +(A2(5)+B2(5)*TE+C2(5)*EE)/(PE*VE**4)

      VOL2=CONST2+SB2+R2*TE/PE
      RETURN
      END

       R-114 SPECIFIC VOLUME FUNCTION

      FUNCTION VOL4(T,P,V4)
      DIMENSION A4(5),B4(5),C4(5)
      REAL K4
      DATA A4/0.0,-2.3856704,0.034055687,-3.857481E-4,1.6017659E-6/
      DATA B4/0.0,1.08012C7E-3,5.333469E-6,0.0,6.2632341E-10/
      DATA C4/0.0,-6.5643648,0.16366057,0.0,-1.0165314E-5/
      DATA K4/3.0/
      DATA TC4/753.95/
      DATA SB4/.005914907/
      DATA R4/.062780807/

      TF=TR114(T)
      EF=EXP(-K4*TR114(T)/TC4)
      PF=P/6.894757
      VF=V4-SB4
```

APPENDIX III.

EXPERIMENTAL DATA ON TESTS OF THE SEPARATING CYCLE

Test number	95	97	99
Percent R-114 by mass	50	50	25
Pressure, kPa abs.			
compressure discharge	650	652	944
compressor suction	56	56	72
Refrigerant flow rates, kg/s			
through LTE	0.0106	0.0107	0.0112
through HTE	0.0081	0.0090	0.0080
Temperature at positions indicated by Fig. 5.4, °C			
0	78.5	81.7	87.4
1	60.7	63.3	70.0
2	42.7	44.7	53.9
3	43.0	44.8	50.9
4	39.9	42.7	47.9
5	40.1	41.8	47.3
6	38.5	40.1	45.9
7	27.9	28.6	30.7
8	34.1	34.7	41.1
9	37.7	39.3	46.1
10	43.1	44.7	53.6
11	42.3	43.0	51.4
12	39.0	40.9	46.7
13	36.3	38.0	43.4
14	36.5	38.0	44.4
15	33.9	35.1	40.2
16	32.4	33.6	34.3
17	30.9	31.8	27.5
18	28.2	28.6	25.5
19	27.8	27.0	25.3
20	24.4	25.1	24.8
21	25.0	25.6	24.9
22	26.1	26.8	26.5
23	28.4	29.2	31.0

24	0.2	0.2	0.2
25	26.1	26.8	25.9
26	24.8	25.4	24.9
27	-17.2	-15.7	-14.1
28	-8.7	-8.0	-7.4
29	-35.3	-35.0	-34.0
30	-34.6	-34.4	-33.6
31	-33.4	-33.2	-32.9
32	-29.2	-29.6	-31.4
33	-30.0	-30.2	-29.4
34	-29.6	-29.1	-31.0
35	-14.5	-14.6	-14.9
36	-15.5	-15.2	-16.1
37	-15.1	-15.1	-15.8
38	-19.3	-18.8	-19.5
39	-17.6	-17.6	-18.5
40	-20.5	-19.8	-20.4
41	-17.8	-17.4	-17.9
42	21.3	22.0	27.5
43	-21.7	-21.9	-23.0
44	-21.1	-20.9	-22.0
45	-28.0	-27.6	-29.9
46	-20.6	-21.3	-22.9
47	-17.3	-20.4	-21.0
48	-12.5	-14.0	-13.9
49	-6.1	-7.7	-5.8
50	0.1	0.2	-0.1
51	-0.3	-0.2	-0.4
52	-1.9	-2.1	-2.1
53	-1.8	-1.8	-1.9
54	-4.6	-4.7	-5.2
55	-2.1	-2.1	-2.5
56	-0.1	0.8	3.5
57	-4.4	-5.0	-5.6
58	-1.6	-2.7	-1.5
59	14.8	13.9	18.9

REFERENCES

1. Aurora, C. P., "Boiling Heat Transfer Data for Pure and Mixed Refrigerants," Proc. XII International Congress of Refrigeration, Madrid, 1967.

2. Aittomaki, A., "Use of Refrigerant Mixtures in Exhaust-Air Heat Pump," Proc. of Meeting of Commissions B1, B2, E1, and E2 of the International Institute of Refrigeration Mons, Belgium, Sept. 1980.

3. Jakobs, R., and Kruse, H., "The Use of Nonazeotropic Refrigerant Mixtures in Heat Pumps for Energy Saving," Proc., Meeting of Commission B2 of the International Institute of Refrigeration, Delft, The Netherlands, 1978.

4. Cooper, W. D., and Borchardt, H. D., "The Use of Refrigerant Mixtures in Air-to-Air Heat Pumps," Paper no. E1-60, XV Int. Congress of Refrigeration, Venice, Sept. 1979.

5. Stoecker, W. F. and McCarthy, C. I., "The Simulation and Performance of a System Using an R-12/R-114 Refrigerant Mixture," University of Illinois, for the Oak Ridge National Laboratory, United States Department of Energy, Report No. ORNL/Sub/81-7762/3&01, May 1984.

6. Kornota, E., and Stoecker, W. F., "Flow Regimes of Refrigerant Mixtures Condensing Inside Tubes," University of Illinois at Urbana-Champaign, for Oak Ridge National Laboratory, Report No. ORNL/Sub/81-7762/4&01, 1985.

7. Launay, P. F., "Improving the Efficiency of Refrigerators and Heat Pumps by Using a Nonazeotropic Mixture of Refrigerants," University of Illinois for the Oak Ridge National Laboratory United States Department of Energy, Report No. ORNL/Sub-81/7762/1, Oct. 1981.

8. Stoecker, W. F., "Improving the Energy Effectiveness of Domestic Refrigerators by the Application of Refrigerant Mixtures," University of Illinois, for the Oak Ridge National Laboratory, United States Department of Energy, Report No. ORNL/Sub-78/55463/1, Sept. 1978.

9. Downing, R. C., "Refrigerant Equations", ASHRAE Trans., Vol. 80, Part 2, pp. 158-159, 1974.

10. Connon, H. A., E. I. du Pont de Nemours and Company, Wilmington, Del., Personal Communication, 1984.

11. Kazacki, G., "Refrigerant Cycles Using Nonazeotropic Refrigerant Mixtures," Potravinarska a Cladici Technika, Vol. 7, No. 5, pp. 515.147 to 520.152, 1976.

12. Labochnik, A. E., and Ceonov, M. A., Patent on Two Chamber Refrigerator, Kholod. Tech., Vol. 52, No. 8, p. 51, 1975

13. Connon, H. A., "A Generalized Computer Program for Analysis of Mixture Refrigeration Cycles," ASHRAE Trans., Vol. 89, Part 2A, pp. 628-639, 1983.